Coordination Chemistry Reviews 254 (2010) 46–76

Contents lists available at ScienceDirect

Coordination Chemistry Reviews

journal homepage: www.elsevier.com/locate/ccr

Review

Stereochemical activity of lone pairs of electrons and supramolecular aggregation patterns based on secondary interactions involving tellurium in its 1,1-dithiolate structures

Edward R.T. Tiekink[a,b,c,*], Julio Zukerman-Schpector[a,**]

[a] *Universidade Federal de São Carlos, Laboratório de Cristalografia, Estereodinâmica e Modelagem Molecular, Departamento de Química, C.P. 676, São Carlos, São Paulo 13565-905, Brazil*
[b] *School of Materials Science and Engineering, Nanyang Technological University, Singapore 639798, Singapore*
[c] *Department of Chemistry, University of Malaya, 50603 Kuala Lumpur, Malaysia*

Contents

ARTICLE INFO

Article history:
Received 8 May 2009
Accepted 6 September 2009
Available online 11 September 2009

Keywords:
Tellurium(II)/(IV)
Stereochemistry
Supramolecular association
Secondary bonding

ABSTRACT

A survey of the crystallographic literature of tellurium(II)/(IV) 1,1-dithiolates (dithiocarbamate, xanthate, dithiophosphate, or dithiophosphinate) is presented. Coordination numbers range from a low of three in some organotellurium(II) 1,1-dithiolates to a high of eight in the binary tellurium(IV) dithiocarbamates. The coordination geometries are rich and varied due to the stereochemical influence exerted by up to two lone pairs of electrons and the penchant of tellurium to increase its coordination number by forming secondary Te···X interactions, where X = sulphur, halide, tellurium, oxygen, and, in one case, a π system defined by a four-membered TeS_2C chelate. Stereochemical roles of the lone pairs of electrons are always evident in the tellurium(II) structures. By contrast, a stereochemical position is not always evident for the lone pair of electrons in the tellurium(IV) derivatives, in particular in circumstances where the tellurium centre has a high coordination number. Supramolecular aggregation mediated by Te···X secondary interactions often leads to the formation of dimeric aggregates but sometimes to supramolecular polymers, and rarely three-dimensional networks. Comparisons between closely related structures

---

* Corresponding author at: Department of Chemistry, University of Malaya, 50603 Kuala Lumpur, Malaysia. Tel.: +60 3 7967 4204; fax: +60 3 7967 4193.
** Corresponding author. Tel.: +55 16 3351 8208; fax: +55 16 3351 8350.
E-mail addresses: edward.tiekink@gmail.com (E.R.T. Tiekink), julio@power.ufscar.br (J. Zukerman-Schpector).

0010-8545/$ – see front matter
doi:10.1016/j.ccr.2009.09.007

clearly indicate that the dithiocarbamate ligand is a more effective chelating ligand compared with the other 1,1-dithiolate ligands covered in this survey. This difference in coordinating ability is clearly correlated with the observation that non-dithiocarbamate structures are more likely to form high-dimensional supramolecular architectures.

1. Introduction

Metal 1,1-dithiolate compounds continue to attract significant attention owing to their many and varied applications ranging from agriculture, to medicine, and organic synthesis; see Fig. 1 for chemical structures of selected examples of 1,1-dithiolate anions relevant to the present review. In agriculture, a prominent example is the continued use of the pesticide Mancozeb®, an ethylenebis(dithiocarbamate) containing manganese and zinc [1–3]. In medicine, the aldehyde dehydrogenase inhibitor tetraethylthiuram disulfide (Disulfiram, Antabuse®), an oxidation product of the diethyldithiocarbamate anion, is still used as a treatment for chronic alcoholism and, when co-administered with metals, as an anti-cancer agent [4–6]. In addition, there is an ever increasing number of metal compounds being evaluated for biological activity with gold [7–9] and bismuth [10] dithiocarbamates, in particular, attracting attention as potential anti-tumour agents. The 1,1-dithiolate anions themselves may be used in organic synthesis [11–13]. Many of their metal compounds serve as highly efficient precursors for metal sulphide nanoparticle generation [14–18]. The 1,1-dithiolate ligands are relatively easy to prepare and once made, many of their metal complexes are stable [19]. As such, and given the practical importance of metal 1,1-dithiolates, crystallographic studies are a favoured mode of structural characterisation [20–23]. Consequently, the relative ease of crystallisation of metal dithiolate complexes has resulted in their being exploited in the rapidly emerging field of crystal engineering, i.e. in the realm of both transition metal [24–27] and main group element chemistry [28–33]. In a related theme and as an example of “data mining”, the availability of a relatively large number of structures has allowed structural correlations to be made whereby different types of intermolecular interactions are investigated in closely related structures. Specifically, the prevalence of secondary bonding interactions operating in the crystal structures of main group element compounds has been investigated [34–37]. Secondary interactions have been long recognized as important in stabilising crystal structures, see the seminal discussions of Alcock [38,39], and in their simplest form may be regarded as solid-state Lewis acid (metal centre)···Lewis base (sulphur or other donor atom) interactions. The aforementioned systematic surveys have shown that it is possible to control the formation of secondary interactions by varying the steric bulk of organic groups, either/or in a remote substituent of a ligand or directly bound to the metal centre, as in organometallic derivatives [34–37]. It is the determination of the prevalence and, when formed, the persistence of Te···S secondary interactions operating in the crystal structures of tellurium 1,1-dithiolates that is one of two major motivations for the present survey of their crystallographically determined structures.

In addition to comments on structural aspects of tellurium compounds in the aforementioned reviews focussing on 1,1-dithiolate ligands [20–23], more generally, the structural chemistry of tellurium has been reviewed periodically over the years by Abel et al. [40], Sudha and Singh [41], with the latest comprehensive survey, appearing in 1994, by Haiduc et al. [42].

The complementary focus of this survey of tellurium 1,1-dithiolate structures is a systematic investigation of the coordination environments in these molecules which may be influenced by two lone pairs of electrons in the tellurium(II) structures or one lone pair in the case of tellurium(IV) species. The pivotal role of stereochemically active lone pairs of electrons in rationalising geometries is readily appreciated by the wide applicability of the Valence Shell Electron Pair Repulsion (VSEPR) model for organic molecules [43,44]. Stereochemically active lone pairs are also well known to influence coordination geometries in main group element compounds but in certain examples containing the heavier atoms, it is well known that the lone pair can be stereochemically inert [45–47]. This comes about as often greater coordination numbers are found in compounds of the heavier elements, meaning a diminishing contribution of the s-orbital to the overall bonding. An additional consequence of crowded coordination geometries is that it can sometimes be difficult to definitely detect the influence of a putative lone pair of electrons upon the molecular structure. A useful concept relating to the detection of lone pairs in high coordinate molecules involves considering the topological distribution of donor atoms about the central atom [48]. Here, a holodirected arrangement shows the ligand donor atoms to be distributed uniformly on the surface of sphere about the central donor which contrasts a hemidirected distribution whereby an obvious gap is apparent on the sphere that is ascribed to the presence of a lone pair of electrons [48]. Systematic studies of the heavier main group element compounds examining the influence of the lone pair of electrons are probably most developed for lead(II) compounds [49–51] with less attention been directed towards antimony(III) [35,52–54] and bismuth [55,56]. The role of lone pairs of electrons obviously has attracted considerable attention in tellurium structures [20–23,40–42] with the classic example of “stereochemical inertness” for tellurium(IV) compounds found in the $[TeCl_6]^{2-}$ salts [57,58].

With varying oxidation states, chemical compositions, and the putative influence of stereochemically active lone pairs, it is no surprise that a wide variety of coordination geometries are possible in the structures described herein. Table 1 summarises the more frequently encountered coordination geometries, and their designations. Coordination geometries are analysed in terms of formal covalent bonds along with the secondary Te···X interactions, whenever present. The criterion used to determine the “significance” of a Te···X interaction is simply based on the sum of the van der Waals radii, as tabulated by Bondi [59], e.g. 2.06A for tellurium, 1.80A for sulphur, etc.

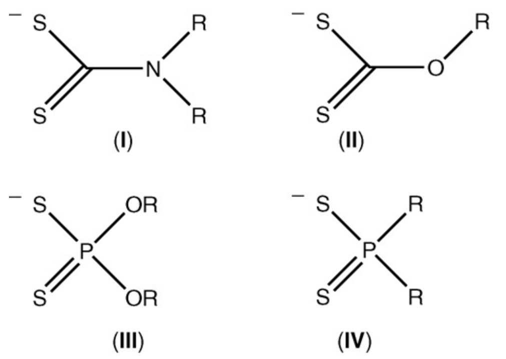

Fig. 1. (**I**) Chemical structures for the (**I**) *N*,*N*′-dialkyl(aryl)dithiocarbamate anion; (**II**) *O*-alkly(aryl)dithiocarbonate (xanthate) anion; (**III**) *O*,*O*′-dialkyl(aryl)dithiophosphate anion; (**IV**) dialkyl(aryl)dithiophosphinate anion.

Table 1
Coordination geometries encountered in tellurium 1,1-dithiolate structures, and their abbreviations.

Description	Donor atoms	Lone pairs	Symbol
Distorted pseudo-tetrahedral	2	2	d ψ-t
Pseudo-trigonal bipyramid	3	2	ψ-$t_r$bp
Pseudo-trapezoidal bipyramid	4	2	ψ-tbp
Trapezoidal bipyramid	6	0	tbp
Distorted trapezoidal bipyramid	6	0	d tbp
Distorted pseudo-trapezoidal bipyramid	4	2	d ψ-tbp
Capped pseudo-trapezoidal bipyramid[a]	5	2	c ψ-tbp
	6	1	
Pseudo-pentagonal bipyramid[a]	5	2	ψ-pbp
	6	1	ψ-pbp
Distorted pseudo-pentagonal bipyramid[a]	5	2	d ψ-pbp
	6	1	
Highly distorted pseudo-pentagonal bipyramid[a]	5	2	hd ψ-pbp
Pentagonal bipyramid	7	0	pbp
Distorted pentagonal bipyramid	7	0	d pbp
Axially distorted pentagonal bipyramid	7	0	ad pbp
Bicapped pseudo-trapezoidal bipyramid	6	2	bc ψ-tbp
Capped pseudo-pentagonal bipyramid	7	1	c ψ-pbp
Capped pentagonal bipyramid	8	0	c pbp
Capped distorted pentagonal bipyramid	8	0	c d pbp

[a] The three coordination geometries are distinguished in the following manner: if one of the atoms deviates by less than 10° from the plane formed by the other four donor atoms, then it is considered ψ-pbp, if the deviation is between 10° and 20°, the coordination geometry then is considered d ψ-pbp, if the deviation is greater than 20°, it is considered hd ψ-pbp.

In this survey, the structural chemistry of the tellurium(II) 1,1-dithiolates are described first followed by those of tellurium(IV). Within each division, binary compounds are discussed first, followed by ternary derivatives, usually containing one or more halide (pseudo-halide) donors. Finally, organotellurium compounds are described in order of increasing number of tellurium-bound organic substituents. All structural data were extracted from the Cambridge Crystallographic Data Centre [60]. Particularly relevant to the present survey are the 1,1-dithiolate ligands shown in Fig. 1, namely (**I**) N,N′-dialkyl(aryl)dithiocarbamate; (**II**) O-alklyl(aryl)dithiocarbonate (xanthate); (**III**) O,O′-dialkyl(aryl)dithiophosphate; and (**IV**) dialkyl(aryl)dithiophosphinate, as all of these form compounds with tellurium(II)/(IV) that have been crystallographically determined. Within each of the specified categories, the structures are described in order of those containing (**I**), the most numerous, (**II**), (**III**) and finally, (**IV**), the least represented. When applicable, mixed 1,1-dithiolate ligand structures are discussed at the conclusion of each category. All crystallographic illustrations are original and were drawn with the aid of DIAMOND programme [61] using arbitrary spheres; hydrogen atoms are not illustrated to aid clarity.

2. Tellurium(II) compounds

Tellurium(II) 1,1-dithiolates are less numerous that their tellurium(IV) counterparts but, arguably display a greater diversity of coordination geometries and more varied supramolecular association patterns. An obvious explanation for the greater disparity in their coordination environments is explained in terms of the presence of two lone pairs of electrons around the tellurium(II) centre rather than one pair as for the tellurium(IV) structures.

2.1. Binary tellurium(II) 1,1-dithiolates

Key structural features for the binary tellurium 1,1-dithiolate compounds (**1**)–(**21**) [48–65] are collected in Table 2; see Supplementary Table S1 for a compilation of selected geometric parameters.

In the structures of the known binary dithiocarbamates, the immediate geometry about the tellurium(II) centre is defined by two asymmetrically coordinating ligands: the Te–S bond distances fall into two well-separated ranges, i.e. Te–S_{short} of 2.50–2.56 Å and Te–S_{long} of 2.79–2.90 Å. The angles subtended at the central tellurium atom by the more tightly held sulphur atoms of approximately 80° are significantly narrower than 145°, defined by the two more loosely attached sulphur atoms. As the longer distances lie to one side of the essentially planar TeS_4 arrangement, the coordination geometry may to a first approximation be described as planar trapezoidal (pt). When the lone pairs above and below the TeS_4 plane are considered, the geometry is best described as pseudo-trapezoidal bipyramidal (ψ-tbp), with the lone pairs orientated over the weaker Te–S_{long} bonds. It turns out that this isolated ψ-tbp geometry occurs in only one example, namely for $Te[S_2CNCy_2]_2$ (**8**) [69], illustrated in Fig. 2a, as the other examples form secondary interactions to increase the coordination around the tellurium atom.

Most of the binary tellurium(II) dithiocarbamates, i.e. six out of the eight available structures, adopt a dimeric motif in their solid-state structures, as illustrated for $Te[S_2CN(i\text{-}Pr)_2]_2$ (**7**) [68] in Fig. 2b. Dimers are held together by a pair of secondary Te···S contacts, 3.50–3.68 Å, which occur between centrosymmetrically related molecules. The close approach of a neighbouring sulphur atom increases the coordination number and leads to an essentially planar TeS_5 arrangement. When included in the coordination sphere, the coordination geometry is based on a pentagonal bipyramid, with the lone pairs of electrons normal to, and above and below the TeS_5 pentagonal plane, and is designated ψ-pbp (Table 1). Variations in the assigned coordination geometry for these systems relate to the relative disposition of the molecules comprising the dimer. Whereas in Fig. 2b, the two molecules lie in the same plane, as also occurs in (**3**) [64] and (**7**) [68], in the crystal structures of (**4**)–(**6**) [65–67], this is not so as seen from Fig. 2c for $Te[S_2CN(CH_2)_5]_2$ (**5**) [66]. Accordingly, the coordination geometry found in (**4**)–(**6**) is defined as highly distorted pseudo-pentagonal bipyramid (hd ψ-pbp); see footnote to Table 1 for quantification of “degrees of distortion”. The remaining binary dithiocarbamate structure, $Te[S_2CN(CH_2CH_2OH)_2]_2$ (**3**) [64], while having similar coordination geometry to the majority of structures in this category, i.e. d ψ-pbp, associates into a supramolecular chain generated by a crystallographic 2_1 screw axis, Fig. 2d. When viewed down the 2_1 axis, Fig. 2e, the polymeric chain has the appearance of the dimeric motif, Fig. 2b, but this is deceptive as successive molecules in the chain are, from symmetry, approximately orthogonal.

While the lack of association in the structure of (**8**) [69] is correlated with the steric bulk of the nitrogen-bound cyclohexyl groups which preclude the close approach of neighbouring sulphur atoms, as discussed for related 1,1-dithiolate systems [34–37], the reason for the adoption of the observed motif for (**3**) [64] is not readily apparent. The n-propyl derivative (**6**) [67], also with three non-hydrogen atoms in each nitrogen-bound substituent, adopts the common dimeric motif. While it might be supposed that the presence of hydrogen-bonding functionality in the terminal CH_2CH_2OH groups is responsible for the different supramolecular motif, subsequent structures to be described herein do not reveal a similar influence.

In the binary tellurium(II) xanthates, monomeric structures and geometric features akin to that illustrated in Fig. 2a are found for (**13**) [74] and (**16**) [69], an observation correlated with the steric bulk of the R groups [34–37], and dimeric motifs similar to that seen in Fig. 2b are adopted by (**9**) [70] as well as for each of polymorphic (**10**) [71] and (**11**) [72]. The three remaining structures adopt chain motifs, with that found for (**12**) [73] resembling

Table 2
Key structural data for binary(II) 1,1-dithiolate structures.

No.	Compound	Motif	CN geometry[a]	Ref.	No.	Compound	Motif	CN geometry[a]	Ref.
Dithiocarbamate					Xanthate				
(**1**)	$Te(S_2CNEt_2)_2$	Dimer (0-D)	ψ-pbp	[62]	(**9**)	$Te(S_2COMe)_2$	Dimer (0-D)	d ψ-pbp	[70]
(**2**)	$Te[S_2CN(CH_2)_4]_2$[b]	Dimer (0-D)	hd ψ-pbp	[63]	(**10**)	$Te(S_2COEt)_2$[e]	Dimer (0-D)	ψ-pbp	[71]
(**3**)	$Te[S_2CN(CH_2CH_2OH)_2]_2$	1-D	d ψ-pbp	[64]	(**11**)	$Te(S_2COEt)_2$[f,g]	Dimer (0-D)	ψ-pbp	[72]
(**4**)	$Te[S_2CN(CH_2CH_2)_2O]_2$[c]	Dimer (0-D)	hd ψ-pbp	[65]	(**12**)	$Te[S_2CO(n\text{-}Pr)_2]_2$	1-D	d ψ-pbp	[73]
(**5**)	$Te[S_2CN(CH_2)_5]_2$[d]	Dimer (0-D)	hd ψ-pbp	[66]	(**13**)	$Te[S_2CO(i\text{-}Pr)_2]_2$[g]	1-D	ψ-tbp	[74]
(**6**)	$Te[S_2CN(n\text{-}Pr)_2]_2$	Dimer (0-D)	hd ψ-pbp	[67]	(**14**)	$Te[S_2CO(i\text{-}Bu)]_2$	1-D	d ψ-pbp	[69]
(**7**)	$Te[S_2CN(i\text{-}Pr)_2]_2$	Dimer (0-D)	ψ-pbp	[68]	(**15**)	$Te(S_2COCH_2CH_2CMe_3)_2$	1-D	bc ψ-tbp	[73]
(**8**)	$Te(S_2CNCy_2)_2$	0-D	ψ-tbp	[69]	(**16**)	$Te(S_2COCH_2Ph)_2$	0-D	ψ-tbp	[69]
Dithiophosphate					Dithiophosphinate				
(**17**)	$Te[S_2P(OMe)_2]_2$[h]	2-D	ψ-tbp	[75]	(**19**)	$Te(S_2PPh_2)_2$[g]	1-D	ψ-tbp	[77]
(**18**)	$Te[S_2P(OEt)_2]_2$[i]	3-D	ψ-tbp	[76]	(**20**)	$Te(S_2PPh_2)_2$[g,j]	1-D	ψ-tbp	[78]
Mixed dithiocarbamate/xanthate									
(**21**)	$Te(S_2CNEt_2)(S_2COEt)$	Dimer (0-D)	ψ-tbp	[79]					

[a] See Table 1 for the abbreviations of the coordination geometries.
[b] The ligand is tetramethylenedithiocarbamate.
[c] The ligand is morpholinedithiocarbamate.
[d] The ligand is pentamethylenedithiocarbamate.
[e] Monoclinic form.
[f] Triclinic form.
[g] Two independent molecules in the asymmetric unit with the same CN geometry.
[h] The molecule has 2-fold symmetry.
[i] Three independent molecules with the same CN geometry.
[j] Benzene solvate.

dithiocarbamate (**3**) [64], Fig. 2d and e. The supramolecular chain found in (**15**) [73] is a variation of dithiocarbamate (**3**) [64] and xanthate (**12**) [73] in that that there are two secondary Te···S interactions linking molecules, rather than one, Fig. 3a and b. A variation on the former occurs in (**14**) [69], Fig. 3c, whereby successive molecules are inclined by approximately 30° as emphasised in the view down the polymer backbone, Fig. 3d. In terms of coordination geometries, the xanthate structures resemble their dithiocarbamate analogues, with the exception of (**15**) [73] which features a bicapped ψ-tbp arrangement whereby the intermolecularly associated sulphur atoms occupy capping positions. However, in (**15**) [73], each of the Te···S interactions are weaker and at the limits of the van der Waals radii compared with those observed in the other binary xanthate structures, Table S1, again correlated with the relative large size of the R substituents on the xanthate ligand [34–37].

There are two examples each of binary tellurium(II) dithiophosphates, i.e. (**17**) [75] and (**18**) [76], and dithiophosphinates (**19**) [77] and (**20**) [78]: all four structures display significant supramolecular association in the solid-state owing to the propensity of these 1,1-dithiolate ligands to bridge tellurium centres rather than chelate a single atom. The immediate coordination geometry in $Te[S_2P(OMe)_2]_2$ (**17**) [75] is bent as both dithiophosphate ligands are monodentate, Fig. 4a. However, each non-coordinating sulphur atoms forms a bridge to a neighbouring tellurium centre so as to form a two-dimensional grid comprising 16-membered [···S–P–S–Te]$_4$ rings. A more complicated situation is found in the ethyl derivative, $Te[S_2P(OEt)_2]_2$ (**18**) [76], where three independent molecules comprise the crystallographic asymmetric unit. In this structure, a similar bridging coordination mode as just described for $Te[S_2P(OMe)_2]_2$ is found for three of the six dithiophosphate ligands. Two ligands are strictly monodentate and for the sixth independent ligand, one of the non-coordinating sulphur atoms bridges two tellurium atoms (Table S1). A layer arrangement, as illustrated in Fig. 4b is found but additional Te···S interactions connect the layers into a three-dimensional array, Fig. 4c. The coordination geometries for the tellurium atoms in the aforementioned structures is ψ-tbp, with the lone pairs of electrons projected to lie over the weaker Te···S interactions, Table 2. In summary, two- and three-dimensional supramolecular aggregation patterns are evident in (**17**) [75] and (**18**) [76] despite the fact that the only chemical difference between the structures is found in the nature of the oxygen-bound R groups, i.e. R = Me (**17**) and R = Et (**18**). Such structural variations have precedents in the literature [34–37].

The supramolecular chains found in each of $Te(S_2PPh_2)_2$ (**19**) [77] and its 1:1 benzene solvate (**20**) [78] are quite distinct owing to the prevalence of Te···S secondary interactions in (**19**) [77] and Te···Te interactions in (**20**) [78]. In these structures, ditellurium entities (see Table S1 for Te–Te bond distances) are linked by two bidentate but asymmetrically coordinating dithiophosphinate ligands with the coordination environment about each tellurium atom in (**19**) [77] completed by an intermolecular Te···S interaction, resulting in a ψ-tbp geometry. The supramolecular chain thus formed in (**19**) results from Te···S interactions derived from both dithiophosphinate ligands, Fig. 5a, see Fig. 5b for an end-on view. By contrast, in (**20**) [78], the intermolecular interactions are of the type Te···Te (3.67 Å), see Fig. 5c. The supramolecular chain formed in (**20**) is reinforced by Te···S contacts of 3.79 and 3.88 Å, i.e. at the margin of significance. The different modes of association between the molecules in (**19**) [77] and (**20**) [78] results in significant kinking in the chain formed in (**20**), Fig. 5d.

The structure of (**20**) [78] is the first example encountered herein of a supramolecular structure stabilised by Te···Te interactions. While not nearly as frequent as Te···S secondary interactions, these are, Te–Te contacts feature in several more structures to be described herein. According to the van der Waals criterion, Te···Te separations less than 2 × 2.06 Å need to be considered as being significant [59]. However, often Te···Te contacts less than 4.12 Å appear to occur as a consequence of one or more prominent Te···S secondary interactions. The literature contains relatively few reports of Te···Te interactions [80,81]. Separations of approximately 2.75 Å indicate a Te–Te single bond while separations less than 3.7 Å probably represent "significant" Te···Te secondary interactions. The nature of this type of interaction have been investigated theoretically and dispersion forces appear to dominate [82,83].

The structures of (**19**) [77] and (**20**) [78] can be regarded as supramolecular isomers [84] in that different modes of associa-

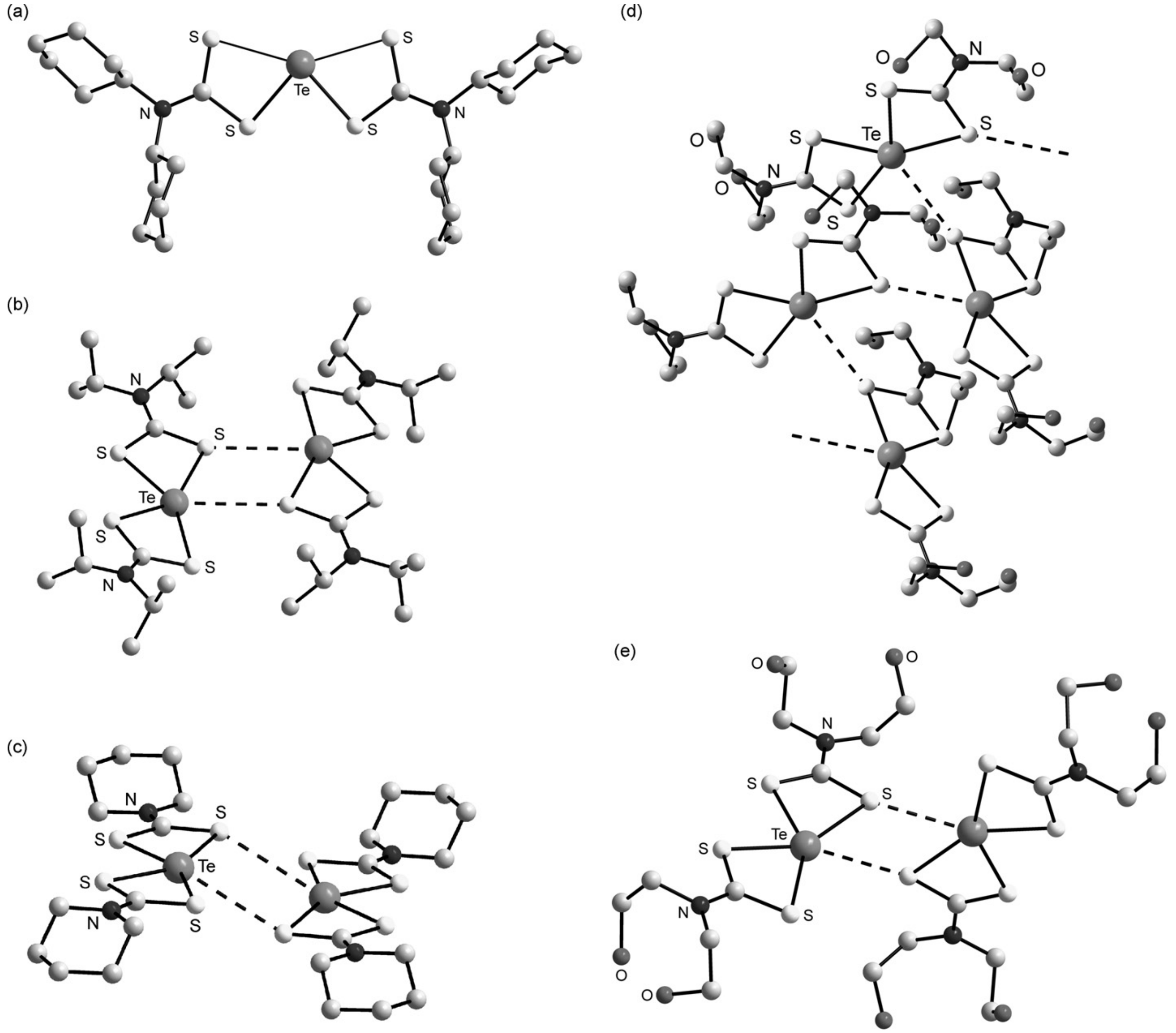

Fig. 2. (a) Molecular structure of monomeric Te[S_2CNCy_2]$_2$ (**8**) [69]; (b) supramolecular dimer mediated by two Te···S contacts in the crystal structure of Te[$S_2CN(i\text{-}Pr)_2$]$_2$ (**7**) [68]; (c) supramolecular dimer for Te[$S_2CN(CH_2)_5$]$_2$ (**5**) [66] viewed side-on showing the off-set disposition of the interacting molecules; (d) supramolecular aggregation mediated by Te···S contacts leading to a chain in the crystal structure of Te[$S_2CN(CH_2CH_2OH)_2$]$_2$ (**3**) [64] and (e) projection down the axis of the supramolecular polymer shown in (d) which deceptively resembles the dimeric aggregate observed in (b) but, in fact represents molecules arranged orthogonally along the axis.

tion are found in the supramolecular aggregation patterns for the same chemical compositions; the benzene molecules in (**20**) do not directly participate in the formation of the supramolecular chains. The important conclusion made from the observed structures of (**19**) [77] and (**20**) [78] is that Te···S contacts may be subsumed by Te···Te contacts and vice versa in that the supramolecular chain can be sustained by either type of supramolecular synthon, and therefore, provide similar energies of stabilisation to their respective crystal structures.

The final structure to be described in this category is that of the mixed dithiocarbamate species, Te(S_2CNEt_2)(S_2COEt) (**21**) [79]. The molecular structure resembles those of the Te(S_2CNEt_2)$_2$ (**1**) [62] and polymorphic Te(S_2COEt)$_2$ (**10** [71] and **11** [72]) compounds in terms of coordination geometry but adopts a distinct pattern of supramolecular association, Fig. 6, i.e. a chain most closely resembling that formed in the structure of Te[$S_2CN(CH_2CH_2OH)_2$]$_2$ (**3**) [64], Fig. 2d. It is salutary to compare the geometric parameters for (**21**) [79] with those of (**1**) [62] and (**10** [71] and **11** [72]), Table S1. The Te–S bond distances formed by the dithiocarbamate ligand contract in the mixed ligand compound and the Te–S_{short} distance formed by the xanthate ligand are elongated. It is also noteworthy that it is a dithiocarbamate-sulphur atom that forms the intermolecular Te···S interaction. These results point to the greater coordination potential of the dithiocarbamate ligand compared with the xanthate ligand.

2.2. Mixed ligand tellurium(II) 1,1-dithiolates

Structure information for the mixed ligand tellurium(II) 1,1-dithiolates described herein are collated in Table 3. The first two structures to be described in this category are adducts, namely {[Te(S_2CNEt_2)$_2$]$_2$(4,4′-bipyridine)} (**22**) [85] and

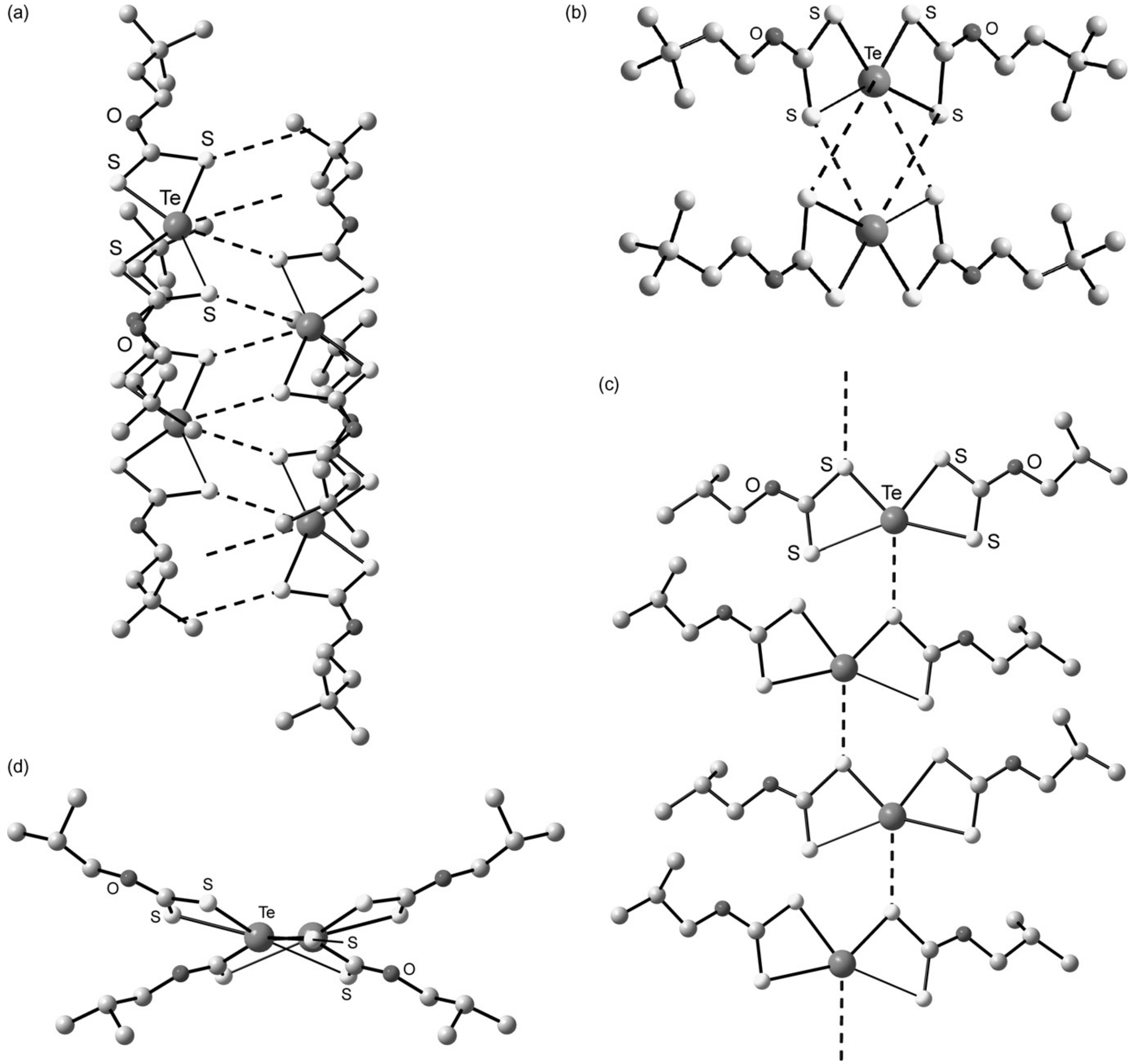

Fig. 3. (a) Supramolecular chains in binary tellurium(II) xanthates mediated by Te···S contacts: (a) in Te($S_2COCH_2CH_2CMe_3$)$_2$ (**15**) [73] in which molecules are connected on average by two Te···S interactions; (b) end-on view of the chain in (a); (c) somewhat flattened supramolecular chain in Te[S_2CO(i-Bu)]$_2$ (**14**) [69]; and (d) end-on view of the chain in (c) showing the inclination of successive molecules.

{Te(S_2COEt_2)$_2$(4,4′-bipyridine)} (**23**) [86], with the former shown in Fig. 7. Comparing the geometric parameters in these structures, Table S2, with those observed in the respective parent compounds, i.e. (**1**) [62] and (**10** [71] and **11** [72]), shows a general elongation of the Te–S_{short} bond distances in the 4,4′-bipyridine adducts accompanied by a reduction in the Te–S_{long} bond distances. The $TeNS_4$ coordination environments in (**22**) [85] and (**23**) [86] resemble the ψ-pbp TeS_5 geometries observed in the parent compounds in which

Table 3
Key structural data for neutral mixed ligand tellurium(II) 1,1-dithiolate structures.

No.	Compound	Motif	CN geometry[a]	Ref.	No.	Compound	Motif	CN geometry[a]	Ref.
Simple adducts					Te(1,1-dithiolate)X				
(**22**)	{[Te(S_2CNEt_2)$_2$]$_2$ (4,4′-bipyridine)}	Dimer (0-D)	ψ-pbp	[85]	(**24**)	{Te(S_2CNEt_2)Cl}$_n$	1-D	ψ-pbp	[87]
(**23**)	{Te(S_2COEt_2)$_2$ (4,4′-bipyridine)}	Dimer (0-D)	ψ-pbp	[86]	(**25**)	{Te(S_2CNEt_2)Br}$_n$	1-D	ψ-pbp	[87]
					(**26**)	{Te(S_2CNEt_2)I}$_n$	1-D	ψ-pbp	[88]
					(**27**)	{Te(S_2COEt)Br}$_n$	1-D	ψ-pbp	[89]
Adduct									
(**28**)	{[Te(S_2CNEt_2)$_2$] [Te(S_2CNEt_2)SCN]}	Dimer (0-D)	ψ-pbp	[90]					

[a] See Table 1 for the abbreviations of the coordination geometries.

the pyridine–nitrogen atom simply substitutes for the intramolecularly coordinated sulphur atom.

There are four structures available, (**24**)–(**27**) [87–89], where the substitution of a 1,1-dithiolate by a halide has been accomplished, i.e. structures of general formula Te(1,1-dithiolate)X. Selected geometric parameters are collected in Table S2 and a representative structure, namely $\{Te(S_2CNEt_2)I\}_n$ (**26**) [88], is shown in Fig. 8. In each structure, the halide atoms bridge tellurium centres forming asymmetric Te–X distances, and the resulting polymeric chains each have a helical topology. For the homologous series of structures $\{Te(S_2CNEt_2)X\}_n$, there is the expected elongation of the Te–X distances, for X = Cl, Br and I. The degree of asymmetry in the bridging Te–X distances decreases in the same order, i.e. 0.42, 0.30 and 0.17 Å. A search of the Cambridge Structure Database [60] was conducted for structures containing Te–X bonds for X = Cl, Br and I, and the average Te–X distances, $Te–X_{intra}$, calculated. These distances were compared with average intermolecular Te···X separations less than the sum of the respective van der Waals radii, $Te\cdots X_{inter}$. The differences computed for $[Te–X_{intra} – Te\cdots X_{inter}]$ calculated to 1.01, 0.95 and 0.82 Å for X = Cl, Br and I, respectively, in line with the observations for (**24**)–(**26**) [87–89], Table S2. This trend is consistent with the decreasing electronegativity differences between tellurium and the respective halide. The coordination geometries in (**24**)–(**27**) conform to ψ-pbp.

The final structure included in this category is an adduct formed between $Te(S_2CNEt_2)_2$ and $Te(S_2CNEt_2)SCN$, i.e. $\{[Te(S_2CNEt_2)_2][Te(S_2CNEt_2)SCN]\}$ (**28**) [90], Fig. 9 and Table S2. The dimeric aggregate is sustained by Te···Te (3.22 Å) and Te···S interactions (Table S2). The Te–S bond distances within the $Te(S_2CNEt_2)_2$ component of (**28**) [90] are close to those found in the parent compound (**1**), Table S1. The coordination geometry for this atom is ψ-pbp based on the assumption that one lone pair of electrons resides in the pentagonal plane. One of the apical positions is occupied by the loosely associated tellurium atom with the second lone pair of electrons being trans to this. The tellurium coordination geometry in $Te(S_2CNEt_2)SCN$ is distorted pentagonal

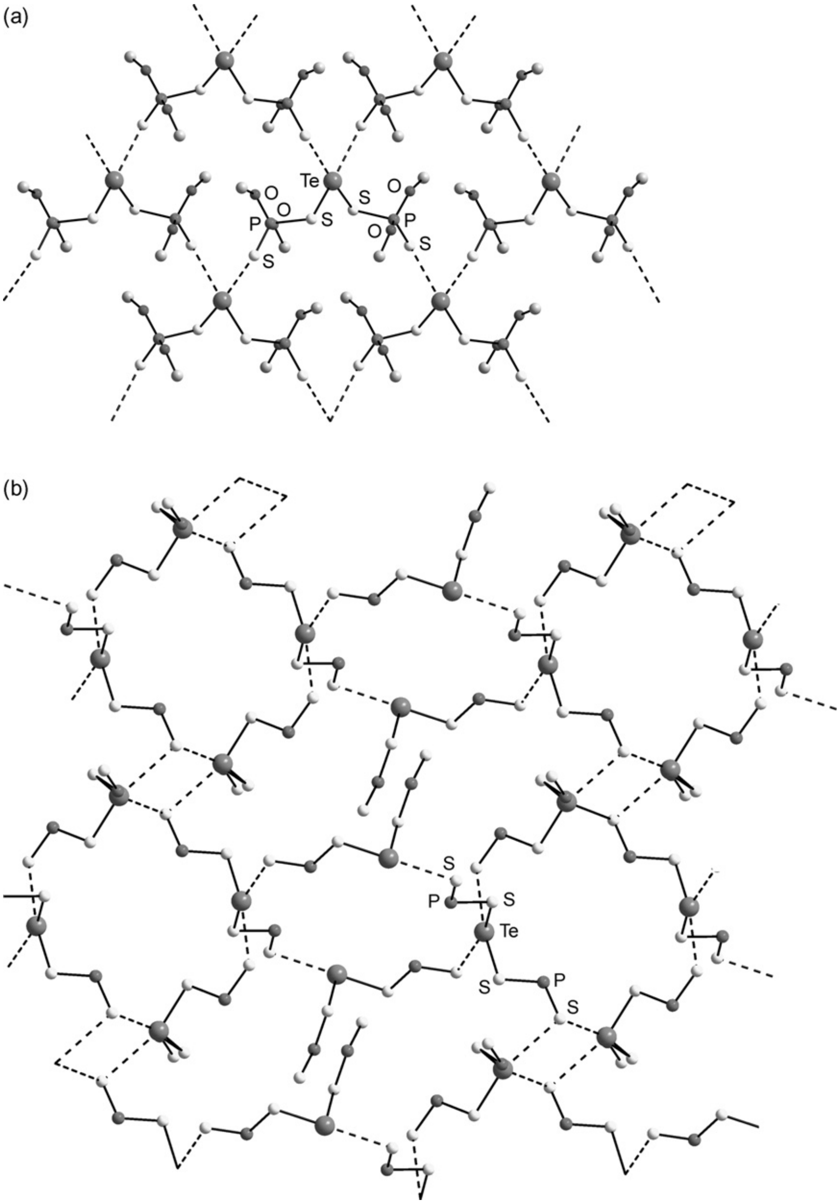

Fig. 4. (a) Supramolecular association in binary tellurium(II) dithiophosphates mediated by Te···S contacts: (a) in $Te[S_2P(OMe)_2]_2$ (**17**) [75] in which 16-membered $[\cdots S–P–S–Te]_4$ rings are connected into a two-dimensional array; (b) two-dimensional array in $Te[S_2P(OEt)_2]_2$ (**18**) [76]; and (c) connections between layers shown in (b) to form a three-dimensional network with the layer shown in (b) highlighted. In (a) and (b) the alkoxyl groups have been removed for reasons of clarity.

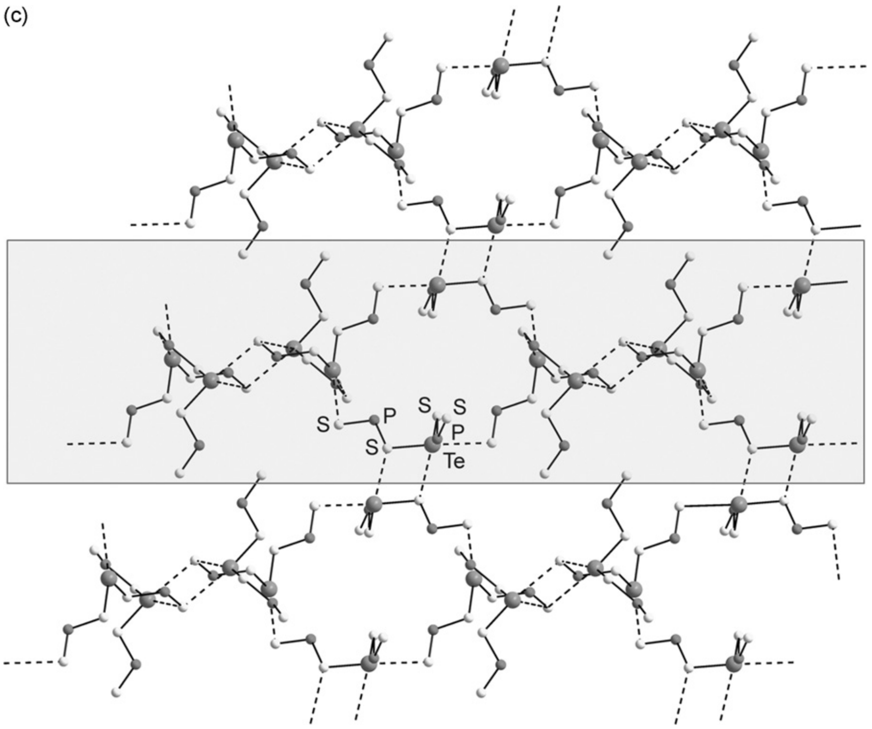

Fig. 4. (*Continued*).

bipyramidal (d ψpbp) based on an approximately planar S_4Te donor set, with the lone pairs of electrons above and below the pentagonal plane.

2.3. Ionic tellurium(II) 1,1-dithiolates

There is a series (**29**)–(**35**) [91–94] of charged species involving tellurium(II) centres: these are described below and summarised in Table 4; selected geometric parameters for these are collected in Table S3.

A regular planar TeS_5 pentagon is found for the anion in $[NEt_4][Te(S_2COEt)_3]$ (**29**) [91] defined by two asymmetrically chelating xanthate ligands and a monodentate ligand. The anion has a ψ-pbp coordination environment with the lone pairs above and below the TeS_5 plane, and is illustrated in Fig. 10.

Binary species comprising dimeric and trimeric aggregates are found in the structures of (a) dimeric $\{[Te(S_2CNEt_2)_2][Te(S_2CNEt_2)_3]\}[ClO_4]$ (**30**) [92] and (b) trimeric $\{[Te(S_2CNEt_2)_2][Te(S_2CNEt_2)_3]_2\}[PF_6]_2$ (**31**) [92]. In (**30**), the $Te(S_2CNEt_2)_2$ molecule has an immediate environment and comparable Te–S bond distances as found for the parent $Te(S_2CNEt_2)_2$ compound (**1**) [62], Table S1. The tellurium(IV) centre in the $[Te(S_2CNEt_2)_3]^+$ cation is coordinated by six sulphur atoms that define a distorted pentagonal pyramid. There is one Te···S interaction linking these species and the connection between them is reinforced by a significant Te···Te contact of 3.35 Å, Fig. 11a. Taking into consideration these additional interactions, the tellurium(II) centre has a coordination environment, ψ-pbp, whereby one lone pair of electrons occupies a position in the pentagonal plane and the other a position opposite the Te···Te interaction. The tellurium(IV) centre is in a capped distorted pentagonal bipyramidal geometry (c d pbp) with the capping position occupied by the sulphur derived from the tellurium(II) moiety. From the foregoing, it is concluded that the lone pair of electrons on the tellurium(IV) centre in (**30**) [92] does not occupy a well defined position. The trimeric species (**31**) [92] has crystallographically imposed 2-fold symmetry in which a $Te(S_2CNEt_2)_2$ molecule is sandwiched between two $[Te(S_2CNEt_2)_3]^+$ cations. As for (**30**) [92], the $Te(S_2CNEt_2)_2$ molecule in (**31**) [92] is essentially as for (**1**) [62]. In the same way, the immediate geometries for the $[Te(S_2CNEt_2)_3]^+$ cations are very similar in (**30**) and (**31**). There is a single Te···S secondary interaction between the neutral and charged species, and this is reinforced by a Te···Te contact of 3.39 Å, Fig. 11b. With these additional interactions, the coordina-

Table 4
Key structural data for ionic tellurium(II) 1,1-dithiolate structures.

No.	Compound	Motif	CN geometry[a]	Ref.	No.	Compound	Motif	CN geometry[a]	Ref.
Binary anions					Mixed ligand salts				
(**29**)	$[Te(S_2COEt)_3]^{-b}$	0-D	ψ-pbp	[91]	(**32**)	$[Te(S_2CNEt_2)Br_2]^{-d}$	0-D	ψ-tbp	[93]
(**30**)	$\{[Te(S_2CNEt_2)_2][Te(S_2CNEt_2)_3]\}[ClO_4]$			[92]	(**33**)	$[Te(S_2CNEt_2)I_2]^{-b}$	0-D	ψ-tbp	[93]
	$[Te(S_2CNEt_2)_2]$	Dimer (0-D)	ψ-pbp		(**34**)	$[Te(S_2CNEt_2)I_2]^{-d}$	0-D	ψ-tbp	[93]
	$[Te(S_2CNEt_2)_3]^+$		c d pbp		(**35**)	$\{Te[S_2CN(i\text{-}Pr)_2]_2I\}[I]\{Te[S_2CN(i\text{-}Pr_2)_2]I\}$			[94]
(**31**)	$\{[Te(S_2CNEt_2)_2][Te(S_2CNEt_2)_3]_2\}[PF_6]_2{}^c$			[92]		$\{Te[S_2CN(i\text{-}Pr_2)_2]I\}$	1-D	ψ-tbp	
	$[Te(S_2CNEt_2)_2]$	Trimer (0-D)	ψ-pbp			$\{Te[S_2CN(i\text{-}Pr)_2]_2I\}^+$	Dimer (0-D)	ψ-pbp	
	$[Te(S_2CNEt_2)_3]^+$	Dimer (0-D)	c d pbp						

[a] See Table 1 for the abbreviations of the coordination geometries.
[b] The cation is tetraethylammonium.
[c] This trimeric structure has crystallographic 2-fold symmetry.
[d] The cation is 1,10-phenanthrolinium.

tion geometry for the central $Te(S_2CNEt_2)_2$ molecule is ψ-pbp with the Te–Te interactions above and below the trapezoidal plane. In this description, the lone pairs of electrons occupy the relatively large void bordered by the Te–Te interactions and weaker Te–S bonds. The coordination geometry for the tellurium(IV) centre in (**31**) [92] is c d pbp with the capping position occupied by the by the sulphur derived from the tellurium(II) moiety as described for (**30**) [92].

The next three structures have the general formula $[M][Te(S_2CNEt_2)X_2]$, (**32**)–(**34**) [93], with a representative example, i.e. [1,10-Phenanthrolinium]$[Te(S_2CNEt_2)Br_2]$ (**32**) shown in Fig. 12; the structures of (**33**) and (**34**) closely resemble (**32**) [93]. The anion is four-coordinate, distorted trapezoidal, defined by a chelating dithiocarbamate ligand and two halides, with the lone pairs lying over the Te–X bonds. In each of the structures, the shorter Te–S bond distance is opposite the longer Te–X bond, Table S3. In terms of supramolecular interactions involving the tellurium(II) centre, the anions may be considered as isolated, there being no Te$\cdots$X interactions of note.

The next structure to be described, $\{Te[S_2CN(i\text{-}Pr)_2]_2I\}[I]\{Te[S_2CN(i\text{-}Pr_2)_2]I\}$ (**35**) [94], involves the interaction between a neutral $Te[S_2CN(i\text{-}Pr_2)_2]I$ molecule, a cationic tellurium(IV) species $\{Te[S_2CN(i\text{-}Pr)_2]_2I\}^+$ and iodide, Fig. 13. The $Te[S_2CN(i\text{-}Pr_2)_2]I$ molecule forms a relatively longer bond with iodide, i.e. 3.34 Å, which if included in the immediate environment gives an TeS_2I_2 arrangement closely resembling the structures of (**32**)–(**34**) [93]. However, there is a close Te$\cdots$Te contact of 3.54 Å to consider, giving rise to a ψ-pbp geometry akin to that seen for the tellurium(II) centre in (**30**) [92]. The iodide also forms a contact with the $\{Te[S_2CN(i\text{-}Pr)_2]_2I\}^+$ cation at 3.37 Å, and therefore, structure (**35**) [94] is best represented with the iodide as loosely bridging the tellurium-containing species. The immediate geometry about the $\{Te[S_2CN(i\text{-}Pr)_2]_2I\}^+$ cation is defined by two symmetrically chelating dithiocarbamate ligands and an iodide. When the aforementioned Te$\cdots$I interaction along with the Te$\cdots$Te contact are taken into account, the geometry is described as pbp, with the lone pair being stereochemically inert.

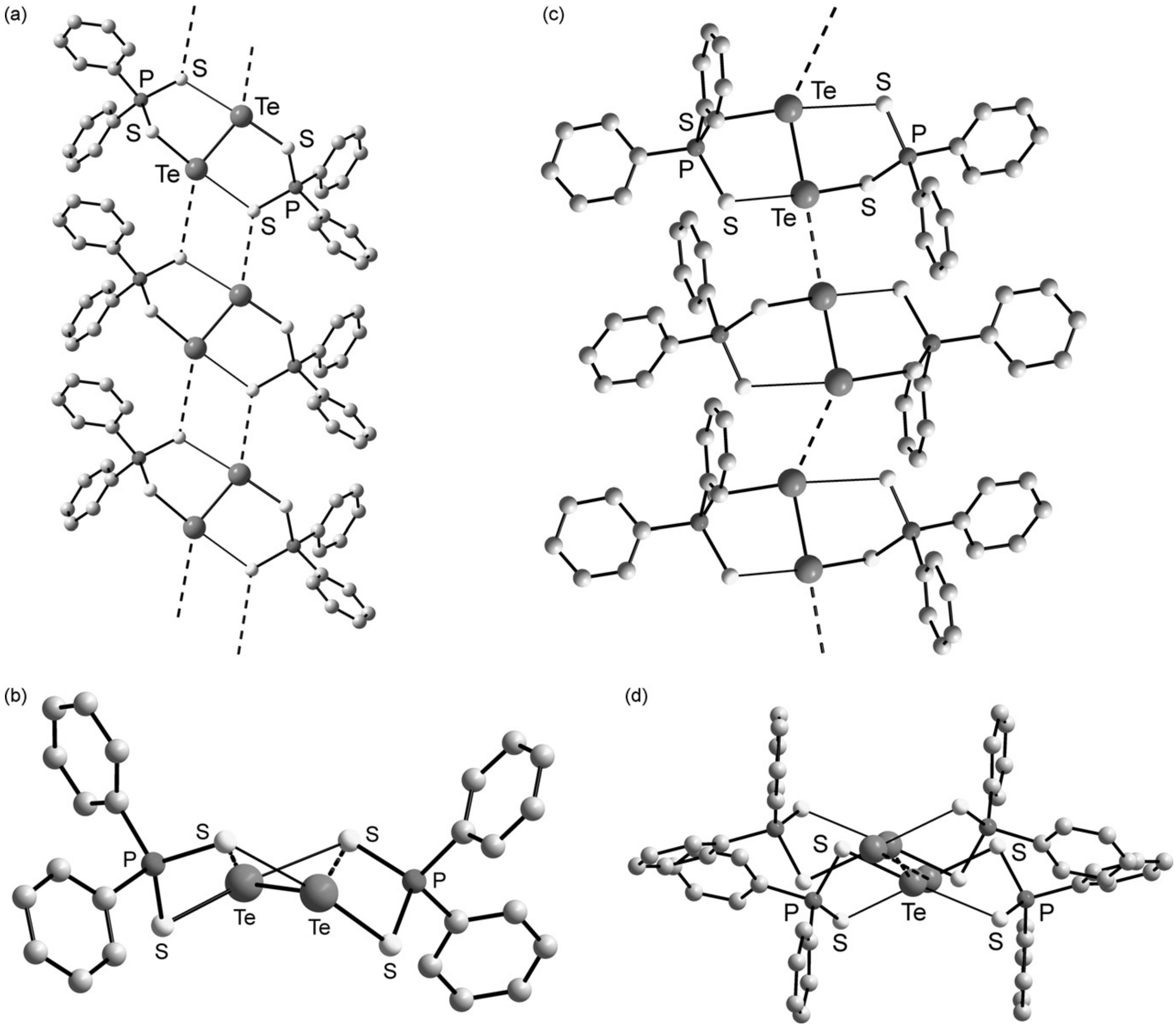

Fig. 5. (a) Supramolecular chains in binary tellurium(II) dithiophosphinates mediated by Te$\cdots$S contacts: (a) in $Te(S_2PPh_2)_2$ (**19**) [77]; (b) end-on view of the chain in (a) showing the inclination of successive molecules; (c) in $Te(S_2PPh_2)_2$, characterised as a benzene solvate (**20**) [78], showing connections between successive molecules mediated by one dithiophosphinate ligand only; and (d) end-on view of the chain in (c).

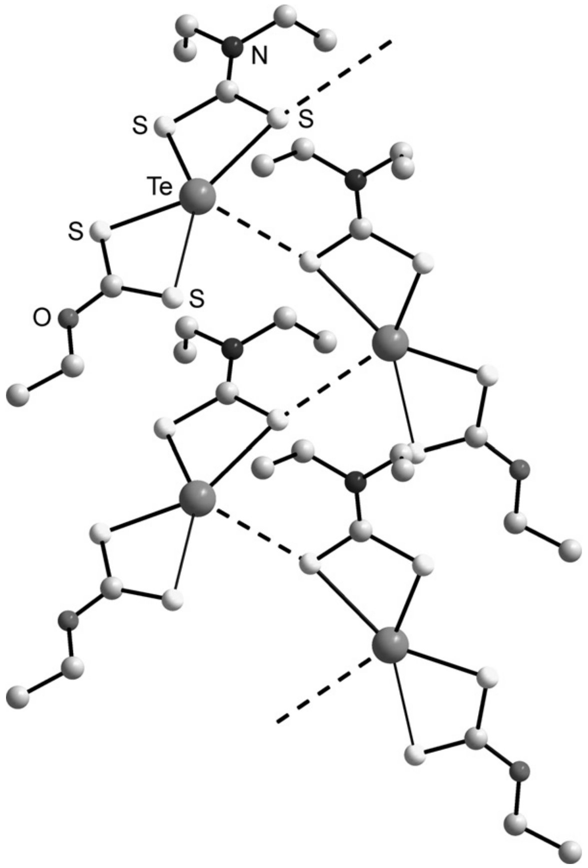

Fig. 6. Supramolecular chain mediated by Te···S contacts involving the dithiocarbamate ligand in the crystal structure of Te(S_2CNEt_2)(S_2COEt) (**21**) [79]. An analysis of geometric parameters shows the dithiocarbamate ligand to be a more effective ligand than the xanthate in this compound.

2.4. Organotellurium(II) 1,1-dithiolates

There is a fair representation of different supramolecular motifs ranging from monomeric, to a chain and up to a 2-D array, amongst the 19 organotellurium(II) 1,1-dithiolates, (**36**)–(**54**) [63,95–106], available for review. Key structural descriptors are collected in Table 5 and selected geometric parameters for these structures are presented in Table S4.

Each of the four neutral organotellurium dithiocarbamates, (**36**)–(**39**) [95–98], features a nitrogen donor atom within the organic substituent and this forms a significant interaction to tellurium in each case. A representative structure, i.e. [2-(2-pyridyl)phenyl]Te(S_2CNMe_2) (**36**) [95], is shown in Fig. 14a. The tellurium atom is tri-coordinated by an asymmetrically coordinating dithiocarbamate ligand, and effectively chelated by the carbon- and nitrogen- atoms of the organic substituent. The coordination geometry is based on ψ-tbp. In the sole example where the organic substituent does not carry an additional donor atom, i.e. (naphthyl)Te[$S_2CN(CH_2)_4$] (**40**) [99], a distinct supramolecular aggregation pattern is observed. There are two independent molecules comprising the asymmetric unit in (**40**) [99], each with

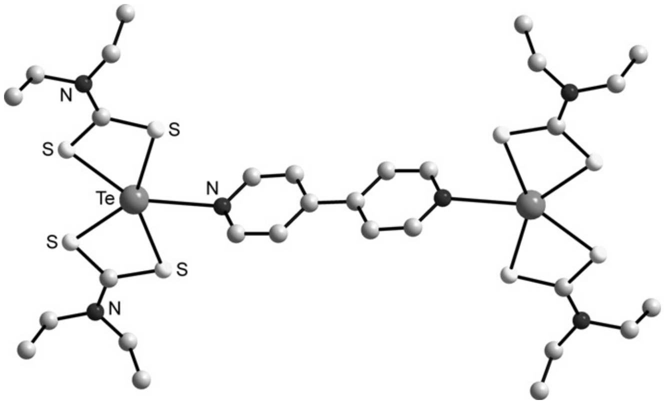

Fig. 7. Dimeric structure of {[Te(S_2CNEt_2)$_2$]$_2$(4,4′-bipyridine)} (**22**) [85]. The analogous xanthate adopts a similar motif.

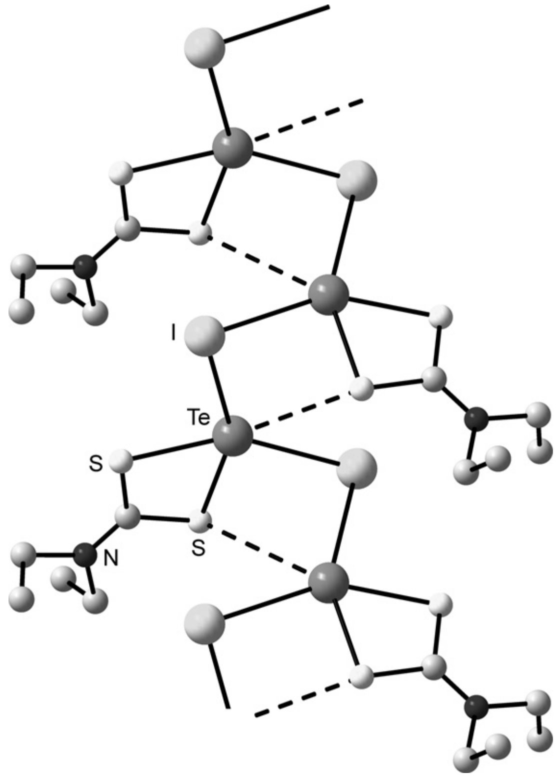

Fig. 8. Helical chain constructed about –Te–I–Te–I– bridges found in the structure of {Te(S_2CNEt_2)I}$_n$ (**26**) [88], being representative of Te(1,1-dithiolate)X structures.

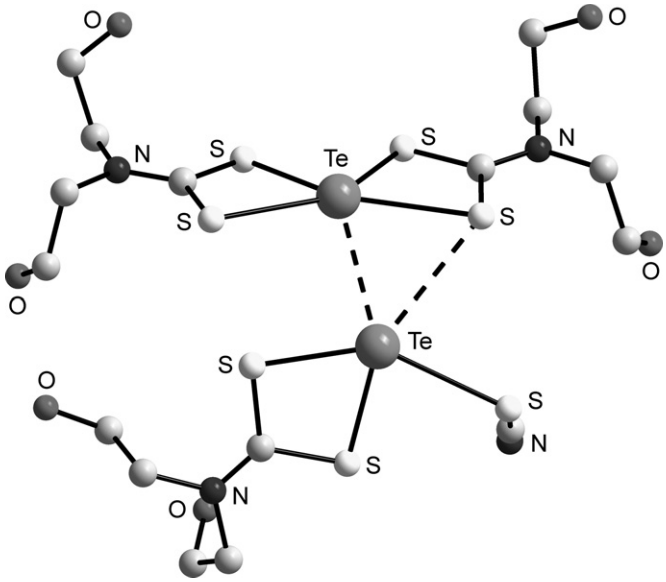

Fig. 9. Dimeric aggregate mediated by Te···S and Te···Te interactions in the structure of {[Te(S_2CNEt_2)$_2$][Te(S_2CNEt_2)SCN]} (**28**) [90].

Table 5
Key structural data for organotellurium(II) 1,1-dithiolate structures.

No.	Compound	Motif	CN geometry[a]	Ref.	No.	Compound	Motif	CN geometry[a]	Ref.
RTe(1,1-dithiolate)									
Dithiocarbamate					Xanthate				
(**36**)	$R^1Te(S_2CNMe_2)$[b]	0-D	ψ-tbp	[95]	(**41**)	$(p\text{-}EtOC_6H_4)Te(S_2COMe)$	Double-chain (1-D)	c ψ-tbp	[100]
(**37**)	$R^2Te(S_2CNMe_2)$[c]	0-D	ψ-tbp	[96]	(**42**)	$(p\text{-}MeOC_6H_4)Te(S_2COEt)$	Double-chain (1-D)	c ψ-tbp	[101]
(**38**)	$R^3Te(S_2CNMe_2)$[d,e]	0-D	ψ-tbp	[97]					
(**39**)	$R^4Te(S_2CNMe_2)$[f]	0-D	ψ-tbp	[98]					
(**40**)	$(naphthyl)Te[S_2CN(CH_2)_4]$[g]	Dimer (0-D)	d ψ-tbp	[99]					
Dithiophosphate					Dithiophosphinate				
(**43**)	$R^5Te[S_2P(O\text{-}i\text{-}Pr)_2]$[h]	0-D	ψ-t$_r$bp	[102]	(**47**)	$PhTe(S_2PPh_2)$[i]	1-D	ψ-t$_r$bp	[105]
(**44**)	$(Mesityl)Te[S_2P(O\text{-}i\text{-}Pr)_2]$	1-D	ψ-t$_r$bp	[103]	(**48**)	$PhTe(S_2PPh_2)$[j]	1-D	ψ-t$_r$bp	[106]
(**45**)	$(p\text{-}MeOC_6H_4)Te[S_2P(OMe)_2]$[e]	2-D	ψ-tbp	[104]	(**49**)	$(mesityl)Te(S_2PPh_2)$	0-D	d ψ-t	[103]
(**46**)	$(p\text{-}EtOC_6H_4)Te[S_2P(OMe)_2]$	2-D	ψ-tbp	[101]	(**50**)	$R^5Te(S_2PMe_2)$[h]	0-D	ψ-tbp	[102]
					(**51**)	$R^5Te(S_2PPh_2)$[h]	0-D	ψ-t$_r$bp	[101]
Ionic dithiocarbamates									
(**52**)	$[caesium\ bis(15\text{-}crown\text{-}5)]\ \{(CF_3)Te[S_2CN(CH_2)_4]_2\}$	0-D	ψ-pbp	[63]					
(**53**)	$Ph_3P{=}N{=}PPh_3]\{(CF_3)Te[S_2CN(CH_2)_4]_2\}$	0-D	ψ-pbp	[63]					
(**54**)	$[Ph_3P{=}N{=}PPh_3]\{(CF_3)Te[S_2CN(CH_2)_4]Cl\}$	0-D	ψ-tbp	[63]					

[a] See Table 1 for the abbreviations of the coordination geometries.

[b] The R^1 group is derived from 2-(2-pyridyl)phenyl.

[c] The R^2 group is derived from 2-phenylazophenyl.

[d] The R^3 group is derived from 2-(2-quinolinyl)phenyl.

[e] Two independent molecules in the asymmetric unit with the same CN geometry.

[f] The R^4 group is derived from (N,N-dimethylamino)naphthyl.

[g] The compound crystallises as a hemi dichloromethane solvate.

[h] The R^5 group is derived from 2-(dimethylaminomethyl)phenyl.

[i] Red form.

[j] Yellow form.

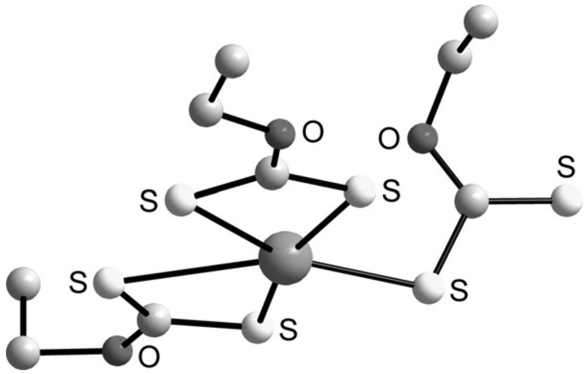

Fig. 10. Molecular structure of the anion in the structure of $[NEt_4][Te(S_2COEt)_3]$ (**29**) [91], showing the pentagonal arrangement of five sulphur atoms around the tellurium(II) centre.

a distinct pattern of bonding interactions. The immediate geometry in (**40**) is defined as for (**36**)–(**39**) [95–98] but in the absence of Te···N contacts, Te···S interactions are noted in (**40**). For each tellurium atom, a weak intramolecular Te···S contact is formed to complete a pseudo-chelate. However, one of these weakly associated sulphur atoms also forms a rather strong Te–S interaction (3.04 Å) with a neighbouring tellurium centre to form a dimer aggregate, Fig. 14b. Centrosymmetrically related dimeric associate via further Te···S interactions (3.27 Å) to form a tetrameric aggregate as illustrated in Fig. 14b. The coordination geometries for both independent tellurium atoms conform to a distorted pseudo-trapezoidal bipyramid, d ψ-tbp, arrangement. By contrast to the zero-dimensional structures observed for the organotellurium(II) dithiocarbamates, the two known organotellurium(II) xanthates each adopt supramolecular chain motifs.

In (p-$MeOC_6H_4$)Te(S_2COMe) (**41**) [100] and the ethyl analogue (**42**) [101], shown in Fig. 15, the xanthate ligand forms a bond to the tellurium atom but forms a weaker bridge to a symmetry related atom to form a one-dimensional chain. These chains are connected into a double-chain by secondary Te···S interactions consolidated by four-membered $\{\cdots Te\cdots S\}_2$ synthons. In each of (**40**) [100] and (**41**) [101], weak Te···O interactions are also noted, i.e. 3.25 and 3.24 Å, respectively. When the Te···O contact is included in the coordination geometry, the arrangement is c ψ-tbp with the capping position occupied by the oxygen atoms and the lone pairs lying over the weakly bound sulphur atoms.

The greatest variety of structures in this category is exhibited by the organotellurium(II) dithiophosphates, (**43**)–(**46**) [101–104]. A non-aggregated structure occurs in [2-(dimethylaminomethyl)phenyl]Te[$S_2P(O$-i-$Pr)_2$] (**43**) [102], Fig. 16a, where the tellurium(II) centre is coordinated by a monodentate dithiophosphate ligand, and is chelated by the carbon and nitrogen atoms of the organic substituent. By contrast to the dithiocarbamate structures, (**36**)–(**40**) [95–99], the non-coordinating sulphur atom is directed away from the tellurium(II) centre so that the coordination geometry is based on a T-shaped CNS donor set with the carbon being normal to the sulphur and nitrogen donor atoms within a distorted trigonal bipyramidal, ψ-t$_r$bp, arrangement of electron pairs. Removing the potential donor atom from the organic ligand releases a coordination site so that the once pendent sulphur atom in (**43**) [102], now bridges a neighbouring tellurium atom as in the structure of (mesityl)Te[$S_2P(O$-i-$Pr)_2$] (**44**) [103], Fig. 16b. The donor set for each of the two independent molecules is approximately T-shaped based on a CS_2 donor set within a ψ-t$_r$bp arrangement. The next two structures display additional secondary bonding in their structures to generate two-dimensional arrays, an observation that is correlated with the reduced steric bulk associated with the tellurium-bound organic group. In (p-$MeOC_6H_4$)Te[$S_2P(OMe)_2$] (**45**) [104], Fig. 16c, the supramolecular chains described for (**43**) [102] are further connected by Te···O secondary interactions into a layer structure; a similar arrangement is found for the ethoxy derivative, (**46**) [101]. The coordination geometry is ψ-tbp.

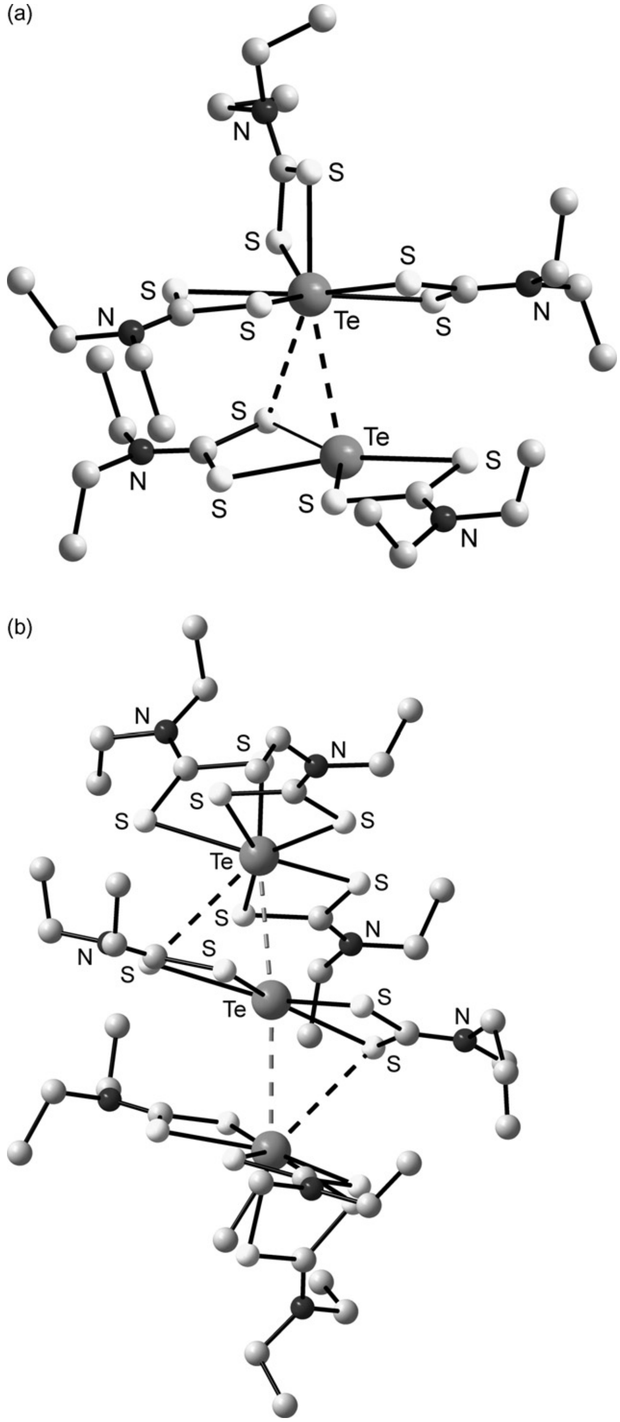

Fig. 11. Supramolecular association via Te···S and Te···Te interactions formed between neutral tellurium(II) $Te(S_2CNEt_2)_2$ species and tellurium(IV) $[Te(S_2CNEt_2)_3]^+$ cations in the structures of (a) dimeric $\{[Te(S_2CNEt_2)_2][Te(S_2CNEt_2)_3]\}[ClO_4]$ (**30**) [92], which has crystallographic 2-fold symmetry; and (b) trimeric $\{[Te(S_2CNEt_2)_2][Te(S_2CNEt_2)_3]_2\}[PF_6]_2$ (**31**) [92].

There are five organotellurium(II) dithiophosphinate structures, (**47**)–(**51**) [101–103,105,106] and these vary from zero- to one-dimensional. In each of the red (**47**) [105] and yellow (**48**)

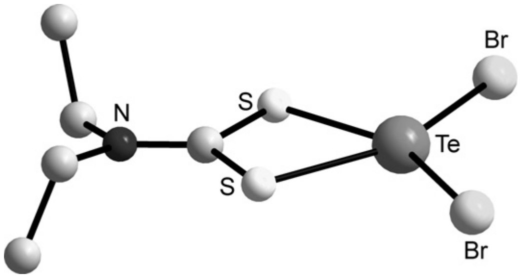

Fig. 12. Molecular structure of the anion in the structure of [1,10-Phenanthrolinium][Te(S_2CNEt_2)Br_2] (**32**) [93], showing the trapezoidal Br_2S_2 arrangement and being representative of other [Te(S_2CNEt_2)X_2]$^-$ structures.

[106] (low-temperature) forms of PhTe(S_2PPh_2), supramolecular chains are present in their crystal structures. These structures exhibit thermochromism, are virtually identical and feature bridges between tellurium(II) centres provided by only one of the dithiophosphinate-sulphur atoms as shown in Fig. 17a for PhTe(S_2PPh_2) (**47**) [105]. Such a coordination pattern imparts a zig-zag topology in the chain as opposed to the effectively linear chains observed for related structures (see above). The coordination geometry is ψ-t$_r$bp in each case. When the steric profile of the tellurium-bound organic substituent is increased by the inclusion of mesityl, i.e. as in (mesityl)Te(S_2PPh_2) (**49**) [103], supramolecular association is precluded and a monomeric structure is observed with a bent geometry about tellurium, based on a distorted pseudo-tetrahedral arrangement, d ψ-t, of electron pairs. The remaining two structures, (**50**) [102] and (**51**) [101], carry nitrogen donor atoms in their tellurium-bound organic substituent which, akin to the dithiocarbamate analogues, precludes intermolecular aggregation.

The remaining three tellurium(II) structures, (**52**)–(**54**) [63], each with dithiocarbamate ligands, are anionic species. Two structures are formulated as {(CF_3)Te[$S_2CN(CH_2)_4$]$_2$}$^-$ anions, i.e. (**52**) and (**53**) [63], and each feature pentagonal planar CS_4 donor set leading to a ψ-pbp geometry, as illustrated in Fig. 18a for (**52**). No supramolecular aggregation involving tellurium is noted in these structures. In (**54**) [63], one dithiocarbamate ligand has been replaced by a chloride, i.e. {(CF_3)Te[$S_2CN(CH_2)_4$]Cl}$^-$ shown in Fig. 18b, leading to a ψ-tbp geometry; no evidence for secondary interactions was found. The lack of supramolecular aggregation in these species is readily correlated with the combined presence of tellurium-bound organic substituents and chelating dithiocarbamate ligands giving rise to coordinative saturation.

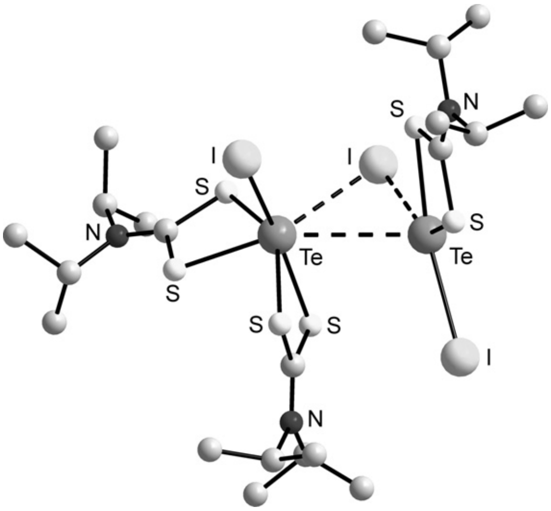

Fig. 13. Supramolecular association via Te···Te and Te···I interactions formed between neutral tellurium(II) {Te[$S_2CN(i\text{-}Pr)_2$]$_2$I}, the tellurium(IV) [Te(S_2CNEt_2)$_2$I]$^+$ cation and iodide in the structure of {Te[$S_2CN(i\text{-}Pr)_2$]$_2$I}[I]{Te[$S_2CN(i\text{-}Pr_2)_2$]I} (**35**) [94].

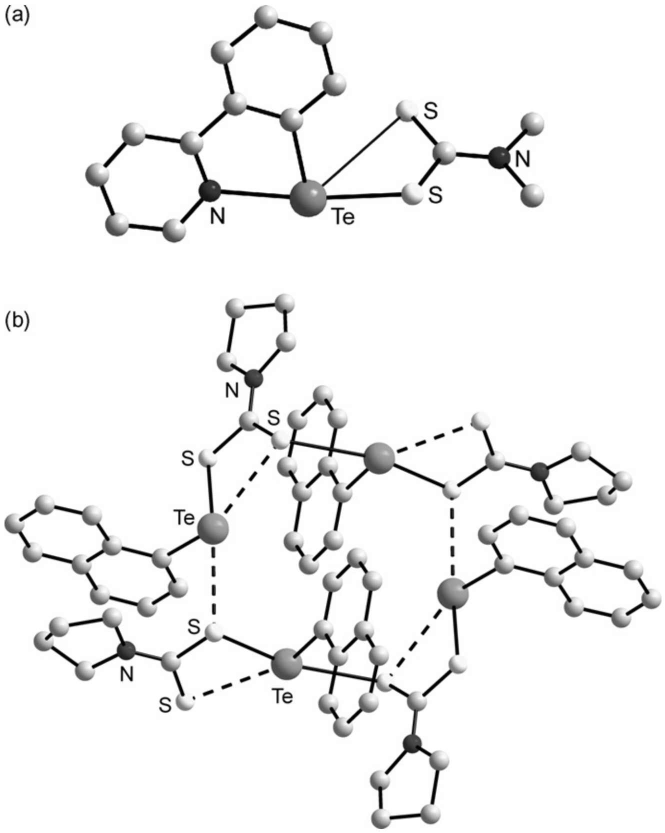

Fig. 14. (a) Molecular structure of [2-(2-pyridyl)phenyl]Te(S_2CNMe_2) (**36**) [95] showing the additional coordination provided by the heteroatom in the organic substituent; this is representative of the other RTe(S_2CNR_2) structures where the R group carries a nitrogen donor atom; (b) Supramolecular aggregation via Te···S interactions in (napthyl)Te[$S_2CN(CH_2)_4$] (**40**) [99].

3. Tellurium(IV) compounds

Tellurium(IV) is a reducing centre and 1,1-dithiolate ligands can be readily oxidised, e.g. $^-S_2CNEt_2$ to disulfiram, $Et_2NC(=S)SSC(=S)NEt_2$, $^-S_2COEt$ to dixanthogen, $EtOC(=S)SSC(=S)COEt$, and $^-S_2P(OEt)_2$ to $(EtO)_2P(=S)SSP(=S)(OEt)_2$, etc. [19]. Under these circumstances, the only binary 1,1-dithiolate compounds to have been characterised with tellurium(IV) are those containing dithiocarbamate ligands which are renowned for their ability to stabilise high oxidation states. Mixed ligand compounds, for example containing halides, are also restricted to dithiocarbamates although some other 1,1-dithiolate ligands appear in mixed 1,1-dithiolate compounds. The situation changes somewhat when organotellurium compounds are considered where all 1,1-dithiolate ligands are featured. More so than for the tellurium(II) examples, the stereochemical activity of the lone pair of electrons is more problematic in these systems.

3.1. Binary tellurium(IV) dithiocarbamates

A summary of the structural data for the binary tellurium(IV) dithiocarbamates, (**55**)–(**61**) [63,107–112] is given in Table 6 and selected geometric parameters are collected in Table S5; no other binary tellurium(IV) 1,1-dithiolates have been structurally characterised (see above). All structures, (**55**)–(**61**), conform to the same basic structural motif as illustrated in Fig. 19 for (**58**) [110]. Two

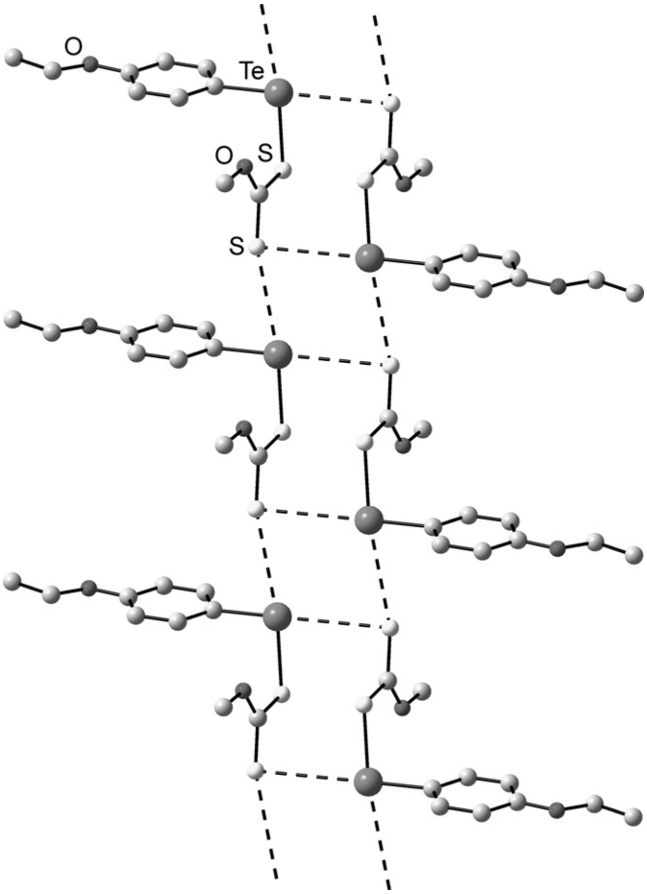

Fig. 15. Supramolecular association via Te$\cdots$S interactions leading to a double-chain in the structure of (p-EtOC$_6$H$_4$)Te(S$_2$COMe) (**41**) [100]. Intramolecular Te$\cdots$O interactions are not shown for reasons of clarity.

of the structures have crystallographic $\bar{4}$ symmetry, i.e. (**59**) [63] and (**60**) [111], the tetragonal polymorph of Te(S$_2$CNEt$_2$)$_4$ (**56**) [108] has 2-fold symmetry, whereas the orthorhombic polymorph (**55**) [107] features two independent molecules on the asymmetric unit. In each structure, the dithiocarbamate ligands bind the tellurium atom forming almost equidistant Te–S interactions (the range of Te–S in the seven independent molecules is 2.63–2.86 Å) so that the tellurium centre is eight-coordinate. The coordination geometry is highly distorted and does not conform to an easily recognisable geometry. While some authors have described the geometry as being based on a square anti-prism, the two putative square faces in this description are highly buckled in each of (**55**)–(**61**) [63,107–112] to render this designation inappropriate. Using the molecular structures of the binary tellurium(II) dithiocarbamates as a starting point, a facile description of the coordination geometries in (**55**)–(**61**) is one based on two trapezoidal planar S$_4$ arrangements pivoted at the tellurium atom and inclined orthogonally; this description is highlighted in the view shown in Fig. 19. Whatever the ultimate designation of the coordination geometry, it is concluded that the lone pair of electrons is stereochemically inert in these eight-coordinate structures.

3.2. Mixed ligand tellurium(IV) dithiocarbamates

The structures under this heading each feature at least one dithiocarbamate ligand and are separated into four categories depending on the number of X = halide/pseudo-halide ligands present. Table 7 summarises salient structural data and selected geometric parameters are collected in Table S6.

The majority of structures in this section (**62**)–(**69**) [111,113–119] have the general formula Te(dithiocarbamate)$_3$X and conform to the same structural motif based on a pentagonal bipyramid of varying degrees of distortion as indicated in Table 7. A representative structure for (**62**)–(**68**), namely Te(S$_2$CNMe$_2$)$_3$Cl (**62**) [113] is shown in Fig. 20a. The pentagonal plane is defined by two symmetrically chelating dithiocarbamate ligands and a sulphur atom of a dithiocarbamate ligand that spans both equatorial and axial positions. This latter ligand forms quite disparate Te–S bond distances and forms the shortest and generally the longest Te–S bond distances within each structure, see Table S6 for geometric parameters. The seventh position is occupied by the halide/pseudo-halide donor atom. A variation on this theme is seen in the structure of [Te(S$_2$CNEt$_2$)$_3$][ClO$_4$] (**69**) [119], shown in Fig. 20b. The perchlorate anion in (**69**) forms two Te$\cdots$O interactions, one a little shorter at 2.88 Å compared to 3.12 Å; the coordination geometry is described as capped pentagonal bipyramidal (c pbp). The distortion in (**66**) [117] is additionally labelled with an "a" as the distortion occurs in the axial position compared with the other structures where the distortion is in the equatorial plane. In the foregoing descriptions of coordination geometries, no stereochemical position is assigned to the lone pair of electrons, consistent with the situation for the binary tellurium(IV) dithiocarbamates.

Four structures conform to the general formula Te(dithiocarbamate)$_2$X$_2$, i.e. (**70**)–(**73**) [120–123], and these adopt two distinct motifs, Table 7. In each of (**70**) [120] and (**71**) [121], represented in Fig. 21a, the pseudo-pentagonal bipyramidal coordination geometry is based on a S$_4$X$_2$ donor set with the dithiocarbamate ligands coordinating symmetrically. The pentagonal plane is defined by two sulphur atoms of a chelating dithiocarbamate ligand, one sulphur atom of a dithiocarbamate ligand that spans both equatorial and axial positions, a chloride, and the lone pair of electrons. The axial positions are occupied by a sulphur atom and the remaining chloride atom. Reducing the steric bulk in (**71**) [121] by substituting the nitrogen-bound iso-propyl groups by ethyl, allows the close approach of molecules

Table 6
Key structural data for binary tellurium(IV) dithiocarbamate structures[a].

No.	Compound	Motif	Ref.	No.	Compound	Motif	Ref.
(**55**)	Te(S$_2$CNEt$_2$)$_4$[b,c]	0-D	[107]	(**56**)	Te(S$_2$CNEt$_2$)$_4$[d,e]	0-D	[108]
(**57**)	Te[S$_2$CN(i-Pr)$_2$]$_4$	0-D	[109]	(**58**)	Te[S$_2$CN(CH$_2$CH$_2$OH)$_2$]$_4$	0-D	[110]
(**59**)	Te[S$_2$CN(CH$_2$Ph)$_2$]$_4$[f]	0-D	[63]	(**60**)	Te[S$_2$CN(CH$_2$CH$_2$OH)Me]$_4$[f]	0-D	[111]
(**61**)	Te[S$_2$CN(CH$_2$CH$_2$)$_2$O]$_4$	0-D	[112]				

[a] Structures are described as two trapezoidal planar S$_4$ units connected at the tellurium atom and orientated orthogonally, the angle represents the dihedral angle between the two TeS$_4$ planes.
[b] Orthorhombic form.
[c] Two independent molecules in the asymmetric unit.
[d] Tetragonal form.
[e] The molecule has crystallographic 2-fold symmetry.
[f] The molecule has crystallographic 4-fold symmetry.

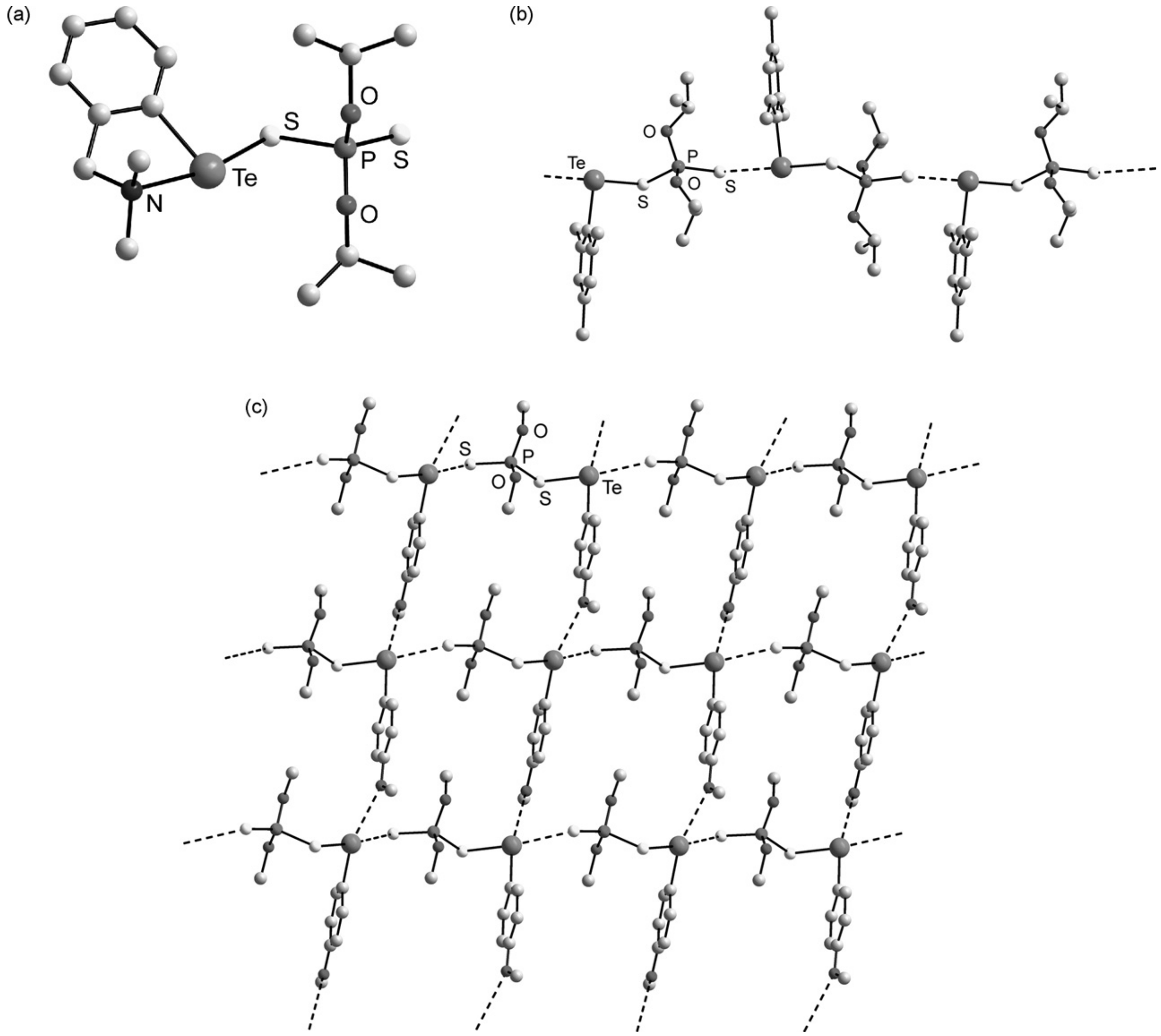

Fig. 16. Varying degrees of supramolecular association in organotellurium(II) dithiophosphate structures: (a) zero-dimensional [2-(dimethylaminomethyl)phenyl]Te[$S_2P(O$-i-$Pr)_2$] (**43**) [102]; (b) one-dimensional in (mesityl)Te[$S_2P(O$-i-$Pr)_2$] (**44**) [103]; and (c) two-dimensional in (p-$MeOC_6H_4$)Te[$S_2P(OMe)_2$] (**45**) [104]. Supramolecular association leading to chains in (**44**) and (**45**) is mediated by Te···S secondary bonding. Additional Te···O interactions in (**45**) lead to a layer structure.

Table 7
Key structural data for tellurium(IV) dithiocarbamate halide/pseudo-halide structures.

No.	Compound	Motif	CN geometry[a]	Ref.	No.	Compound	Motif	CN geometry[a]	Ref.
Te(dithiocarbamate)$_3$X					Te(dithiocarbamate)X$_3$				
(**62**)	$Te(S_2CNMe_2)_3Cl$	0-D	pbp	[113]	(**74**)	$Te(S_2CNEt_2)I_3$	1-D	pbp	[124]
(**63**)	$Te(S_2CNEt_2)_3Cl$	0-D	pbp	[114]					
(**64**)	$Te[S_2CN(CH_2CH_2OH)_2]_3Cl$	0-D	d pbp	[115]	[Te(dithiocarbamate)X$_4$]$^-$				
(**65**)	$Te[S_2CN(CH_2CH_2OH)_2]_3SCN$	0-D	d pbp	[116]	(**75**)	$[NEt_4][Te(S_2CNEt_2)I_4]$	0-D	ψ-pbp	[125]
(**66**)	$Te[S_2CN(CH_2)_5]_3I$	0-D	ad pbp	[117]	(**76**)	$[Te(S_2CNEt_2)_2Br][Te(S_2CNEt_2)Br_4]$			[126]
(**67**)	$Te[S_2CN(CH_2CH_2OH)Me]_3Cl$	0-D	d pbp	[118]		$[Te(S_2CNEt_2)_2Br]$	Dimer (0-D)	pbp	
(**68**)	$Te[S_2CN(CH_2CH_2OH)Me]_3Br$	0-D	d pbp	[111]		$[Te(S_2CNEt_2)Br_4]$		ψ-pbp	
(**69**)	$[Te(S_2CNEt_2)_3][ClO_4]$	0-D	c pbp	[119]					
Te(dithiocarbamate)$_2$X$_2$									
(**70**)	$Te(S_2CNEt_2)_2Cl_2$	0-D	d ψ-pbp	[120]					
(**71**)	$Te[S_2CN(i\text{-}Pr_2)_2]I_2$	0-D	d ψ-pbp	[121]					
(**72**)	$[Te(S_2CNEt_2)_2I_2]_2$	Dimer (0-D)	pbp	[122]					
(**73**)	$Te[S_2CN(CH_2CH_2OH)_2]_2I_2$	Dimer (0-D)	pbp	[123]					

[a] See Table 1 for the abbreviations of the coordination geometries.

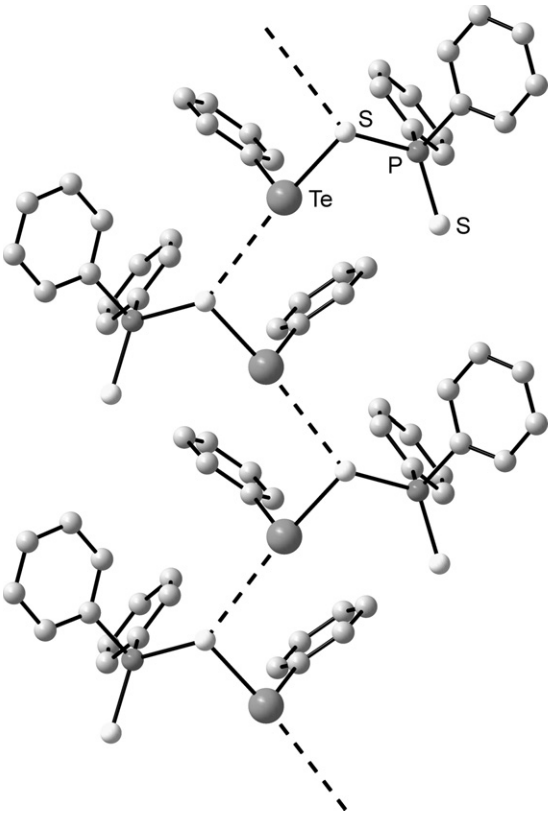

Fig. 17. Supramolecular association mediated by Te···S secondary bonding in the 1-dimensional chain of $PhTe(S_2PPh_2)$ (**47**) [105].

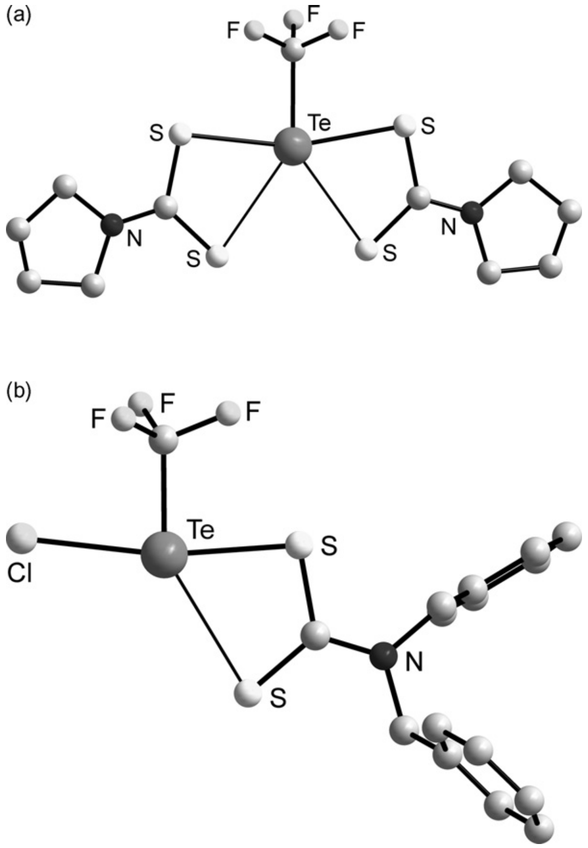

Fig. 18. Monomeric molecular structures of the anionic species in (a) [caesium bis(15-crown-5)]$\{(CF_3)Te[S_2CN(CH_2)_4]_2\}$ (**52**) [63]; and (b) $[Ph_3P{=}N{=}PPh_3]\{(CF_3)Te[S_2CN(CH_2)_4]Cl\}$ (**54**) [63].

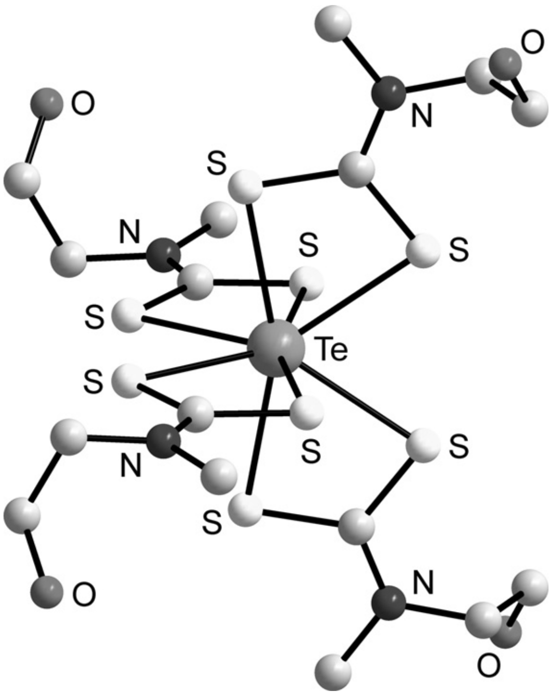

Fig. 19. Monomeric molecular structure of $Te[S_2CN(CH_2CH_2OH)_2]_4$ (**58**) [110]; this is representative of the binary tellurium(IV) dithiocarbamates.

and therefore self-association into centrosymmetric aggregates via Te···I secondary interactions in the structure of (**72**) [122], Fig. 21b; a similar centrosymmetric dimer is found for (**73**) [123]. The coordination geometry is based on a pentagonal bipyramid with sulphur atoms and the weakly associated iodide atom defining the pentagonal plane; the covalently bound iodide atoms occupy axial positions.

There is only one example of a structure with the general formula $Te(dithiocarbamate)X_3$, i.e. $Te(S_2CNEt_2)I_3$ (**74**) [124]. The reduction in the number of chelating ligands results in a relatively coordinatively unsaturated tellurium centre that compensates by forming two secondary Te···I interactions resulting in a supramolecular chain as shown in Fig. 22. The coordination geometry is based on a pentagonal bipyramid with the chelating dithiocarbamate ligand, a covalently bound iodide and two symmetry related iodide atoms defining the pentagonal plane. The two remaining covalently bound iodide atoms occupy axial positions. In this description, there is no obvious stereochemical role for the lone pair of electrons, as concluded for the previous two categories of $Te(dithiocarbamate)_4$ and $Te(dithiocarbamate)_3X$ structures described above.

There are two structures of the general formula $[Te(dithiocarbamate)X_4]^-$, i.e. $[NEt_4][Te(S_2CNEt_2)I_4]$ (**75**) [125] and $[Te(S_2CNEt_2)_2Br][Te(S_2CNEt_2)Br_4]$ (**76**) [126]. In (**75**) [125], Fig. 23a, the anion is discrete and is coordinated symmetrically by the dithiocarbamate ligand. The coordination geometry is pseudo-pentagonal bipyramidal with the two sulphur atoms, two iodide atoms and the lone pair occupying positions in the pentagonal plane; the two remaining iodide atoms define the axial positions. An almost identical geometry is found for the $[Te(S_2CNEt_2)Br_4]^-$ anion in (**76**) [126]. The cation, $[Te(S_2CNEt_2)_2Br]^+$, sees the tellurium atom chelated by two dithiocarbamate ligands and its immediate coordination geometry completed by the bromide

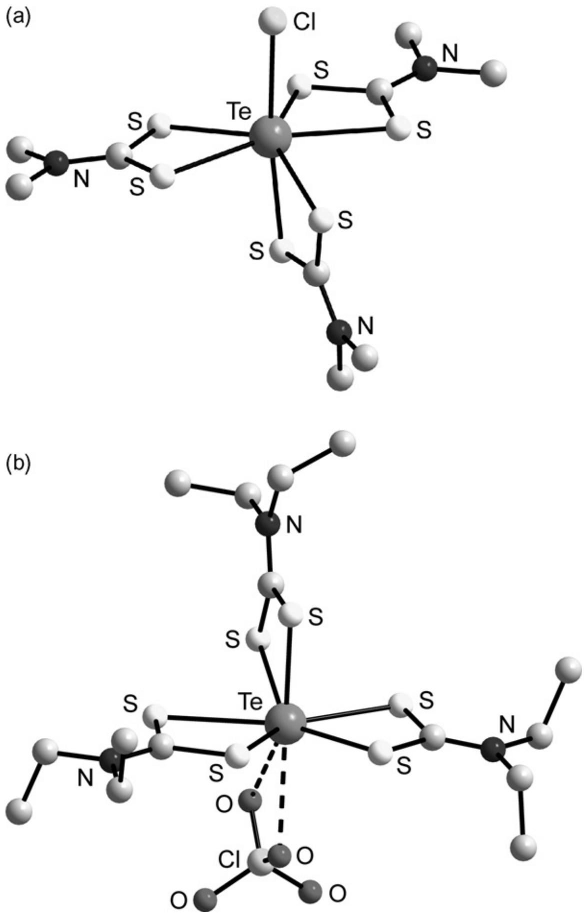

Fig. 20. Monomeric molecular structures of representative Te(dithiocarbamate)$_3$X compounds: (a) Te(S$_2$CNMe$_2$)$_3$Cl (**62**) [113]; and (b) [Te(S$_2$CNEt$_2$)$_3$][ClO$_4$] (**69**) [119].

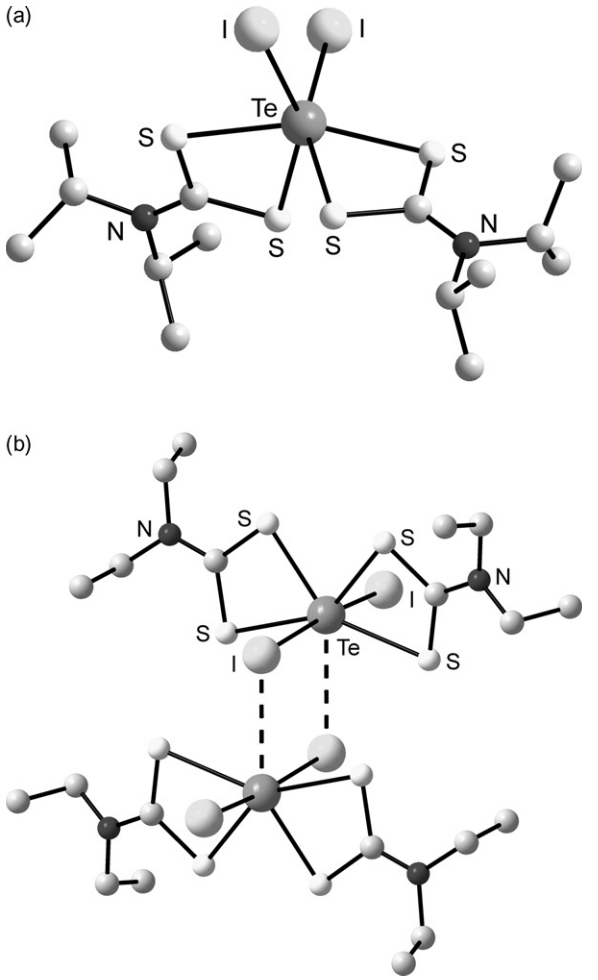

Fig. 21. Structural motifs for Te(dithiocarbamate)$_2$X$_2$ compounds: (a) monomeric Te[S$_2$CN(i-Pr$_2$)$_2$]I$_2$ (**71**) [121]; and (b) dimeric [Te(S$_2$CNEt$_2$)$_2$I$_2$]$_2$ (**72**) [122], mediated by Te···I secondary interactions.

atom. The tellurium atom in the cation, associates with the anion via two secondary Te···Br interactions, as illustrated in Fig. 23b, so that the tellurium atom is surrounded by seven donor atoms that define a pentagonal bipyramid with no obvious role for the lone pair of electrons. The pentagonal plane is defined by two sulphur atoms derived from one dithiocarbamate ligand, one dithiocarbamate ligand derived from the sulphur atom spanning equatorial and axial positions, and the two loosely associated bromide atoms; the axial positions are occupied by the sulphur atom and the covalently bound bromide atom.

Despite the varying compositions of the tellurium(IV) dithiocarbamates, there is significant homogeneity in their coordination geometries. With the exception of the binary tellurium(IV) structures which uniformly adopt eight-coordinate geometries and for which the lone pair of electrons does not play an obvious stereochemical role, the remaining structures, with only two exceptions, i.e. (**70**) [119] and (**71**) [121], adopt distorted pentagonal bipyramidal geometries. This is attained through the presence of seven donor atoms, either intramolecularly or through a combination of intra- and inter-molecularly coordination. In these cases the lone pair of electrons is not ascribed a stereochemical position. Alternatively, when there are not seven donors, the distorted pentagonal bipyramidal arrangement is attained by six donor atoms, by some combination of intra- and inter-molecular coordination, and the lone pair of electrons occupies a stereochemical position, more often than not in the pentagonal plane. The emerging observation is that when there are seven or more donor atoms presented to the tellurium centre, steric crowding presumably precludes the lone pair of electrons from exerting a stereochemical role. In cases where the formal coordination number is six or less, the lone pair of electrons is stereochemically active.

3.3. *Organotellurium(IV) 1,1-dithiolates*

A full range or mono-, di-, and tri-organotellurium(IV) 1,1-thiolates are available in the literature with significant representation from the 1,1-dithiolate ligands not represented in the non-organotellurium(IV) structures. Unlike the former structures, significant supramolecular aggregation leading to extended architectures is evident in many of the structures to be described in this section. Intriguingly, a competition between the formation of Te···S secondary interactions versus Te···halide interactions is apparent, in particular when X = iodide.

3.3.1. *Mono-organotellurium(IV) 1,1-dithiolates*

Structural data for the mono-organotellurium 1,1-dithiolates are summarised in Table 8 and geometric data are collated in Table S7. There are four organotellurium(IV) dithiocarbamate structures, i.e. (**77**)–(**80**) [127–129], and they have a similar structural motif as shown in Fig. 24 for (**79**) [129]. The tellurium atom is coordinated by three dithiocarbamate ligands as well as the carbon atom of the organo substituent. While two of the dithiocarbamate ligands chelate the tellurium centre forming almost equivalent Te–S bond distances, the other is more asymmetric in its mode of coordination, an observation correlated with this lig-

Table 8
Key structural data for monoorganotellurium(IV) 1,1-dithiolate structures.

No.	Compound	Motif	CN geometry[a]	Ref.	No.	Compound	Motif	CN geometry[a]	Ref.
RTe(dithiocarbamate)$_3$					RTe(dithiocarbamate)$_2$X				
(**77**)	$PhTe(S_2CNEt_2)_3$[b,c]	0-D	c ψ-pbp	[127]	(**83**)	$MeTe(S_2CNEt_2)_2I$	0-D	ψ-pbp	[131]
(**78**)	$PhTe(S_2CNEt_2)_3$[d]	0-D	c ψ-pbp	[128]	(**84**)	$MeTe[S_2CN(CH_2)_5]_2I$	Dimer (0-D)	c ψ-pbp	[66]
(**79**)	(p-$MeOC_6H_4)Te(S_2CNMe_2)_3$	0-D	c ψ-pbp	[129]	(**85**)	$PhTe(S_2CNEt_2)_2I$[c]	Dimer (0-D)	c ψ-pbp	[132]
(**80**)	(p-$MeOC_6H_4)Te(S_2CNEt_2)_3$	0-D	c ψ-pbp	[127]	(**86**)	(p-$MeOC_6H_4)Te(S_2CNEt_2)_2Br$	Dimer (0-D)	pbp	[133]
RTe(dithiophosphate)$_3$					(**87**)	(p-$MeOC_6H_4)Te(S_2CNEt_2)_2I$	Dimer (0-D)	pbp	[134]
(**81**)	$PhTe[S_2P(OPh)_2]_3$	0-D	c ψ-pbp	[130]	(**88**)	(p-$MeOC_6H_4)Te(S_2CNEt_2)_2I/Br$[e]	Dimer (0-D)	pbp	[134]
RTe(dithiocarbamate)$_2$(dithiophosphate)					(**89**)	(p-$MeOC_6H_4)Te(S_2CNMe_2)_2Br$[f]	Dimer (0-D)	ψ-pbp	[135]
(**82**)	$PhTe(S_2CNEt_2)_2[S_2P(OEt)_2]$	0-D	c ψ-pbp	[131]	(**90**)	(p-$EtOC_6H_4)Te(S_2CNEt_2)_2Cl$[c]	Dimer (0-D)	c ψ-pbp	[140]
					(**91**)	[(p-$MeOC_6H_4)Te(S_2CNMe_2)_2][ClO_4]$	Dimer (0-D)	pbp	[141]
RTe(dithiocarbamate)X$_2$					RTe(dithiophosphate)X$_2$				
(**92**)	$PhTe(S_2CNEt_2)I_2$[g]	0-D	ψ-tbp	[142]	(**94**)	(p-$MeOC_6H_4)Te[S_2P(OMe)_2]Br_2$	Dimer (0-D)	d tbp	[143]
(**93**)	(p-$MeOC_6H_4)Te(S_2CNEt_2)I_2$	Dimer (0-D)	tbp	[142]					

[a] See Table 1 for the abbreviations of the coordination geometries.
[b] Triclinic form.
[c] Two independent molecules in the asymmetric unit with the same CN geometry.
[d] Monoclinic form.
[e] The iodide site is partially occupied by bromide (41%).
[f] Crystal characterised as a dichloromethane solvate.
[g] Three independent molecules in the asymmetric unit, two with CN geometry ψ-tbp and Motif 0-D and the third one involving the I atom has tbp and dimer (0-D).

and spanning both equatorial (short Te–S bond) and axial sites. The five more tightly held sulphur atoms define the pentagonal plane Table S7. The weakly bound sulphur atom and the organo substituent occupy axial positions. Thus, to a first approximation, the structure just described matches those found for $Te(S_2CNMe_2)_3X$, (**62**)–(**68**) [111,113–118]. However, there are some important differences, most notably the axial angle is significantly distorted from 180° in the organotellurium structures and the axial Te–S bond distance is very long, Table S7. As indicated from the view in Fig. 24, there is a rather large gap in the coordination environment and it is proposed that this is occupied by the lone pair of electrons. In this scenario, the coordination geometry is capped pentagonal bipyramidal with the lone pair occupying the capping position. There are two crystal forms of $PhTe(S_2CNEt_2)_3$, one triclinic with two molecules in the asymmetric unit (**77**) [127] and the other monoclinic (**78**) [128]. The coordination geometries are in close agreement, Tables 8 and S7, and the differences between the molecules arise as a result of the different orientations of the nitrogen-bound ethyl groups. In the monoclinic form (**78**) and in one of the independent molecules of the triclinic form (**77**), two of the NEt_2 adopt the most common arrangement, i.e. one terminal methyl group lying to either side of the NC_2 plane, and the third NEt_2 moiety has both methyl groups lying to the same side of the NC_2 plane. In the second independent molecule of the triclinic polymorph (**77**), the ratio is reversed. A similar structural motif to that just described is found for each of $PhTe[S_2P(OPh)_2]_3$ (**81**) [130] and the mixed 1,1-dithiolate ligand compound, $PhTe(S_2CNEt_2)_2[S_2P(OEt)_2]$ (**82**) [131]. The five sulphur atoms forming the stronger Te–S interactions occupy the pentagonal plane. From the tabulated geometric parameters in Table S7, in particular those for the ligands forming the shorter Te–S distances, it may be concluded that the dithiocarbamate ligand is a more potent coordinating agent for tellurium compared with the dithiophosphate ligand.

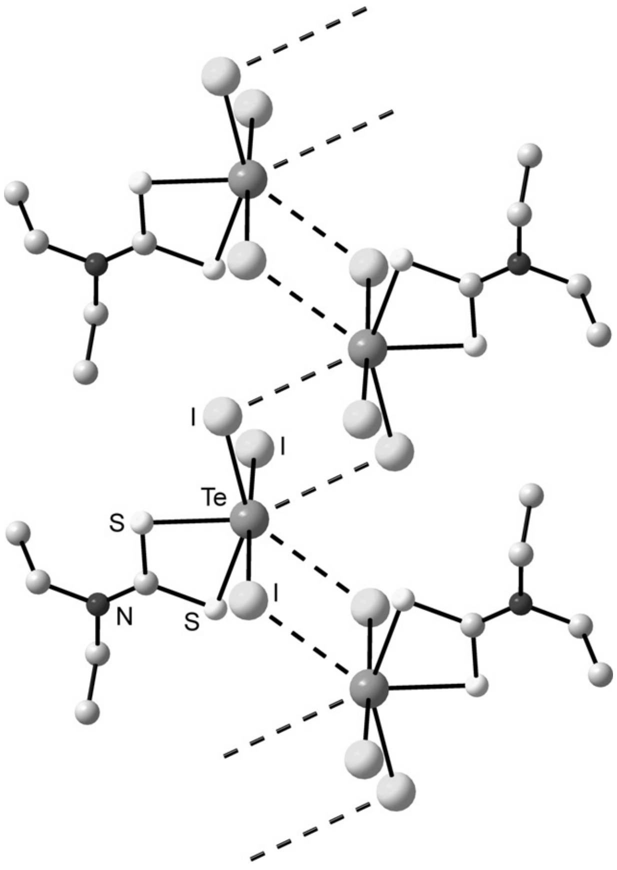

Fig. 22. Supramolecular chain mediated by Te···I secondary interactions in the structure of $Te(S_2CNEt_2)I_3$ (**74**) [124].

The replacement of one dithiocarbamate ligand in $RTe(S_2CNR_2)_3$ leading to $RTe(S_2CNMe_2)_2X$, where X = halide, gives rise to five distinct structural motifs amongst the nine structures conforming to this formulation (**83**)–(**91**) [66,131–135,140,141]; see Table S7 for selected bond distances. A monomeric structure is found for $MeTe(S_2CNEt_2)_2I$ (**83**) [131], illustrated in Fig. 25a. The molecular geometry is based on a pseudo-pentagonal bipyramidal arrangement in which the methyl group and lone pair of electrons occupy axial positions normal to the pentagonal plane defined by the two symmetrically chelating dithiocarbamate ligands and the iodide atom. While each of the remaining $RTe(S_2CNR_2)_2X$ molecules, (**84**)–(**91**) [66,132–135,140,141], display supramolecular aggregation leading to loosely associated dimers in their crystals structures, there is no apparent pattern in the mode of association between them.

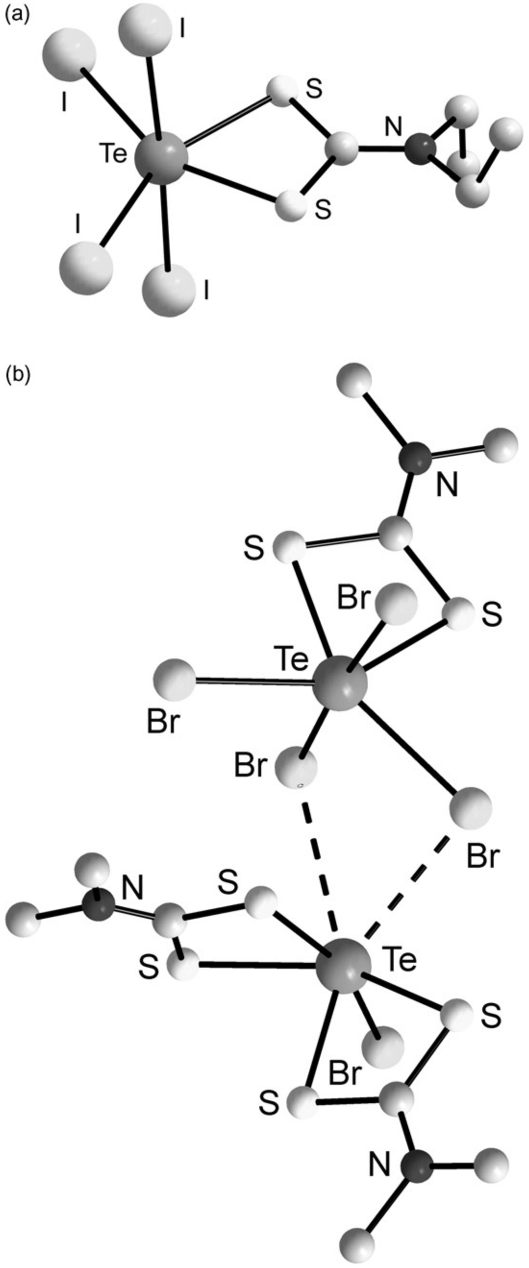

Fig. 23. Structures containing the $[Te(dithiocarbamate)X_4]^-$ anion: (a) monomeric $[Te(S_2CNEt_2)I_4]^-$ in (**75**) [125]; and (b) dimeric $[Te(S_2CNEt_2)_2Br][Te(S_2CNEt_2)Br_4]$ (**76**) [126] held together by Te···Br secondary interactions.

The dimeric aggregate of $MeTe[S_2CN(CH_2)_5]_2I$ (**84**) [66] is mediated by Te···S secondary interactions, Fig. 25b, and similar, at least to a first approximation, aggregation is found in each (**85**) [132] and (**90**) [140]. The presence of the additional sulphur atom in the coordination geometry leads to a capped pseudo-pentagonal bipyramid (c ψ-pbp) arrangement as the weakly associated sulphur atom clearly deviates from the ideal axial position leaving sufficient room for the lone pair of electrons to reside; similar depictions of the coordination geometries apply for (**85**) [132] and (**90**) [140]. Secondary Te···Br rather than Te···S interactions consolidate the dimeric unit in the structure of $(p\text{-}MeOC_6H_4)Te(S_2CNEt_2)_2Br$ (**86**) [133], Fig. 25c. In this structure, as for (**87**) [134] and (**88**) [134], which are sustained by Te···I interactions, the coordination geometries reveal no capacity for the incorporation of the lone pair of electrons: the axial C–Te···X angles approach linearity. Accordingly, the coordination geometries are described as distorted pentagonal bipyramidal. In the crystal structure of $(p\text{-}MeOC_6H_4)Te(S_2CNMe_2)_2Br$ (**89**) [135], neither Te···S nor Te···Br interactions are found. Instead, and, it is worth highlighting, as noted by the authors in the original publication, the dimeric unit is sustained by Te···π interactions where the π-system is defined by the TeS_2C chelate ring. Metal···π interactions [136–138] are attracting increasing attention in supramolecular chemistry and complement lone pair···π interactions found in the realm of organic crystal engineering [139]. It turns out that the Te···$\pi(TeS_2C)$ interaction found in (**89**) [135] is the only such contact amongst the structures surveyed herein suggesting that this is not a prevalent form of association in tellurium 1,1-dithiolate compounds. The final $RTe(S_2CNMe_2)_2X$ structure to be described features a non-coordinating anion, i.e. perchlorate (**91**) [141]. As illustrated in Fig. 25e, two cations associate via Te···S interactions that are about the same order of magnitude observed in the other dimeric aggregates featuring Te···S interactions, Table S7.

The lack of a systematic series of $RTe(S_2CNMe_2)_2X$ structures precludes rationalisation of why one supramolecular synthon forms over another – it is well established that even very minor changes in chemical composition can have major ramifications upon supramolecular aggregation [34–37] – an observation that emphasises the desirability of comprehensive structural analyses. Thus, the substitution of a dithiocarbamate-bound ethyl group in $(p\text{-}MeOC_6H_4)Te(S_2CNEt_2)_2Br$ (**86**) [133] for a methyl group in $(p\text{-}MeOC_6H_4)Te(S_2CNMe_2)_2Br$ (**89**) [135] might just be sufficient to turn off Te···Br interactions in favour of Te···$\pi(TeS_2C)$ interactions, remembering that these interactions are by their very nature, weak.

There are three examples of molecules of the general formula $RTe(1,1\text{-dithiolate})X_2$, (**92**)–(**94**) [142,143]. The asymmetric unit in $PhTe(S_2CNEt_2)I_2$ (**92**) [142] comprises three independent molecules. Two of these molecules exist as monomers, Fig. 26a. The third independent molecule self-associates into a dimeric motif via Te···I interactions, Fig. 26b. While the Te···I distance in the latter is rather long at 3.90 Å, this distance falls within the sum of the van der Waals radii for these atoms [59]. The original two molecules in (**92**) [142] also associate into a dimer but the closest Te···I contact between them is 4.19 Å and therefore these are probably more correctly assigned as monomeric. The coordination geometry for each of the monomeric species is pseudo-trapezoidal

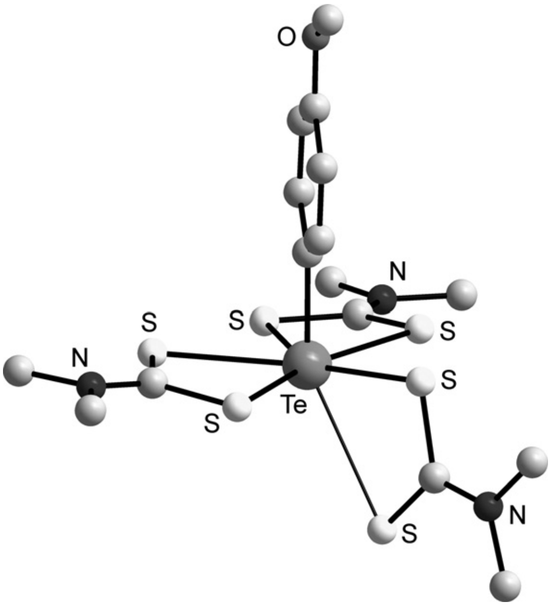

Fig. 24. Molecular structure of monomeric $(p\text{-}MeOC_6H_4)Te(S_2CNMe_2)_3$ (**79**) [129]; this is representative of the $RTe(1,1\text{-dithiolate})_3$ structures.

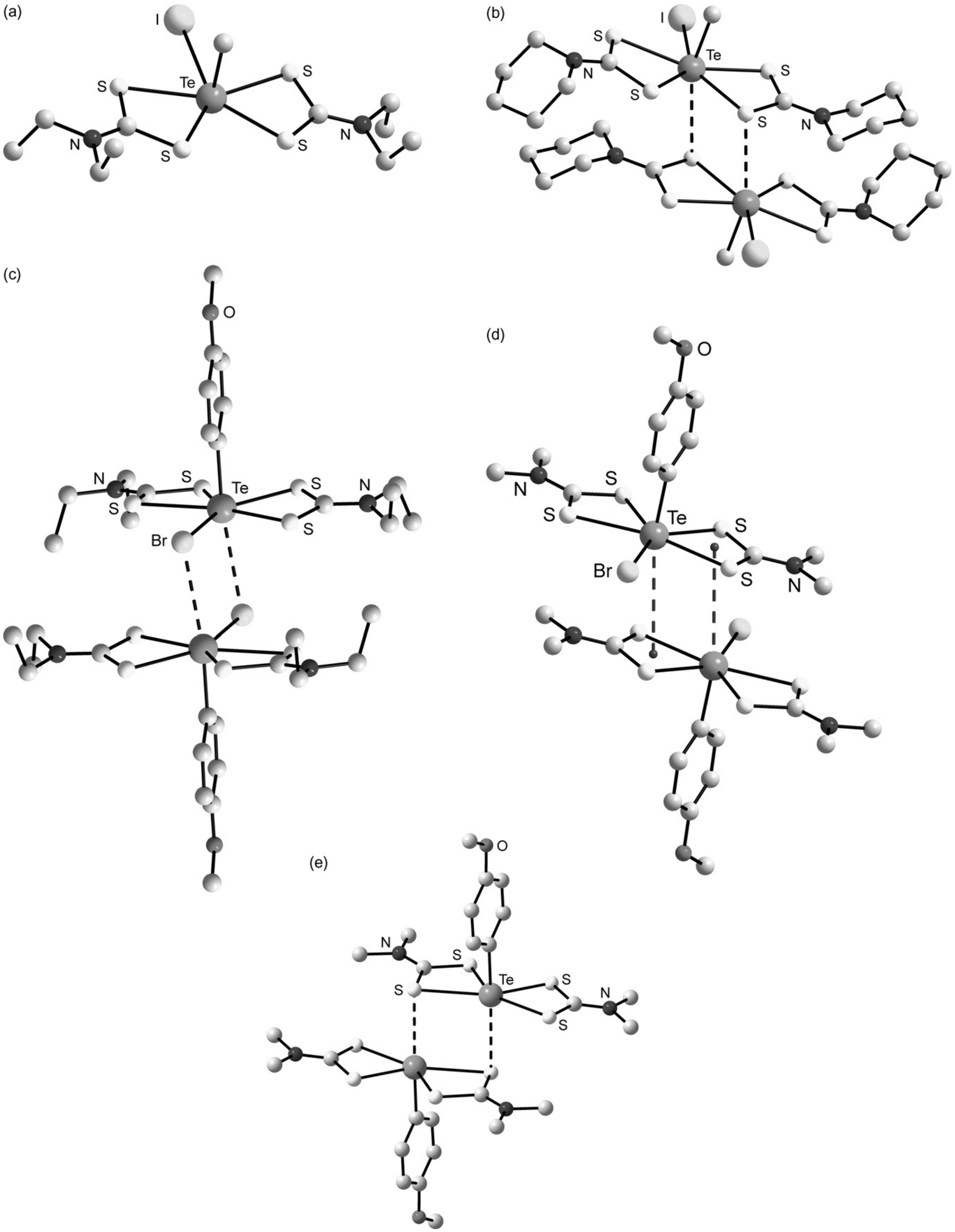

Fig. 25. Structural motifs for RTe(1,1-dithiolate)$_2$X compounds: (a) monomeric MeTe(S_2CNEt_2)$_2$I (**83**) [131]; (b) dimeric MeTe[$S_2CN(CH_2)_5$]$_2$I (**84**) [66] mediated by Te···S secondary interactions; (c) dimeric (p-MeOC$_6$H$_4$)Te(S_2CNEt_2)$_2$Br (**86**) [133] mediated by Te···Br interactions; (d) dimeric (p-MeOC$_6$H$_4$)Te(S_2CNMe_2)$_2$Br (**89**) [135] mediated by lone pair···π (TeS_2C) interactions; and (e) pairs of cations associated via Te···S interactions in the crystal structure of [(p-MeOC$_6$H$_4$)Te(S_2CNMe_2)$_2$][ClO$_4$] (**91**) [141].

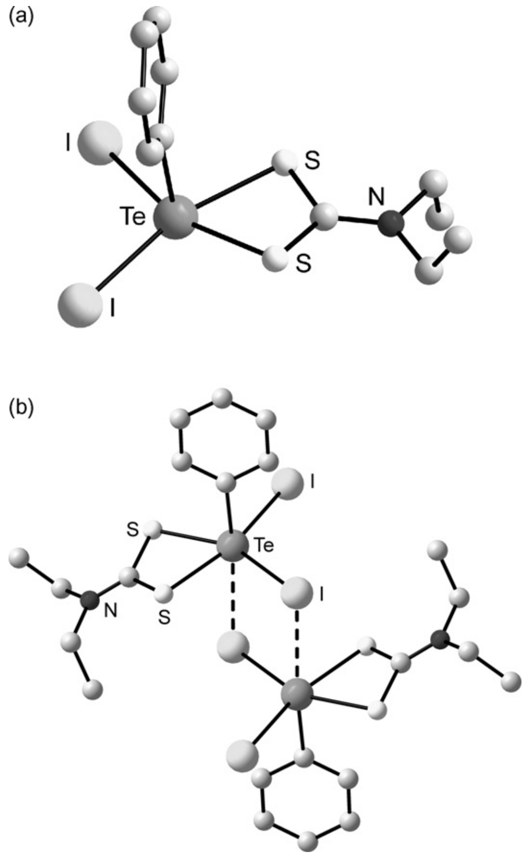

Fig. 26. Structural motifs for $RTe(1,1\text{-dithiolate})X_2$ compounds: (a) monomeric $PhTe(S_2CNEt_2)I_2$ (**92**) [142]; and (b) dimeric $PhTe(S_2CNEt_2)I_2$ (**92**) [142], mediated by Te···I interactions. Both motifs are observed within the one crystal structure, see text [142].

bipyramidal with the lone pair of electrons projected to occupy an axial position. With the additional iodide atom in its coordination sphere, the geometry for the tellurium atom in the third molecule of $PhTe(S_2CNEt_2)I_2$ (**92**) [142] has a CI_3S_2 donor set. Whereas in previous examples the lone pair of electrons occupied a position in the basal plane, here, the angles range 70.3° (chelate angle) to 113.4° (I–Te–I) and so it seems likely that the lone pair of electrons does not occupy a stereochemical position. An analogous dimer to that illustrated in Fig. 26b occurs in $(p\text{-}MeOC_6H_4)Te(S_2CNEt_2)I_2$ (**93**) [142]. The only non-dithiocarbamate monoorganotellurium structure available for description is that of $(p\text{-}MeOC_6H_4)Te[S_2P(OMe)_2]Br_2$ (**94**) [143] and this is also dimeric in the solid-state. A similar trapezoidal bipyramidal environment as found for the third molecule of (**92**) [142] is seen in each of (**93**) [142] and (**94**) [143], with some distortion in the axial angle in the latter structure.

3.3.2. *Diorganotellurium(IV) 1,1-dithiolates*

There are a large number of structures, (**95**)–(**124**) [143–158,160], falling in this category. The structural details for the diorganotellurium(IV) 1,1-dithiolate structures of the general formula $R_2Te(1,1\text{-dithiolate})_2$ are collected in Table 9 and selected geometric parameters may be found in Table S8. Despite the large number of structures that have been determined for $R_2Te(1,1\text{-dithiolate})_2$, the homogeneity of the molecular geometries and supramolecular aggregation for each 1,1-dithiolate ligand is remarkable.

There are no less than 13 structures of the general formula $R_2Te(S_2CNR'_2)_2$, i.e. (**95**)–(**107**) [144–151], and these adopt one of three structural motifs in the solid-state. The majority of the structures, i.e. nine, adopt a monomeric motif as illustrated for $Me_2Te[S_2CN(CH_2)_5]_2$ (**97**) [145] in Fig. 27a, a result correlated with the strong chelating ability of the dithiocarbamate ligand. The coordination geometries are based on capped pseudo-trapezoidal bipyramidal geometry (c ψ-tbp) where the trapezoidal plane is defined by a chelating dithiocarbamate ligand, one of the tellurium-bound organic groups, and one sulphur atom of the second dithiocarbamate ligand. The axial positions are occupied by the second organic group as well as the lone pair of electrons with the remaining second sulphur atom occupying a capping position. This assignment is supported by the C–Te–S angles listed in Table S8 and comes about as the two dithiocarbamate ligands are approximately orthogonal. Subtle differences in terms of forming secondary Te···S or Te···Te secondary interactions are found in the remaining structures.

The structure of $Me_2Te(S_2CNMe_2)_2$ (**95**) [144] is particularly interesting as the asymmetric unit comprises two independent molecules. The first molecule self-associates into a centrosymmetric dimer via Te···S interactions. While the Te···S separations are long, i.e. 3.84 Å, evidence in support of the significance of these interactions in found in the rearrangement of the ligand donor set. The most profound change is seen in the relative orientation of the dithiocarbamate ligands which are now coplanar, Fig. 27b. These plus one of the tellurium-bound organic substituents define a pentagonal plane with the second organic group and lone pair of electrons in the axial position; the weakly associated sulphur atom occupies a capping role in the capped pseudo-pentagonal bipyramidal (c ψ-pbp) coordination geometry. The second independent molecule in $Me_2Te(S_2CNMe_2)_2$ (**95**) [144] adopts essentially the same c ψ-pbp coordination geometry but the capping position is occupied by a symmetry related tellurium atom, Fig. 27c. The structural results for (**95**) [144] provides additional evidence that Te···S and Te···Te interactions can provide equivalent energies of stabilisation in supramolecular aggregation.

The dimeric structure of $(p\text{-}H_2CC_6H_4CH_2)Te[S_2CN(CH_2)_5]_2$ (**106**) [151] mimics the Te···S mediated dimer shown in Fig. 27b. The lone pair of electrons appears not to occupy a stereochemical position in the coordination geometry around the tellurium atom in $Me_2Te[S_2CN(CH_2)_4][S_2CN(CH_2)_5]$ (**107**) [145] as evidenced by the C–Te–S axial angle of 171.3° and hence, the geometry is classified as pbp. The supramolecular structure of $Me_2Te[S_2CN(CH_2)_4]_2$ (**96**) [145] is quite distinct from the other $R_2Te(S_2CNR'_2)_2$ structures, being a linear chain, Fig. 27d. Again, as with some of the previous structures, the Te···S interactions are close to the limits of the established van der Waals criteria but the change in coordination environment dictates that these must be considered significant.

Dimeric units mediated by Te···S secondary bonding are found in the four diorganotellurium bis(xanthate) structures (**108**)–(**111**) [150,152,153]. The same coordination geometries as described for the analogous dithiocarbamate structures are found in three of these structures. Thus, the structures of (**108**) [152] and (**109**) [153] have c ψ-pbp geometries, resembling $Me_2Te(S_2CNMe_2)_2$ (**95**) [144] shown in Fig. 27b. The structure of (**111**) [150], resembling $Me_2Te[S_2CN(CH_2)_4][S_2CN(CH_2)_5]$ (**107**) [145], has a pbp coordination geometry whereby the lone pair does not occupy a stereochemical position, an observation consistent with the relatively close approach of the symmetry related sulphur atom, i.e. 3.48 Å, which crowds the tellurium centre. The exceptional coordination geometry is found for $Ph_2Te(S_2COEt)_2$ (**110**) [153]. Although designated as c ψ-pbp, this molecule has the xanthate ligands approximately orthogonal, Fig. 28a, indicating that the relative orientation of the 1,1-dithiolate ligands is not a criterion for dimerization via Te···S secondary interactions in the structures of $R_2Te(1,1\text{-dithiolate})_2$.

Table 9

Key structural data for diorganotellurium(IV) bis(1,1-dithiolate) structures.

No.	Compound	Motif	CN geometry[a]	Ref.	No.	Compound	Motif	CN geometry[a]	Ref.
R_2Te(dithiocarbamate)$_2$					R_2Te(dithiophosphate)$_2$				
(**95**)	$Me_2Te(S_2CNMe_2)_2$[b]	Dimer (0-D)	c ψ-pbp	[144]	(**112**)	$Me_2Te[S_2P(OC(Me_2)C(Me_2)O)]_2$	0-D	c ψ-tbp	[154]
(**96**)	$Me_2Te[S_2CN(CH_2)_4]_2$	1-D	c ψ-pbp	[145]	(**113**)	$Me_2Te[S_2P(OCH_2C(Et_2)CH_2O)]_2$	0-D	c ψ-tbp	[154]
(**97**)	$Me_2Te[S_2CN(CH_2)_5]_2$	0-D	c ψ-tbp	[145]	(**114**)	$Ph_2Te[S_2P(OMe)_2]_2$	0-D	c ψ-tbp	[143]
(**98**)	$Ph_2Te(S_2CNMe_2)_2$	0-D	c ψ-tbp	[146]	(**115**)	$Ph_2Te[S_2P(OEt)_2]_2$	0-D	c ψ-tbp	[147]
(**99**)	$Ph_2Te(S_2CNEt_2)_2$[c]	0-D	c ψ-tbp	[147]	(**116**)	$Ph_2Te[S_2P(OC(Me_2)C(Me_2)O)]_2$	0-D	c ψ-tbp	[155]
(**100**)	$Ph_2Te(S_2CNEt_2)_2$[d]	0-D	c ψ-tbp	[147]	(**117**)	$[(CH_2)_4]Te\{S_2P[OCH_2C(Me)(n\text{-}Pr)CH_2O]\}_2$	0-D	c ψ-tbp	[156]
(**101**)	$Ph_2Te[S_2CN(n\text{-}Bu)_2]_2$	0-D	c ψ-tbp	[148]	(**118**)	$[(CH_2)_2O(CH_2)_2]Te\{S_2P[OCH_2C(Et_2)CH_2O]\}_2$	0-D	c ψ-tbp	[156]
(**102**)	$Ph_2Te(S_2CNPh_2)_2$[e]	0-D	c ψ-tbp	[149]	(**119**)	$(p\text{-}H_2CC_6H_4CH_2)Te[S_2P(OEt)_2]_2$	1-D	c ψ-pbp	[150]
(**103**)	$Ph_2Te[S_2CN(Et)Ph]_2$	0-D	c ψ-tbp	[149]	R_2Te(dithiophosphinate)$_2$				
(**104**)	$(p\text{-}MeOC_6H_4)_2Te(S_2CNMe_2)_2$	0-D	c ψ-tbp	[144]	(**120**)	$Ph_2Te(S_2PPh_2)_2$	0-D	c ψ-tbp	[157]
(**105**)	$(p\text{-}H_2CC_6H_4CH_2)Te(S_2CNEt_2)_2$	0-D	c ψ-tbp	[150]	R_2Te(dithiocarbamate)(1,1-dithiolate)[g]				
(**106**)	$(p\text{-}H_2CC_6H_4CH_2)Te[S_2CN(CH_2)_5]_2$	Dimer (0-D)	c ψ-pbp	[151]	(**121**)	$Me_2Te(S_2CNEt_2)(S_2COMe)$	(Dimer) 0-D	pbp	[158]
(**107**)	$Me_2Te[S_2CN(CH_2)_4][S_2CN(CH_2)_5]$[f]	Dimer (0-D)	pbp	[145]	(**122**)	$Me_2Te(S_2CNMe_2)(S_2COEt)$	(Dimer) 0-D	pbp	[158]
R_2Te(xanthate)$_2$					(**123**)	$(p\text{-}H_2CC_6H_4CH_2)Te(S_2CNEt_2)[S_2P(OEt)_2]$	0-D	c ψ-tbp	[160]
(**108**)	$Me_2Te(S_2COMe)_2$	Dimer (0-D)	c ψ-pbp	[152]	R_2Te(dithiophosphate)X adduct				
(**109**)	$Me_2Te(S_2COEt)_2$	Dimer (0-D)	c ψ-pbp	[153]	(**124**)	$Ph_2Te\{S_2P[OCH_2C(Me_2)CH_2O]\}_2[Ph_2TeCl_2]$	Dinuclear	pbp	[155]
(**110**)	$Ph_2Te(S_2COEt)_2$	Dimer (0-D)	c ψ-pbp	[153]					
(**111**)	$(p\text{-}H_2CC_6H_4CH_2)Te(S_2COEt)_2$	Dimer (0-D)	pbp	[150]					

[a] See Table 1 for the abbreviations of the coordination geometries.

[b] Two independent molecules in the asymmetric unit.

[c] Molecule has 2-fold symmetry.

[d] Monoclinic form ($P2_1$).

[e] Monoclinic form (C2/c).

[f] Toluene solvate.

[g] Molecule crystallised as a $CHCl_3$ solvate.

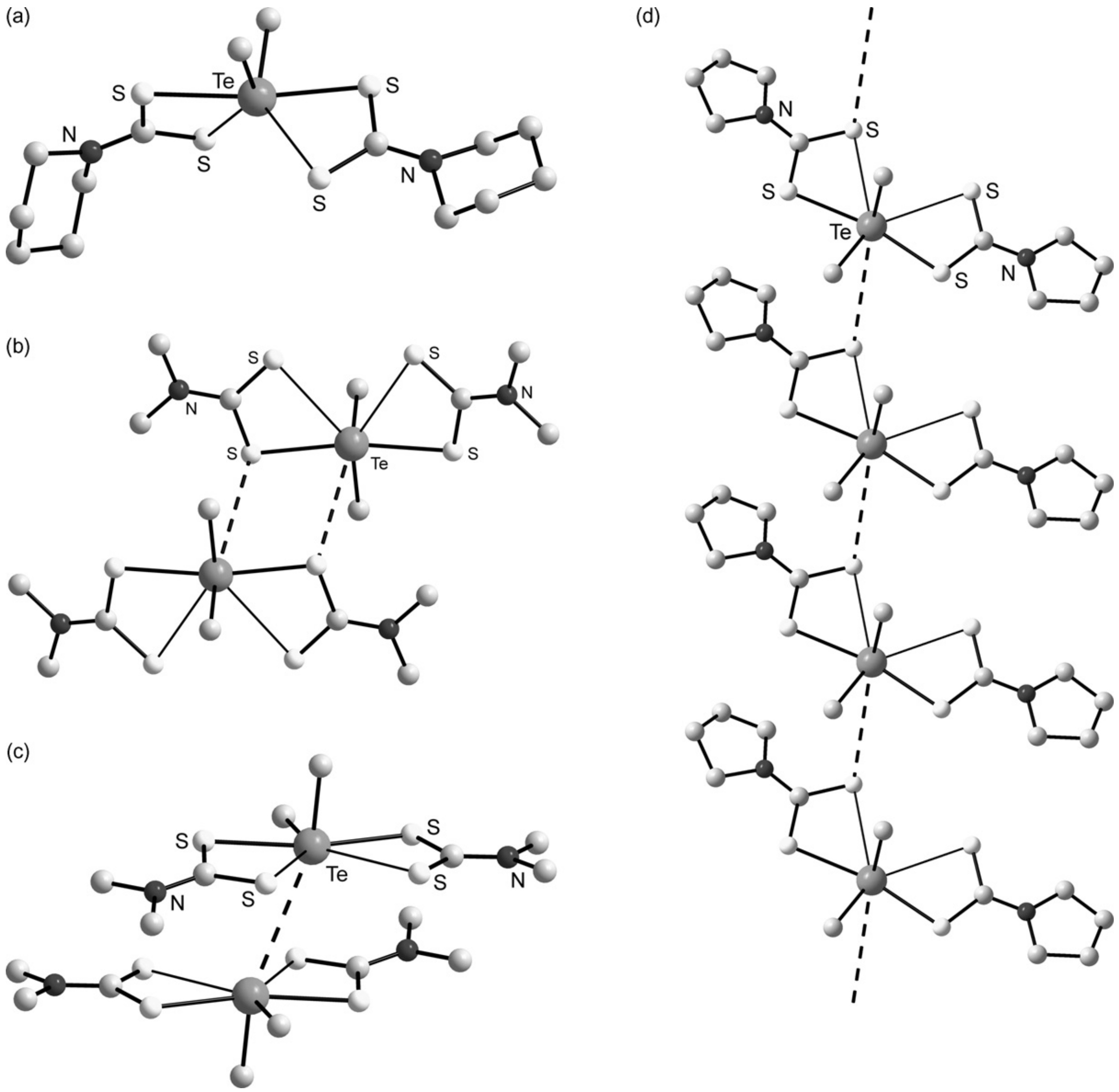

Fig. 27. Structural motifs for $R_2Te(1,1\text{-dithiolate})_2$ compounds: (a) monomeric $Me_2Te[S_2CN(CH_2)_5]_2$ (**9**) [145]; (b) dimeric $Me_2Te(S_2CNMe_2)_2$ (**95**) [144], first independent molecule, mediated by Te···S interactions; (c) dimeric $Me_2Te(S_2CNMe_2)_2$ (**95**) [144], second independent molecule, mediated by Te···Te interactions; (d) the supramolecular chain mediated by Te···S secondary interactions in $Me_2Te[S_2CN(CH_2)_4]_2$ (**96**) [145].

The dithiophosphate analogues (**112**)–(**118**) [143,147,154–156] adopt monomeric structures and coordination geometries as represented for $Me_2Te[S_2CN(CH_2)_5]_2$ (**97**) [145] in Fig. 27a. The exceptional structure of this series is found for $(p\text{-}H_2CC_6H_4CH_2)Te[S_2P(OEt)_2]_2$ (**119**) [150] which crystallises as a supramolecular chain, Fig. 28b, in which the tellurium centre has a c ψ-pbp geometry as for the other linear chain motif, (**96**) [145]. The sole example of a dithiophosphinate structure in this category, i.e. $Ph_2Te(S_2PPh_2)_2$ (**120**) [157], adopts the common monomeric motif and geometry, see Fig. 27a. The final structures in this category to be described are mixed ligand structures containing different 1,1-dithiolate ligands.

The first of three mixed ligand structures, $Me_2Te(S_2CNEt_2)(S_2COMe)$ (**121**) [158], is dimeric as seen in the xanthate derivative, $Me_2Te(S_2COMe)_2$ (**108**) [152]; the “parent” $Me_2Te(S_2CNEt_2)_2$ compound is not available for comparison. The pbp coordination geometry in (**121**) [158] is different than that observed in (**108**) [152], i.e. c ψ-pbp, as the lone pair does not occupy an apparent position in the coordination geometry, Fig. 29a. The presence of the strongly coordinating dithiocarbamate ligand results in a more significant intermolecular Te···S interaction and the straightening of axial C–Te–S angle to 169.5°. Evidence for the better coordinating ability of the $^{-}S_2CNEt_2$ ligand versus the $^{-}S_2COMe$ anion is found in the shorter Te–S bond distances (Table S8) formed by the dithiocarbamate ligand, the apparent lengthening of the Te–S bond distances formed by the $^{-}S_2COMe$ ligand compared to those in (**108**) [152], and the fact that it is the dithiocarbamate ligand that provides the sulphur atom for intermolecular association.

The closely related mixed ligand structure $Me_2Te(S_2CNMe_2)(S_2COEt)$ (**122**) [158] sees a change in the mode of coordination of one of the xanthate ligands, Fig. 29b. The exceptional xanthate ligand coordinates via one of the sulphur atoms as well as the oxygen atom. Similar coordination modes have been observed in other xanthate structures [23]; including a triorganotellurium xanthate derivative, see below. In a systematic experimental and theoretical analysis of S,S versus S,O coordination modes in dimethyltin bis(xanthate) structures, $R_2Sn(S_2COR)_2$, it was concluded that the coordination modes were adopted so as to meet the dictates

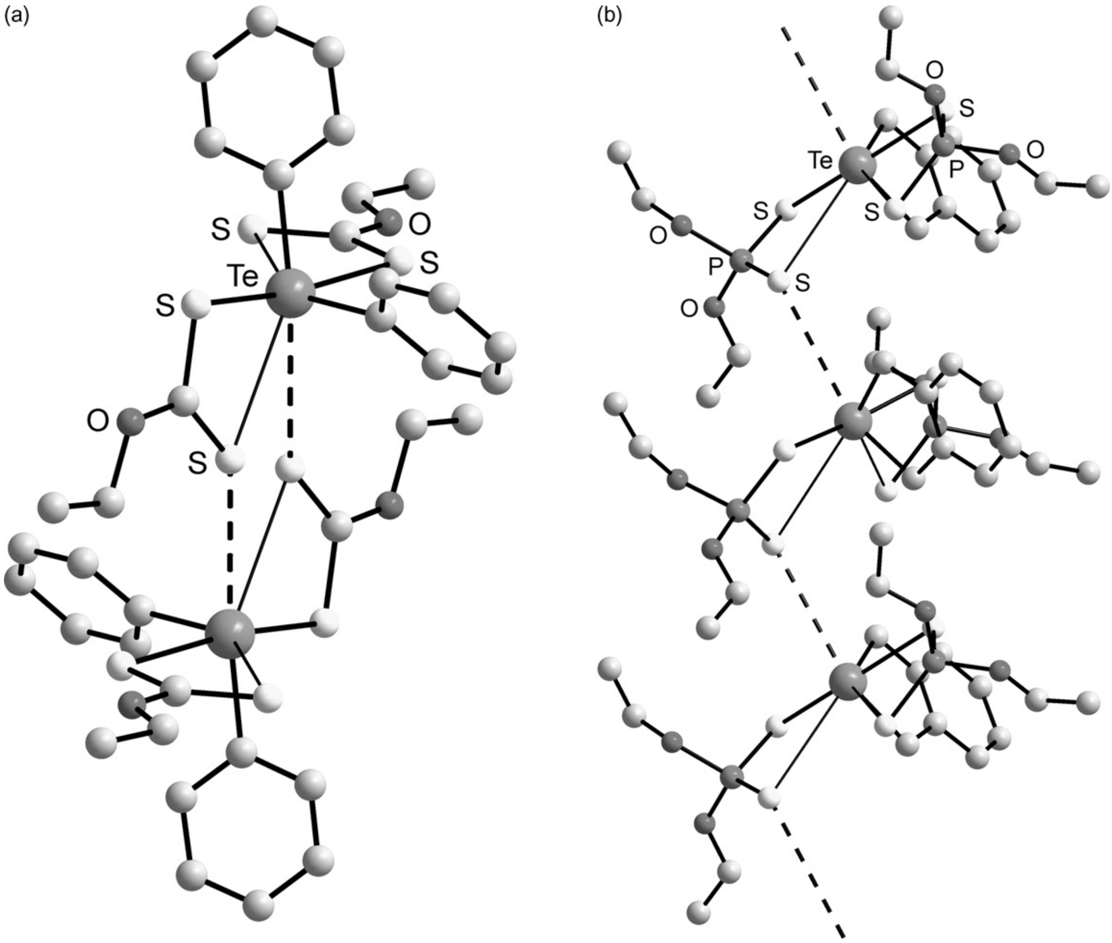

Fig. 28. Structural motifs for R_2Te(1,1-dithiolate)$_2$ compounds: (a) dimeric $Ph_2Te(S_2COEt)_2$ (**110**) [153] mediated by Te···S interactions and where the xanthate ligands are almost orthogonal in contrast to the majority of related dimers; and (b) supramolecular structure in (p-$H_2CC_6H_4CH_2$)$Te[S_2P(OEt)_2]_2$ (**119**) [150] mediated by Te···S interactions.

of crystal packing [159]. It is pertinent to recall that in these compounds, formally, the second bond formed by the xanthate ligand is a dative (coordinate) bond and hence, expected to be weaker than the primary covalent Sn–S interaction. Thus, it is feasible to imagine a scenario where S,S-coordination versus S,O-coordination can be found. Often, S,S-coordination for xanthate ligands is favoured as there is delocalization in the resulting four-membered chelate, e.g. in transition metal complexes. However, in main group elements, this is not always the case, especially when the central atom to sulphur bond distances are disparate, and thus, S,O-coordination modes may be found. The difference in coordination mode notwithstanding, the supramolecular aggregation pattern and coordination geometry in (**122**) [158] is similar to that described for (**108**) [152]. The next structure to be described in this category is of monomeric (p-$H_2CC_6H_4CH_2$)$Te(S_2CNEt_2)[S_2P(OEt)_2]$ (**123**) [160], Fig. 29c, with a coordination geometry akin to that illustrated in Fig. 27a for $Me_2Te[S_2CN(CH_2)_5]_2$ (**97**) [145]. The examination of Te–S bond distances, Table S8, clearly demonstrates the greater coordinating ability of the dithiocarbamate ligand over the dithiophosphate ligand in (**123**) [160].

The last structure in this category is in fact an 1:1 adduct formed between $Ph_2Te\{S_2P[OCH_2C(Me_2)CH_2O]\}_2$ and Ph_2TeCl_2 (**124**) [155], see Fig. 29d The tellurium atom in the dithiophosphate associates with the Ph_2TeCl_2 molecule via Te···S and Te···Cl contacts. The resultant seven coordinate geometry is pentagonal bipyramidal with no obvious position occupied by the lone pair of electrons, as noted in several examples above.

3.3.3. *Mixed ligand diorganotellurium(IV) 1,1-dithiolates*

There are 35 structures of the general formula $R_2Te(S_2CNR'_2)X$, (**125**)–(**149**) [66,145,146,148,151,161–169], and they are remarkable in terms of adopting one basic coordination geometry across the series with the only exception being for the structure of $Me_2Te(S_2CNEt_2)I$ (**127**) [161]. Table 10 summarises important structural characteristics for (**125**)–(**149**), and listings of geometric parameters are available in Table S9. The coordination geometries for the majority of structures are based on a pseudo-pentagonal bipyramid with the lone pair of electrons occupying a position in the pentagonal plane along with a chelating dithiocarbamate ligand, the X substituent and one of the tellurium-bound organic groups. In this description, the second tellurium-bound organic group and the, normally, intermolecularly coordinated atom define the axis. The homogeneity observed for the coordination geometries does not extend to the observed supramolecular aggregation patterns.

Six of the structures are monomeric and the common feature of (**138**)–(**140**) [163] and (**142**)–(**144**) [164] is the presence of the chelating $^{-}SP(Ph_2){=}N^{+}{=}P(Ph_2)S^{-}$ ligand as “X”, see Fig. 30a. The tellurium atom is coordinatively saturated owing to the chelating X ligand and therefore, does not participate in intermolecular aggregation. The remaining structures aggregate into dimers or supramolecular chains: dimerisation occurs in 14 of the structures with the remaining five aggregating to form supramolecular chains.

In the dimeric aggregates, association occurs via Te···S secondary interactions in the majority of the structures, i.e. nine,

Table 10
Key structural data for mixed ligand diorganotellurium(IV) 1,1-dithiolate structures.

No.	Compound	Motif	CN geometry[a]	Ref.	No.	Compound	Motif	CN geometry[a]	Ref.
R_2Te(dithiocarbamate)X									
(**125**)	$Me_2Te(S_2CNEt_2)Cl$	Dimer (0-D)	ψ-pbp	[161]	(**138**)	$[(CH_2)_4]Te(S_2CNEt_2)[SP(Ph_2)=N=P(Ph_2)S]$	0-D	ψ-pbp	[163]
(**126**)	$Me_2Te(S_2CNEt_2)Br$	Dimer (0-D)	ψ-pbp	[161]	(**139**)	$[(CH_2)_4]Te[S_2CN(CH_2)_5][SP(Ph_2)=N=P(Ph_2)S]$	0-D	ψ-pbp	[163]
(**127**)	$Me_2Te(S_2CNEt_2)I$	Dimer (0-D)	c ψ-tbp	[161]	(**140**)	$[(CH_2)_4]Te[S_2CN(CH_2CH_2SCH_2CH_2)][SP(Ph_2)=N=P(Ph_2)S]$	0-D	ψ-pbp	[163]
(**128**)	$Me_2Te[S_2CN(CH_2)_4]Cl$	1-D	ψ-pbp	[145]	(**141**)	$[(CH_2)_5]Te[S_2CN(CH_2CH_2)_2O]I$	Dimer (0-D)	ψ-pbp	[66]
(**129**)	$Me_2Te[S_2CN(CH_2)_4]Br$	1-D	ψ-pbp	[145]	(**142**)	$(o\text{-}H_2CC_6H_4CH_2)Te(S_2CNEt_2)[SP(Ph_2)=N=P(Ph_2)S]$[d]	0-D	ψ-pbp	[164]
(**130**)	$Me_2Te[S_2CN(CH_2)_4]I$	Dimer (0-D)	ψ-pbp	[145]	(**143**)	$(o\text{-}H_2CC_6H_4CH_2)Te[S_2CN(CH_2)_5][SP(Ph_2)=N=P(Ph_2)S]$	0-D	ψ-pbp	[164]
(**131**)	$Me_2Te[S_2CN(CH_2)_5]Cl$	Dimer (0-D)	ψ-pbp	[145]	(**144**)	$(o\text{-}H_2CC_6H_4CH_2)Te[S_2CN(CH_2CH_2)_2S][SP(Ph_2)=N=P(Ph_2)S]$	0-D	ψ-pbp	[164]
(**132**)	$Me_2Te[S_2CN(CH_2)_5]I$	1-D	ψ-pbp	[145]	(**145**)	$(p\text{-}H_2CC_6H_4CH_2)Te(S_2CNEt_2)I$	Dimer (0-D)	ψ-pbp	[165]
(**133**)	$Ph_2Te(S_2CNEt_2)Cl$[b]	Dimer (0-D)	ψ-pbp	[146]	(**146**)	$[C_6H_4OC_6H_4]Te[S_2CN(CHC(H)=C(H)CH_2)]Cl$[e]	Dimer (0-D)	ψ-pbp	[166]
(**134**)	$Ph_2Te(S_2CNEt_2)Br$[b,c]	Dimer (0-D)	ψ-pbp	[148]	(**147**)	$[CH_2Si(Me_2)OSi(Me_2)CH_2]Te[S_2CN(CH_2)_4]I$	Dimer (0-D)	ψ-pbp	[167]
(**135**)	$Ph_2Te[S_2CN(i\text{-}Pr)_2]Cl$	1-D	ψ-pbp	[146]	(**148**)	$[CH_2Si(Me_2)OSi(Me_2)CH_2]Te$ $[S_2CN(CH_2CH_2)_2O]I$	Dimer (0-D)	ψ-pbp	[167]
(**136**)	$[(CH_2)_4]Te(S_2CNEt_2)I$	1-D	ψ-pbp	[162]	(**149**)	$[CH_2Si(Me_2)OSi(Me_2)CH_2]Te[S_2CN(CH_2CH_2)_2S]I$	Dimer (0-D)	ψ-pbp	[167]
(**137**)						$[(CH_2)_4]Te[S_2CN(CHC(H)=C(H)CH_2)]I$	Dimer (0-D)	ψ-pbp	[162]
R_2Te(xanthate)X					R_2Te(dithiophosphinate)X				
(**150**)	$Me_2Te(S_2COMe)Br$	1-D	ψ-pbp	[161]	(**156**)	$[(CH_2)_4]Te(S_2PMe_2)I$	1-D	ψ-pbp	[162]
(**151**)	$Me_2Te(S_2COEt)Cl$[b]	1-D	ψ-pbp	[168]	(**157**)	$[(CH_2)_4]Te(S_2PEt_2)I$	1-D	ψ-pbp	[162]
(**152**)	$Me_2Te(S_2CO\text{-}i\text{-}Pr)I$	1-D	ψ-pbp	[168]	(**158**)	$(o\text{-}H_2CC_6H_4CH_2)Te(S_2PMe_2)I$	1-D	ψ-pbp	[151]
R_2Te(dithiophosphate)X					(**159**)	$(o\text{-}H_2CC_6H_4CH_2)Te(S_2PEt_2)I$	Dimer (0-D)	ψ-pbp	[151]
(**153**)	$Me_2Te\{S_2P[OC(Me_2)C(Me_2)O]\}Cl$[b]	1-D	ψ-pbp	[161]					
(**154**)	$Me_2Te\{S_2P[OC(Me_2)C(Me_2)O]\}I$	0-D	ψ-tbp	[161]					
(**155**)	$\{(o\text{-}H_2CC_6H_4CH_2)Te[S_2P(OEt)_2]O\}_6Te$[f]	0-D	ψ-pbp	[169]					

[a] See Table 1 for the abbreviations of the coordination geometries.

[b] Two independent molecules in the asymmetric unit.

[c] Structure crystallised as a hemi carbondisulphide solvate.

[d] Structure crystallised as a monohydrate.

[e] Structure crystallised as a chloroform solvate.

[f] Three independent $Te[S_2P(OEt)_2]O$ units in the asymmetric unit, each with the same coordination geometry.

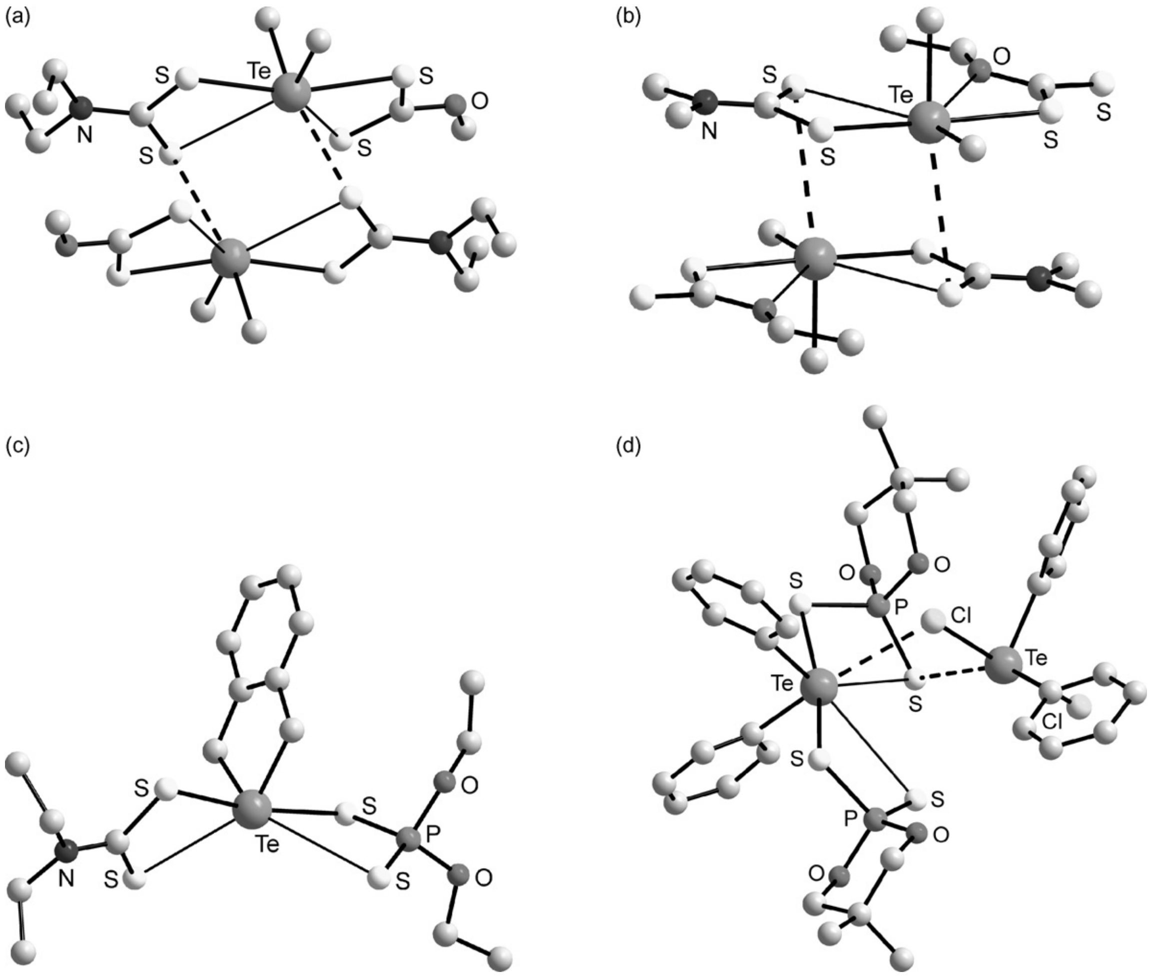

Fig. 29. Structural motifs for mixed ligand $R_2Te(1,1\text{-dithiolate})_2$ compounds: (a) dimeric $Me_2Te(S_2CNEt_2)(S_2COMe)$ (**121**) [158] mediated by Te···S interactions; (b) dimeric $Me_2Te(S_2CNMe_2)(S_2COEt)$ (**122**) [158] showing the unusual S,O-coordination mode of the xanthate ligand; (c) monomeric structure of $(p\text{-}H_2CC_6H_4CH_2)Te(S_2CNEt_2)[S_2P(OEt)_2]$ (**123**) [160]; and (d) dinuclear structure of the adduct $Ph_2Te\{S_2P[OCH_2C(Me_2)CH_2O]\}]_2[Ph_2TeCl_2]$ (**124**) [155].

as illustrated for $[CH_2Si(Me_2)OSi(Me_2)CH_2]Te[S_2CN(CH_2CH_2)_2S]I$ (**149**) [167] in Fig. 30b. Interestingly, five of the dimers are mediated by Te···halide interactions, as shown in Fig. 30c for $Me_2Te(S_2CNEt_2)Cl$ (**125**) [161]. While it is not immediately obvious as to why some of the dimeric aggregates associate via Te···X rather than Te···S interactions, all the Te···X mediated dimers feature dimethyltellurium centres, i.e. (**125**)–(**127**) [161] and (**131**) [145], and the closely related *p*-phenylenedimethyltellurium centre, i.e. (**145**) [165], and that the organic groups in these examples are classified as electropositive. However, the relatively electropositive character of the tellurium atom is not the sole explanation for this mode of association as a Te···S mediated dimer occurs in the dimethyltellurium species, i.e. $Me_2Te[S_2CN(CH_2)_4]I$ (**130**) [145]. Qualitatively, there appears to be a fine balance between supramolecular association patterns dictated by Te···S or Te···I interactions in these systems, indicating that systematic studies are obviously required to resolve this matter. Additional interest in the structure of $Me_2Te(S_2CNEt_2)I$ (**127**) [161] arises from its exceptional coordination geometry. The capped pseudo-trapezoidal bipyramidal (c ψ-tbp) geometry in (**127**) [161] arises as the nominal axial C–Te···S angle is 144.3°, leaving an unobstructed region available for occupancy by the lone pair of electrons, Fig. 30d. The trapezoidal plane is defined by the chelating dithiocarbamate ligand, one of the tellurium-bound methyl groups and the iodide atom. The maximum angle in the trapezoidal plane of 114.0° clearly precludes occupancy by a lone pair of electrons.

The situation in terms of the interactions responsible for the formation of the five supramolecular chains, i.e. Te···S in $Me_2Te[S_2CN(CH_2)_4]Cl$ (**128**) [145], $Me_2Te[S_2CN(CH_2)_4]Br$ (**129**) [145], and $[(CH_2)_4]Te(S_2CNEt_2)I$ (**136**) [162] versus Te···Cl in $Ph_2Te[S_2CN(i\text{-}Pr)_2]Cl$ (**135**) [146] versus Te···I in $Me_2Te[S_2CN(CH_2)_5]I$ (**132**) [145], is as perplexing as is the formation of dimeric aggregates, with no hint of systematic trends. Two distinct topologies are observed for the chains mediated by Te···S interactions, i.e. zig-zag in (**127**) [161] and (**129**) [145], Fig. 31a, and linear in (**136**) [162], Fig. 31b. Zig-zag chains are seen each of the Te···X mediated supramolecular chains, (**132**) [145], for Fig. 31c, and (**134**) [148].

Judging from the foregoing, it is evident the subtle factors are at play when determining supramolecular aggregation patterns. This is also true for the three $Me_2Te(S_2COR)X$ structures (**150**)–(**152**) [161,168]. In $Me_2Te(S_2COMe)Br$ (**150**) [161], a zig-zag chain mediated by Te···S interactions resembling that in Fig. 31a is found. Secondary Te···S interactions are also found in $Me_2Te(S_2COEt)Cl$ (**151**) [168] where two independent molecules comprise the asymmetric unit. Each of these self-associates to form a chain, one with a zig-zag topology and the other with a distinctly more linear topology. The third xanthate derivative, $Me_2Te(S_2CO\text{-}i\text{-}Pr)I$ (**152**) [168], is dimeric in the solid-state, associating via Te···I interactions,

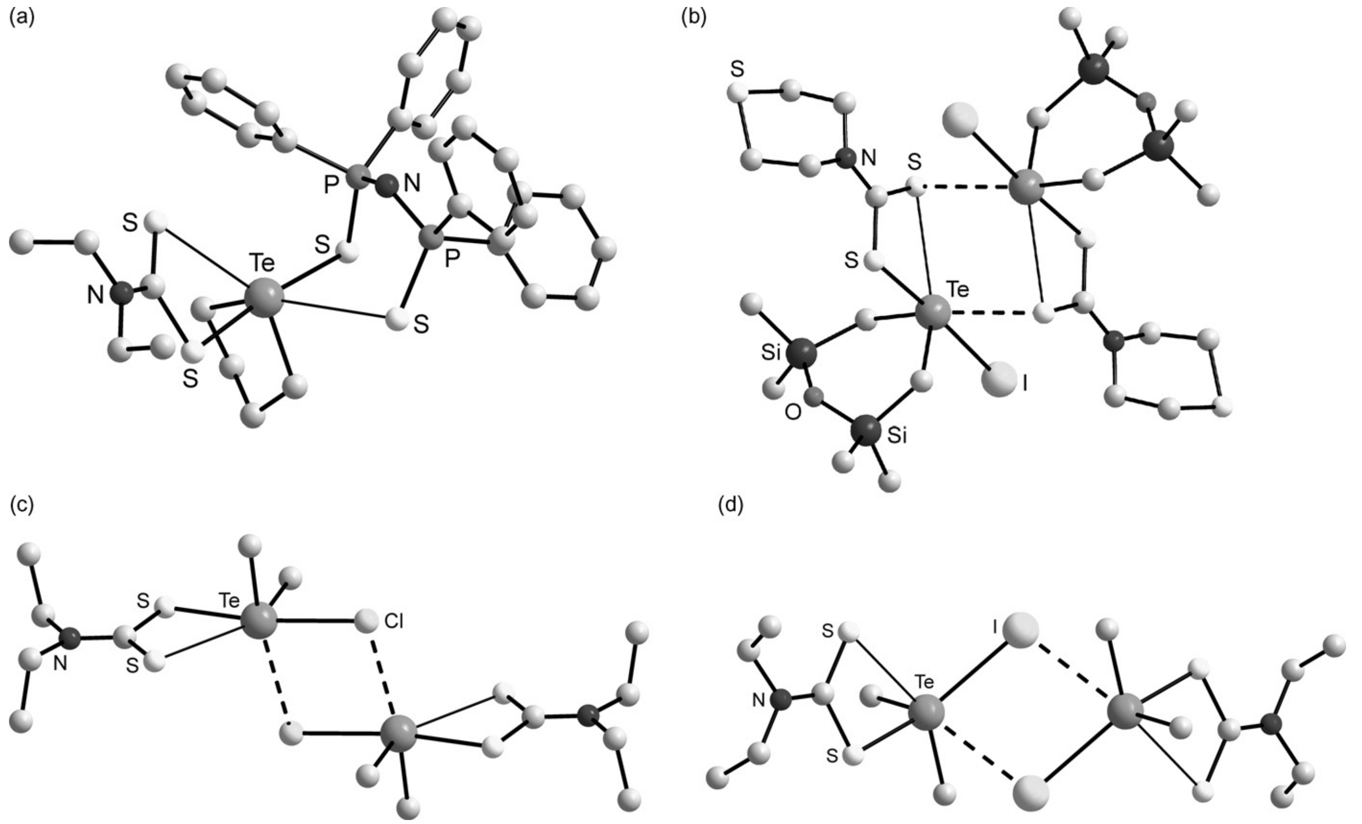

Fig. 30. Structural motifs for zero-dimensional mixed ligand R_2Te(dithiocarbamate)X compounds: (a) monomeric $[(CH_2)_4]Te(S_2CNEt_2)[SP(Ph_2){=}N{=}P(Ph_2)S]$ (**138**) [163]; (b) $[CH_2Si(Me_2)OSi(Me_2)CH_2]Te[S_2CN(CH_2CH_2)_2S]I$ (**149**) [167]; (c) $Me_2Te(S_2CNEt_2)Cl$ (**125**) [161]; and (d) the exceptional capped pseudo-trapezoidal bipyramidal (c ψ-tbp) coordination geometry observed in the $Me_2Te(S_2CNEt_2)I$ (**127**) [161].

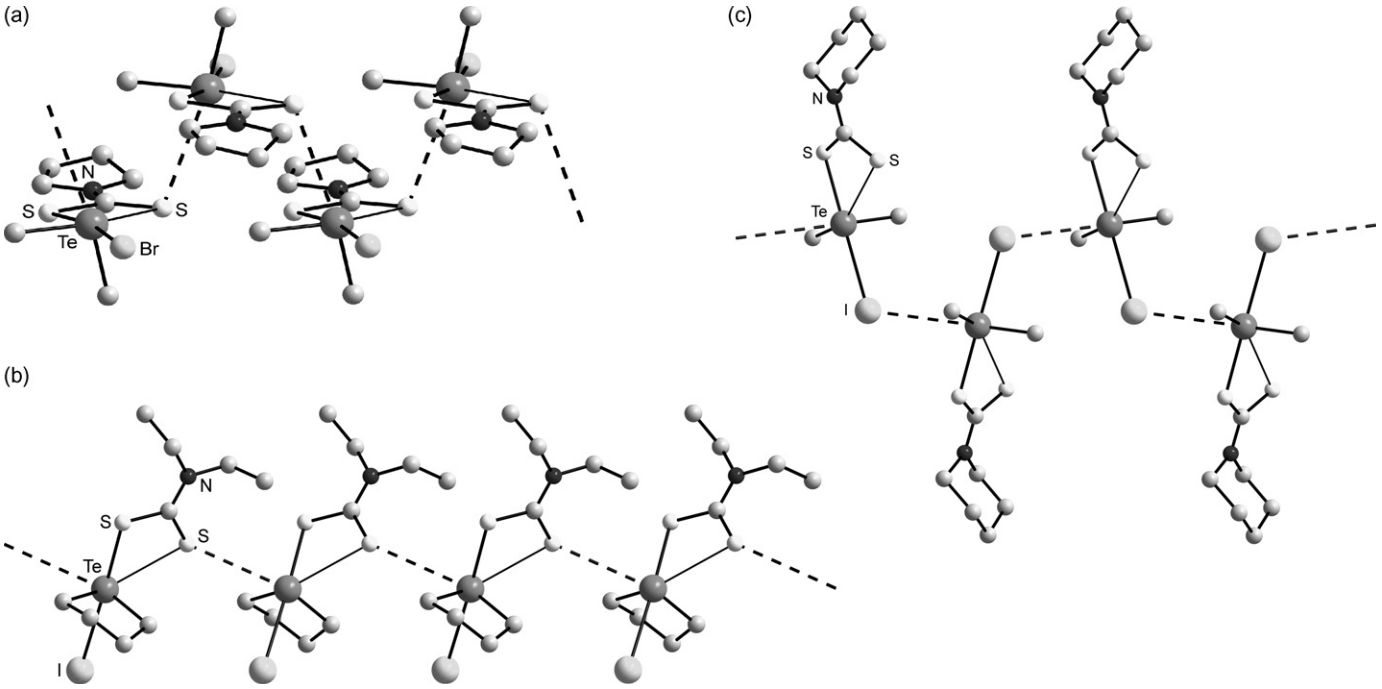

Fig. 31. Structural motifs for mixed ligand R_2Te(dithiocarbamate)X compounds forming supramolecular chains: (a) zig-zag $Me_2Te[S_2CN(CH_2)_4]Br$ (**129**) [145] mediated by Te···S secondary interactions; (b) linear $[(CH_2)_4]Te(S_2CNEt_2)I$ in (**136**) [162] mediated by Te···S interactions; and (c) zig-zag $Me_2Te[S_2CN(CH_2)_5]I$ (**132**) [146] mediated by Te···I secondary interactions.

Table 11
Key structural data for triorganotellurium(IV) 1,1-dithiolate structures.

No.	Compound	Motif	CN geometry[a]	Ref.
R$_3$Te(dithiocarbamate)				
(**160**)	Ph$_3$Te(S$_2$CNEt$_2$)[b]	Dimer (0-D)	c ψ-pbp	[170]
(**161**)	Ph$_3$Te[S$_2$CN(i-Pr)$_2$][b]	Dimer (0-D)	c ψ-pbp	[171]
R$_3$Te(xanthate)				
(**162**)	Ph$_3$Te(S$_2$COMe)[c]	Dimer (0-D)	c ψ-pbpψ-pbp	[172]
(**163**)	Ph$_3$Te(S$_2$COEt)[c]	Dimer (0-D)	ψ-pbpc ψ-pbp	[173]
(**164**)	Ph$_3$Te(S$_2$CO-i-Pr)[b]	Dimer (0-D)	ψ-pbp	[172]
R$_3$Te(dithiophosphate)				
(**165**)	Ph$_3$Te[S$_2$P(OEt)$_2$]	0-D	ψ-tbp	[174]

[a] See Table 1 for the abbreviations of the coordination geometries.
[b] The dimer is centrosymmetric.
[c] Two Te atoms with different polyhedra.

resembling Me$_2$Te(S$_2$CNEt$_2$)Cl (**125**) [161] shown in Fig. 30c. Each of the xanthate molecules features a ψ-pbp coordination geometry.

The coordination geometry (ψ-pbp) and zig-zag topology of the resultant supramolecular chain mediated by Te···S secondary interactions in the dithiophosphate derivative Me$_2$Te{S$_2$P[OC(Me$_2$)C(Me$_2$)O}]Cl (**153**) [161] mimic the structure of (**129**) [145], Fig. 31a. In Me$_2$Te{S$_2$P[OC(Me$_2$)C(Me$_2$)O]}]I (**154**) [161], there are no Te···S nor Te···I interactions less than 4.0 Å and so in accord with the establish distance criteria, the structure should be classified as zero-dimensional with a pseudo-trapezoidal bipyramidal (ψ-tbp) coordination geometry. However, the presence of a Te···S interaction at 4.03 Å and the appearance of a ψ-pbp coordination geometry suggests that the structure could in fact be classified as dimer. The third dithiophosphate structure, {(*o*-H$_2$CC$_6$H$_4$CH$_2$)Te[S$_2$P(OEt)$_2$]O}$_6$Te (**155**) [169], is unusual in several ways. First and foremost, in the context of the present discussion, the X donor atom in R$_2$Te(S$_2$CNR'$_2$)X is an oxygen atom rather than the usual sulphur or halide donor. The structure contains a central tellurium atom coordinated in an octahedral fashion by six oxygen atoms derived from six (*o*-H$_2$CC$_6$H$_4$CH$_2$)Te[S$_2$P(OEt)$_2$]O fragments, Fig. 32a, and is in the +VI oxidation state, Fig. 32b. The tellurium atom in the R$_2$Te(dithiophosphate)X moiety exists within a ψ-pbp coordination geometry.

Zig-zag supramolecular chains mediated by Te···S secondary interactions are found in the dithiophosphinate species (**156**)–(**158**) [151,161]. The fourth structure, (*o*-H$_2$CC$_6$H$_4$CH$_2$)Te(S$_2$PEt$_2$)I (**159**) [151], also features X = iodide, as for (**156**)–(**158**) [151,161], but this crystallises as a dimer mediated by Te···I contacts. Nevertheless, the coordination geometry for tellurium in each of the four compounds is ψ-pbp.

3.3.4. *Triorganotellurium(IV) 1,1-dithiolates*

Structural features for the limited number, i.e. six, structures conforming to the general formula R$_3$Te(1,1-dithiolate) are given in Table 11, and selected geometric data are collated in Table S10. Of the six structures, two are dithiocarbamates (**160**) and (**161**) [170,171], three are xanthates (**162**)–(**164**) [172,173], and there is a sole example of a dithiophosphate (**165**) [174]. The different coordinating abilities of the dithiocarbamate and xanthate ligands are plainly exhibited in these structures which feature two Ph$_3$Te units weakly bridged by two 1,1-dithiolate ligands; the most prominent Te···S interactions are indicated by dashed bonds in the views of Fig. 33. Four of the structures conform to the motif shown in Fig. 33a for Ph$_3$Te(S$_2$CNEt$_2$) (**160**) [170] and Fig. 33b for Ph$_3$Te(S$_2$COMe) (**162**) [172]; the structures of (**163**) [173] and (**165**) [174] are exceptional. From the geometric data collected in Table S10, the dithiocarbamate ligands form shorter Te···S interactions and display a greater tendency towards chelation compared with the xanthate ligands. The structure of Ph$_3$Te(S$_2$COEt) (**163**) [173] represents a variation where one of the xanthate ligand coordinates utilising the oxygen atom as well as the sulphur atoms; the weak nature of these interactions notwithstanding, Fig. 33c. This is a rare example of such a coordination mode observed in tellurium xanthates, the other example being found in the structure of Me$_2$Te(S$_2$CNMe$_2$)(S$_2$COEt) (**122**) [158]. The final structure, Ph$_3$Te[S$_2$P(OEt)$_2$] (**165**) [174], is shown in Fig. 33d and is monomeric, there being no significant supramolecular association involving the tellurium atom.

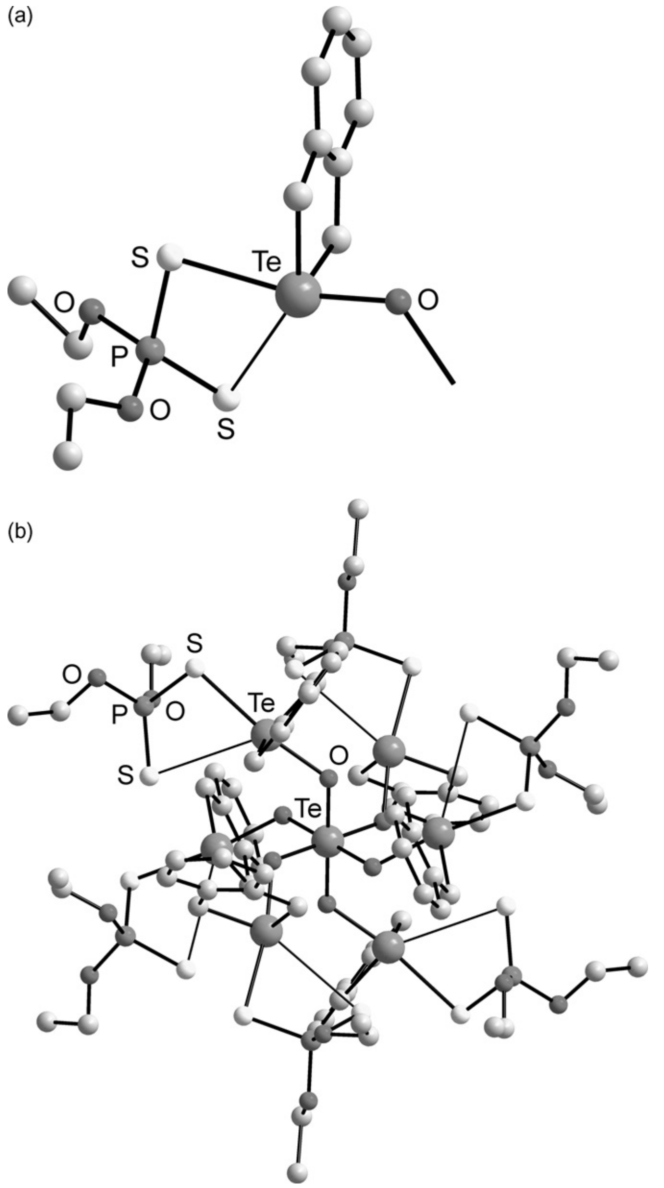

Fig. 32. Structural features of {(*o*-H$_2$CC$_6$H$_4$CH$_2$)Te[S$_2$P(OEt)$_2$]O}$_6$Te (**155**) [169]: (a) the "R$_2$Te(dithiophosphate)X" fragment; and (b) complete molecule.

The weak association between the tellurium centres and the 1,1-dithiolate ligands notwithstanding, the coordination geometries are capped pseudo-pentagonal bipyramidal for the dithiocarbamate structures (**160**) [170] and (**161**) [171] and for one tellurium atom in each of (**162**) [172] and (**163**) [173]. In this description the pentagonal plane being defined by a "chelating" 1,1-dithiolate ligand, two phenyl groups and the lone pair of electrons. The axial positions are occupied by one sulphur atom of the dithiocarbamate ligand formally associated with the second tellurium atom as well as the third phenyl group. The capping position is occupied by the

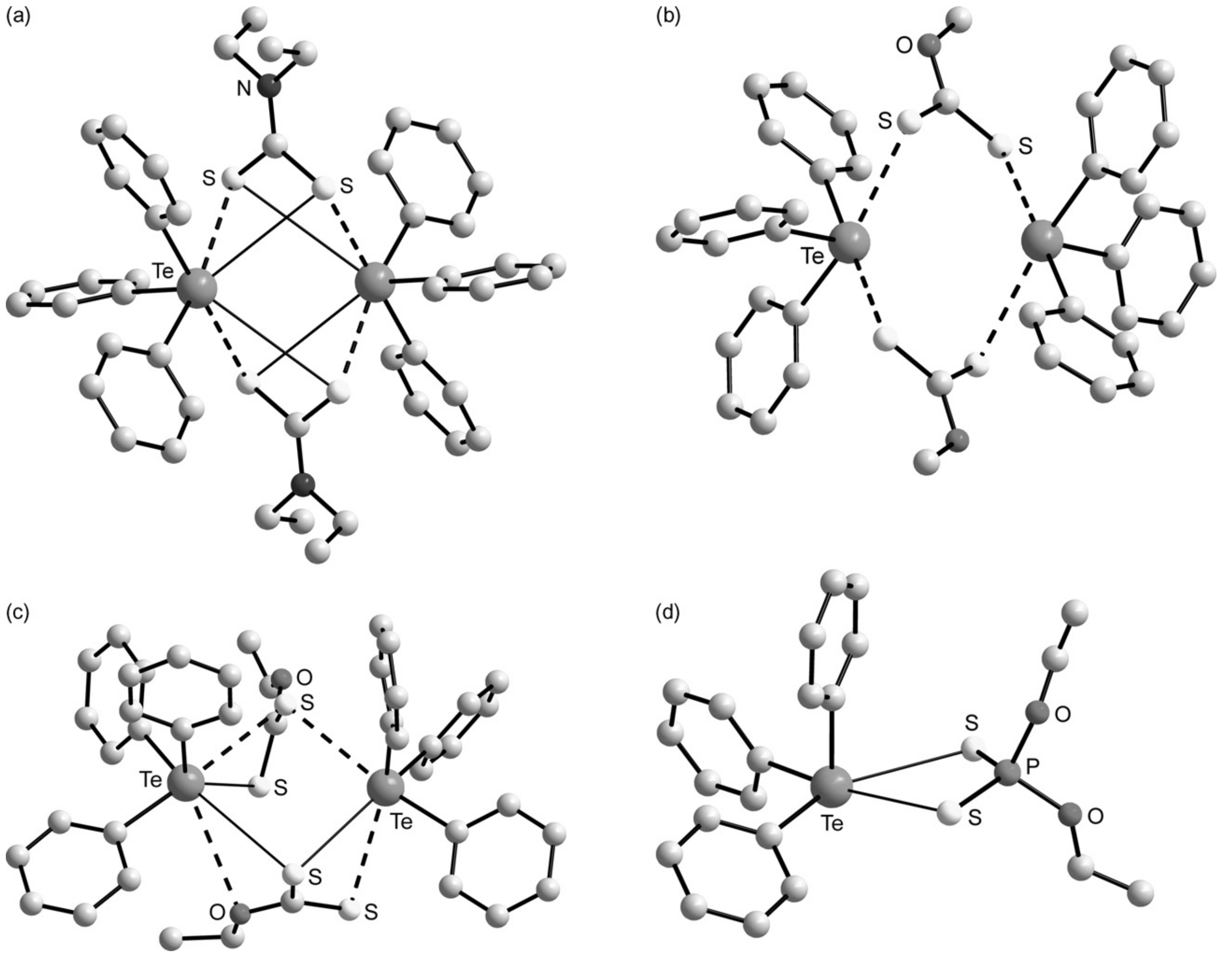

Fig. 33. Structural variations in the R_3Te(1,1-dithiolate) structures: (a) $Ph_3Te(S_2CNEt_2)$ (**160**) [170] showing all Te···S interactions; (b) dinuclear $Ph_3Te(S_2COMe)$ (**162**) [172] highlighting the bridging xanthate ligands and omitting the weaker Te···S interactions; (c) dinuclear $Ph_3Te(S_2COEt)$ (**163**) [173] showing a S,S,O-coordination mode for the xanthate ligand; and (d) the monomeric structure of $Ph_3Te[S_2P(OEt)_2]$ (**165**) [174].

second sulphur atom of the last mentioned dithiocarbamate ligand. Reflecting the poorer coordinating ability of the xanthate ligand, the assigned coordination geometry for the remaining tellurium atoms in (**162**) [172] and (**163**) [173] and for the tellurium atom in (**164**) [172] is pseudo-pentagonal bipyramidal, ψ-pbp, i.e. there is no capping sulphur atom. A pseudo-trapezoidal bipyramidal geometry occurs in the dithiophosphate structure (**165**) [174] where the axial positions are occupied by a phenyl group and the lone pair of electrons.

4. Summary and conclusions

The foregoing description of the structural chemistry of crystallographically characterised tellurium 1,1-dithiolate compounds has focussed upon coordination geometries and supramolecular aggregation patterns. In terms of the former, significant influence exerted by lone pairs of electrons is evident. In the tellurium(II) species, the presence of two lone pairs of electrons is indicated in all coordination geometries. By contrast, often the lone pair of electrons in the tellurium(IV) structures does not exert an obvious stereochemical influence. This difference in behaviour is correlated with steric congestion evident in some tellurium(IV) structures, e.g. the binary tellurium(IV) dithiocarbamates in which the central atom is eight coordinate. When the formal coordination number is lower, e.g. six, the lone pair clearly exerts a stereochemical influence. Organotellurium(IV) species tend to behave differently in that even in the formally seven coordinate RTe(1,1-dithiolate)$_3$ species, a position ascribed to the lone pair of electrons is apparent. For tellurium(II) species coordination numbers range from a low of two to a high of six, when coupled with the two stereochemically active lone pairs of electron, give d ψ-t and bc ψ-tbp coordination geometries, respectively. For tellurium(IV) species, coordination numbers range from a low of six to a high of eight to give ψ-pbp (inclusive of the lone pair of electrons) and cd pbp coordination geometries, respectively. As indicated in Table 1, a total of 19 distinct coordination geometries are exhibited by tellurium 1,1-dithiolate structures, with the complexity due to the presence of secondary Te···X interactions, where X = sulphur, halide, oxygen or tellurium.

Extensive supramolecular association is observed in many of the structures described herein, in particular for the tellurium(II) derivatives. When present, supramolecular aggregation leads to dimeric aggregates or supramolecular polymers, with rare examples of three-dimensional networks. Generally, supramolecular association occurs via Te···S secondary interactions. However, examples exist where association is mediated by secondary Te···Te interactions, sometimes complementing Te···S interactions. It appears that a Te···Te interaction can afford approximately the same energy of stabilisation to a crystal structure as does a Te···S contact. However, steric reasons would favour the formation of Te···S interactions in most cases. While Te···S secondary interactions tend to predominate, the other often observed supramolecular synthon are Te···X interactions, where X = halide. While Te···O secondary interactions complement Te···S contacts in some structures, these are relatively rare. An interesting example of a Te···π interaction, where the π-system is defined by the four-membered TeS_2C chelate system, is found in only one structure of the 165 structures surveyed.

The coordinating ability of the dithiocarbamate ligand is greater than that exhibited by the xanthate ligand which in turn is more effective than dithiophosphate and dithiophosphinate. This observation has a very important ramification in terms of supramolecular aggregation patterns in that dithiocarbamate derivatives are less likely to form high-dimensional architectures whereas dithiophosphate and dithiophosphinate derivatives are more likely to do so.

From the foregoing, it is evident that a rich diversity of coordination geometries are found in tellurium 1,1-dithiolates, often owing to the influence of lone pairs of electrons and the propensity of tellurium to increase its coordination number via secondary interactions that usually involve sulphur.

Acknowledgements

We thank CNPq, FAPESP and CAPES for financial support.

Appendix A. Supplementary data

Supplementary data associated with this article can be found, in the online version, at doi:10.1016/j.ccr.2009.09.007.

References

[1] O.H.J. Szolar, Anal. Chim. Acta 582 (2007) 191.
[2] S. Cecconi, R. Paro, G. Rossi, G. Macchiarelli, Curr. Pharm. Des. 13 (2007) 2989.
[3] C. Rafin, E. Veignie, M.S.-D. Postal, C. Len, P. Villa, G. Ronco, J. Agric. Food Chem. 48 (2000) 5283.
[4] B. Cvek, Z. Dvorak, Curr. Pharm. Des. 13 (2007) 3155.
[5] R. Malcolm, M.F. Olive, W. Lechner, Exp. Opin. Drug Saf. 7 (2008) 459.
[6] Z.E. Sauna, S. Shukla, S.V. Ambudkar, Mol. Biosyst. 1 (2005) 127.
[7] V. Milacic, D. Fregona, Q.P. Dou, Histol. Histopathol. 23 (2008) 101.
[8] L. Ronconi, C. Marzano, P. Zanello, M. Corsini, G. Miolo, C. Maccà, A. Trevisan, D. Fregona, J. Med. Chem. 49 (2006) 1648.
[9] D. de Vos, S.Y. Ho, E.R.T. Tiekink, Bioinorg. Chem. Appl. 2 (2004) 141.
[10] H. Li, C.S. Lai, J. Wu, P.C. Ho, D. de Vos, E.R.T. Tiekink, J. Inorg. Biochem. 101 (2007) 809.
[11] B. Quiclet-Sire, S.Z. Zard, Chem. Eur. J. 12 (2006) 6002.
[12] R.S. Grainger, P. Innocenti, Heteroatom Chem. 18 (2007) 568.
[13] O.J. Plante, E.R. Palmacci, R.B. Andrade, P.H. Seeberger, J. Am. Chem. Soc. 123 (2001) 9545.
[14] D. Fan, M. Afzaal, M.A. Malik, C.Q. Nguyen, P. O'Brien, P.J. Thomas, Coord. Chem. Rev. 251 (2007) 1878.
[15] M.S. Vickers, J. Cookson, P.D. Beer, P.T. Bishop, B. Thiebaut, J. Mater. Chem. 16 (2006) 209.
[16] Y.W. Koh, C.S. Lai, A.Y. Du, E.R.T. Tiekink, K.P. Loh, Chem. Mater. 15 (2003) 4544.
[17] J.R. Castro, K.C. Molloy, Y. Liu, C. Sing Lai, Z. Dong, T.J. White, E.R.T. Tiekink, J. Mater. Chem. (2008) 5399.
[18] N. Alam, M.S. Hill, G. Kociok-Koehn, M. Zeller, M. Mazhar, K.C. Molloy, Chem. Mater. 20 (2008) 6157.
[19] I. Haiduc, in: J.A. McCleverty, T.J. Meyer (Eds.), Comprehensive Coordination Chemistry II, vol. 1, Elsevier Ltd., Oxford, UK, 2004, p. 349.
[20] P.J. Heard, Prog. Inorg. Chem. 53 (2005) 1.
[21] G. Hogarth, Prog. Inorg. Chem. 53 (2005) 71.
[22] I. Haiduc, D.B. Sowerby, S.F. Lu, Polyhedron 14 (1995) 3389.
[23] E.R.T. Tiekink, I. Haiduc, Prog. Inorg. Chem. 54 (2005) 127.
[24] J. Cookson, P.D. Beer, Dalton Trans. (2007) 1459.
[25] E.R. Knight, A.R. Cowley, G. Hogarth, J.D.E.T. Wilton-Ely, Dalton Trans. (2009) 607.
[26] E. Santacruz-Juárez, J. Cruz-Huerta, I.F. Hernández-Ahuactzi, R. Reyes-Martinez, H. Tlahuext, H. Morales-Rojas, H. Höpfl, Inorg. Chem. 47 (2008) 9804.
[27] J. Cruz-Huerta, M. Carillo-Morales, E. Santacruz-Juárez, I.F. Hernández-Ahuactzi, J. Escalante-García, C. Godoy-Alcantar, J.A. Guerrero-Alvarez, H. Höpfl, H. Morales-Rojas, M. Sánchez, Inorg. Chem. 47 (2008) 9874.
[28] C.S. Lai, Y.X. Lim, T.C. Yap, E.R.T. Tiekink, CrystEngComm 4 (2002) 596.
[29] C.S. Lai, S. Liu, E.R.T. Tiekink, CrystEngComm 6 (2004) 221.
[30] C.S. Lai, E.R.T. Tiekink, CrystEngComm 6 (2004) 593.
[31] D. Chen, C.S. Lai, E.R.T. Tiekink, CrystEngComm 8 (2006) 51.
[32] R.E. Benson, C.A. Ellis, C.E. Lewis, E.R.T. Tiekink, CrystEngComm 9 (2007) 930.
[33] R.A. Howie, G.M. de Lima, D.C. Menezes, J.L. Wardell, S.M.S.V. Wardell, D.J. Young, E.R.T. Tiekink, CrystEngComm 10 (2008) 1626.
[34] E.R.T. Tiekink, CrystEngComm 5 (2003) 101.
[35] Y. Liu, E.R.T. Tiekink, CrystEngComm 7 (2005) 20.
[36] E.R.T. Tiekink, CrystEngComm 8 (2007) 104.
[37] E.R.T. Tiekink, Appl. Organomet. Chem. 22 (2008) 553.
[38] N.W. Alcock, Adv. Inorg. Chem. Radiochem. 15 (1972) 1.
[39] N.W. Alcock, Bonding and Structure: Structural Principles in Inorganic and Organic Chemistry, Ellis Horwood, New York, 1990.
[40] E.W. Abel, S.K. Bhargava, K.G. Orrell, Prog. Inorg. Chem. 32 (1984) 1.
[41] N. Sudha, H.B. Singh, Coord. Chem. Rev. 135 (1994) 469.
[42] I. Haiduc, R.B. King, M.G. Newton, Chem. Rev. 94 (1994) 301.
[43] R.J. Gillespie, R.S. Nyholm, Quart. Rev. Chem. Soc. 11 (1957) 339.
[44] R.J. Gillespie, Coord. Chem. Rev. 252 (2008) 1315.
[45] I.D. Brown, Can. J. Chem. 42 (1964) 2758.
[46] D.S. Urch, J. Chem. Soc. 5762 (1964).
[47] R.A. Wheeler, R.A. Heeler, P.N.V.P. Kumar, J. Am. Chem. Soc. 114 (1992) 4776.
[48] L. Shimoni-Livny, J.P. Glusker, C.W. Bock, Inorg. Chem. 37 (1998) 1853.
[49] R.L. Davidovich, Russ. J. Coord. Chem. 31 (2005) 455.
[50] C. Gourlaouen, H. Gerard, J.-P. Piquemal, O. Parisel, Chem. Eur. J. 14 (2008) 2730.
[51] R.L. Davidovich, V. Stavila, D.V. Marinin, E.I. Voit, K.H. Whitmire, Coord. Chem. Rev. 253 (2009) 1316.
[52] N.L. Kilah, S. Petrie, R. Stranger, J.W. Wielandt, A.C. Willis, S.B. Wild, Organometallics 26 (2007) 6106.
[53] D.V. Pushkin, N.V. Aver'yanov, V.N. Serezhkin, Y.E. Gorbunova, Y.V. Kokunov, Russ. J. Inorg. Chem. 47 (2002) 1196.
[54] C.A. Dodds, J. Regelinski, M.D. Spicer, Chem. Eur. J. 12 (2006) 931.
[55] C.S. Lai, E.R.T. Tiekink, Z. Kristallogr. 222 (2007) 532.
[56] K.Y. Monakhov, G. Linti, Inorg. Chem. 48 (2009) 6986.
[57] C. Silvestru, H.J. Breunig, H. Althaus, Chem. Rev. 99 (1999) 3277.
[58] S.S. Dos Santos, E.S. Lang, G.M. de Oliveira, J. Organomet. Chem. 692 (2007) 3081.
[59] A. Bondi, J. Phys. Chem. 68 (1964) 441.
[60] F.H. Allen, Acta Crystallogr. Sect. B: Struct. Crystallogr. Cryst. Chem. 58 (2002) 380.
[61] DIAMOND, Visual Crystal Structure Information System, Version 3.1, CRYSTAL IMPACT, Postfach 1251, D-53002 Bonn, Germany, 2006.
[62] C. Fabiani, R. Spagna, A. Vaciago, L. Zambonelli, Acta Crystallogr. Sect. B: Struct. Crystallogr. Cryst. Chem. 27 (1971) 1499.
[63] W. Tyrra, D. Naumann, S. Buslei, S. Kremer, I. Pantenburg, H. Scherer, Dalton Trans. (2007) 1829.
[64] G.C. Rout, M. Seshasayee, K. Radha, G. Aravamudan, Acta Crystallogr. Sect. C: Cryst. Struct. Commun. 39 (1983) 1021.
[65] S. Husebye, Acta Chem. Scand. 24 (1970) 2198.
[66] P.C. Srivastava, S. Bajpai, R. Lath, R. Kumar, V. Singh, S. Dwivedi, R.J. Butcher, S. Hayashi, W. Nakanishi, Polyhedron 27 (2008) 835.
[67] V. Ganesh, M. Seshasayee, Sp. Chidambaram, G. Aravamudan, K. Goubitz, H. Schenk, Acta Crystallogr. Sect. C: Cryst. Struct. Commun. 45 (1989) 1506.
[68] V. Kumar, G. Aravamudan, M. Seshasayee, P. Selvam, K. Yvon, Acta Crystallogr. Sect. C: Cryst. Struct. Commun. 46 (1990) 2081.
[69] M.J. Cox, E.R.T. Tiekink, Z. Kristallogr. 214 (1999) 584.
[70] H. Graver, S. Husebye, Acta Chem. Scand. A 29 (1975) 14.
[71] S. Husebye, Acta Chem. Scand. 21 (1967) 42.
[72] E.R.T. Tiekink, Acta Crystallogr. Sect. C: Cryst. Struct. Commun. 42 (1986) 633.
[73] M.J. Cox, E.R.T. Tiekink, Z. Kristallogr. 212 (1997) 811.
[74] B.F. Hoskins, E.R.T. Tiekink, G. Winter, Inorg. Chim. Acta 96 (1985) L79.
[75] S. Husebye, Acta Chem. Scand. 20 (1966) 24.
[76] S. Husebye, Acta Chem. Scand. 19 (1965) 1045.
[77] J. Novosad, K.W. Tornroos, M. Necas, A.M.Z. Slawin, J.D. Woollins, S. Husebye, Polyhedron 18 (1999) 2861.
[78] M.G. Newton, R.B. King, I. Haiduc, A. Silvestru, Inorg. Chem. 32 (1993) 3795.
[79] B.F. Hoskins, E.R.T. Tiekink, G. Winter, Inorg. Chim. Acta 105 (1985) 171.
[80] B. Kersting, Z. Naturforsch. 57b (2002) 1115.
[81] N.A.G. Bandeira, L.F. Veiros, M.J. Calhorda, J. Novosad, Inorg. Chim. Acta 356 (2003) 319.
[82] C. Bleiholder, D.B. Werz, H. Köppel, R. Gleiter, J. Am. Chem. Soc. 128 (2006) 2666.
[83] C. Bleiholder, R. Gleiter, D.B. Werz, H. Köppel, Inorg. Chem. 46 (2007) 2249.
[84] B. Moulton, M. Zaworotko, Chem. Rev. 101 (2001) 1629.
[85] S. Rajashree, R. Krishna Kumar, M.R. Udupa, M. Seshasayee, G. Aravamudan, Acta Crystallogr. Sect. C: Cryst. Struct. Commun. 52 (1996) 707.
[86] B.F. Hoskins, P.J. Oliver, G. Winter, Inorg. Chim. Acta 86 (1984) L21.
[87] R.K. Kumar, G. Aravamudan, M.R. Udupa, M. Seshasayee, Polyhedron 15 (1996) 3123.
[88] R.K. Kumar, G. Aravamudan, M.R. Udupa, M. Seshasayee, T.A. Hamor, Polyhedron 12 (1993) 2201.
[89] R.W. Gable, B.F. Hoskins, R.J. Steen, G. Winter, Inorg. Chim. Acta 72 (1983) 173.
[90] K. Radha, G. Aravamudan, A. Rajalakshmi, G.C. Rout, M. Seshasayee, Aust. J. Chem. 39 (1986) 847.
[91] B.F. Hoskins, C.D. Pannan, Chem. Commun. (1975) 408.

[92] R.K. Kumar, G. Aravamudan, M. Seshasayee, K. Sivakumar, H.-K. Fun, I. Goldberg, Polyhedron 17 (1998) 1659.
[93] R. Krishnakumar, G. Aravamudan, M.R. Udupa, M. Seshasayee, T.A. Hamor, J. Chem. Soc. Dalton Trans. (1996) 2253.
[94] V. Ganesh, M. Seshasayee, V. Kumar, S. Chidambaram, G. Aravamudan, K. Goubitz, H. Schenk, J. Crystallogr. Spectrosc. Res. 19 (1989) 745.
[95] N. Al-Salim, A.A. West, W.R. McWhinnie, T.A. Hamor, J. Chem. Soc. Dalton Trans. (1988) 2363.
[96] M.A.K. Ahmed, A.E. McCarthy, W.R. McWhinnie, F.J. Berry, J. Chem. Soc. Dalton Trans. (1986) 771.
[97] A.A. West, W.R. McWhinnie, T.A. Hamor, J. Organomet. Chem. 356 (1988) 159.
[98] A. Panda, G. Mugesh, H.B. Singh, R.J. Butcher, Organometallics 18 (1999) 1986.
[99] M.D. Rudd, A. Defferding, K.K. Klausmeyer, Phosphorus Sulfur Silicon Relat. Elem. 183 (2008) 2361.
[100] S. Husebye, K. Maartmann-Moe, O. Mikalsen, Acta Chem. Scand. 43 (1989) 754.
[101] S. Husebye, K. Maartmann-Moe, O. Mikalsen, Acta Chem. Scand. 44 (1990) 464.
[102] J.E. Drake, M.B. Hursthouse, M. Kulcsar, M.E. Light, A. Silvestru, J. Organomet. Chem. 623 (2001) 153.
[103] F.T. Edelmann, A. Fischer, I. Haiduc, Inorg. Chem. Commun. 6 (2003) 958.
[104] S. Husebye, K. Maartmann-Moe, O. Mikalsen, Acta Chem. Scand. 43 (1989) 868.
[105] A. Silvestru, I. Haiduc, K.H. Ebert, H.J. Breunig, D.B. Sowerby, J. Organomet. Chem. 483 (1994) 253.
[106] A. Silvestru, I. Haiduc, K.H. Ebert, H.J. Breunig, Inorg. Chem. 33 (1994) 1253.
[107] S. Husebye, S.E. Svaeren, Acta Chem. Scand. 27 (1973) 763.
[108] A.V. Virovets, I.V. Kalinina, V.P. Fedin, D. Fenske, Acta Crystallogr. Sect. C: Cryst. Struct. Commun. 56 (2000) e589.
[109] V. Kumar, G. Aravamudan, M. Seshasayee, P. Selvam, K. Yvon, Acta Crystallogr. Sect. C: Cryst. Struct. Commun. 46 (1990) 2100.
[110] G.C. Rout, M. Seshasayee, G. Aravamudan, K. Radha, Acta Crystallogr. Sect. C: Cryst. Struct. Commun. 40 (1984) 1142.
[111] S. Husebye, Acta Chem. Scand. A 33 (1979) 485.
[112] S. Esperas, S. Husebye, Acta Chem. Scand. A 29 (1975) 185.
[113] M.J. Cox, E.R.T. Tiekink, Z. Kristallogr. New Cryst. Struct. 214 (1999) 49.
[114] K. von Deuten, W. Schnabel, G. Klar, Phosphorus Sulfur 9 (1980) 93.
[115] G.V.N.A. Rao, M. Seshasayee, G. Aravamudan, K. Radha, Inorg. Chem. 22 (1983) 2590.
[116] G.C. Rout, M. Seshasayee, G. Aravamudan, K. Radha, J. Crystallogr. Spectrosc. Res. 14 (1984) 193.
[117] S. Chidambaram, G. Aravamudan, M. Seshasayee, M.R. Snow, E.R.T. Tiekink, Aust. J. Chem. 42 (1989) 969.
[118] S. Husebye, A.G. Thowsen, Acta Chem. Scand. A 35 (1981) 443.
[119] S. Chidambaram, G. Aravamudan, M. Seshasayee, T.A. Shibanova, V.I. Simonov, Polyhedron 7 (1988) 1267.
[120] W. Schnabel, K. von Deuten, G. Klar, Cryst. Struct. Commun. 10 (1981) 1405.
[121] V. Kumar, G. Aravamudan, M. Seshasayee, J. Crystallogr. Spectrosc. Res. 21 (1991) 65.
[122] R.K. Kumar, G. Aravamudan, M.R. Udupa, M. Seshasayee, T.A. Hamor, Acta Crystallogr., Sect. C: Cryst. Struct. Commun. 49 (1993) 1328.
[123] G.V.N. Appa Rao, M. Seshasayee, G. Aravamudan, K. Radha, Acta Crystallogr., Sect. C: Cryst. Struct. Commun. 39 (1983) 1018.
[124] R.K. Kumar, G. Aravamudan, M.R. Udupa, M. Seshasayee, P. Selvam, K. Yvon, Polyhedron 15 (1996) 1453.
[125] R.K. Kumar, G. Aravamudan, K. Sivakumar, H.-K. Fun, Acta Crystallogr., Sect. C: Cryst. Struct. Commun. 55 (1999) 1121.
[126] W. Schnabel, K. von Deuten, G. Klar, Phosphorus Sulfur 13 (1982) 345.
[127] S. Husebye, S.V. Lindeman, Acta Crystallogr., Sect. C: Cryst. Struct. Commun. 51 (1995) 2152.
[128] S. Esperas, S. Husebye, Acta Chem. Scand. 26 (1972) 3293.
[129] S. Husebye, K. Maartmann-Moe, W. Steffensen, Acta Chem. Scand. 44 (1990) 579.
[130] M. Wieber, S. Lang, Z. Anorg. Allg. Chem. 620 (1994) 1397.
[131] D. Dakternieks, R. Di Giacomo, R.W. Gable, B.F. Hoskins, J. Am. Chem. Soc. 110 (1988) 6762.
[132] S. Husebye, K. Maartmann-Moe, Acta Chem. Scand. 49 (1995) 834.
[133] S. Husebye, T. Engebretsen, M.D. Rudd, S.V. Lindeman, Acta Crystallogr., Sect. C: Cryst. Struct. Commun. 52 (1996) 2022.
[134] S. Husebye, S. Kudis, S.V. Lindeman, Acta Crystallogr., Sect. C: Cryst. Struct. Commun. 52 (1996) 424.
[135] S. Husebye, S. Kudis, S.V. Lindeman, Acta Crystallogr., Sect. C: Cryst. Struct. Commun. 52 (1996) 429.
[136] J. Zukerman-Schpector, I. Haiduc, CrystEngComm 4 (2002) 178.
[137] I. Haiduc, E.R.T. Tiekink, J. Zukerman-Schpector, in: A.G. Davies, M. Gielen, K.H. Pannell, E.R.T. Tiekink (Eds.), Tin Chemistry—Fundamentals and Frontiers, John Wiley & Sons, Chapter 3.9, 2008.
[138] (a) E.R.T. Tiekink, J. Zukerman-Schpector, CrystEngComm 9 (2009) 1176;
(b) E.R.T. Tiekink, J. Zukerman-Schpector, CrystEngComm 9 (2009), DOI: 10.1039/(b910209d).
[139] T.J. Mooibroek, P. Gamez, J. Reedijk, CrystEngComm 10 (2008) 1501.
[140] S. Husebye, K. Maartmann-Moe, W. Steffensen, Acta Chem. Scand. 44 (1990) 139.
[141] D.S. Yufit, Yu. T. Struchkov, L. Yu. Ukhin, Z.S. Morkovnik, A.A. Maksimenko, I.D. Sadekov, M.M. Levkovich, S.I. Tesgoedova, V.D. Stebletsova, Koord. Khim. (Russ.) (Coord. Chem.) 13 (1987) 1702.
[142] S. Husebye, S. Kudis, S.V. Lindeman, P. Strauch, Acta Crystallogr., Sect. C: Cryst. Struct. Commun. 51 (1995) 1870.
[143] R.K. Chadha, J.E. Drake, N.T. McManus, B.A. Quinlan, A.B. Sarkar, Organometallics 6 (1987) 813.
[144] J.H.E. Bailey, J.E. Drake, Can. J. Chem. 71 (1993) 42.
[145] J.E. Drake, J. Yang, Inorg. Chem. 36 (1997) 1890.
[146] J.H.E. Bailey, J.E. Drake, A.B. Sarkar, M.L.Y. Wong, Can. J. Chem. 67 (1989) 1735.
[147] D. Dakternieks, R. Di Giacomo, R.W. Gable, B.F. Hoskins, J. Organomet. Chem. 349 (1988) 305.
[148] J.H.E. Bailey, J.E. Drake, M.L.Y. Wong, Can. J. Chem. 69 (1991) 1948.
[149] N.W. Alcock, J. Culver, S.M. Roe, J. Chem. Soc., Dalton Trans. (1992) 1477.
[150] D. Dakternieks, R. Di Giacomo, R.W. Gable, B.F. Hoskins, J. Am. Chem. Soc. 110 (1988) 6753.
[151] V. Garcia-Montalvo, R.A. Toscano, A. Badillo-Delgado, R. Cea-Olivares, Polyhedron 20 (2001) 203.
[152] M. Wieber, E. Schmidt, C. Burschka, Z. Anorg. Allg. Chem. 525 (1985) 127.
[153] J.H.E. Bailey, J.E. Drake, L.N. Khasrou, J. Yang, Inorg. Chem. 34 (1995) 124.
[154] J.E. Drake, L.N. Khasrou, A.G. Mislankar, R. Ratnani, Can. J. Chem. 72 (1994) 1328.
[155] J.E. Drake, L.N. Khasrou, A.G. Mislankar, R. Ratnani, Polyhedron 19 (2000) 407.
[156] A.M. Cotero-Villegas, R.A. Toscano, M. Muñoz-Hernández, M. López-Cardoso, P. García y García, R. Cea-Olivares, J. Organomet. Chem. 690 (2005) 2872.
[157] A. Silvestru, I. Haiduc, H.J. Breunig, K.H. Ebert, Polyhedron 14 (1995) 1175.
[158] J.E. Drake, L.N. Khasrou, A.G. Mislankar, R. Ratnani, Can. J. Chem. 77 (1999) 1262.
[159] M.I. Mohamed-Ibrahim, S. See Chee, M.A. Buntine, M.J. Cox, E.R.T. Tiekink, Organometallics 19 (2000) 5410.
[160] J.O. Bogason, D. Dakternieks, S. Husebye, K. Maartmann-Moe, H. Zhu, Phosphorus Sulfur Silicon Relat. Elem. 71 (1992) 13.
[161] J.E. Drake, L.N. Khasrou, A.G. Mislankar, R. Ratnani, Inorg. Chem. 38 (1999) 3994.
[162] V. García-Montalvo, A. Marcelo-Polo, R. Montoya, R.A. Toscano, S. Hernández-Ortega, R. Cea-Olivares, J. Organomet. Chem. 623 (2001) 74.
[163] G. Canseco-Melchor, V. García-Montalvo, R.A. Toscano, R. Cea-Olivares, J. Organomet. Chem. 631 (2001) 99.
[164] G. Canseco-Melchor, V. García-Montalvo, R.A. Toscano, R. Cea-Olivares, Z. Anorg. Allg. Chem. 627 (2001) 2391.
[165] D. Dakternieks, R. Di Giacomo, R.W. Gable, B.F. Hoskins, J. Organomet. Chem. 353 (1988) 35.
[166] J.G. Alvarado-Rodríguez, M.C. García Gutierrez, R. Cea-Olivares, Rev. Mex. Fis. 46 (2000) 44.
[167] D. Fuentes-Alemán, R.-A. Toscano, M. Muñoz-Hernández, M. López-Cardoso, P. García y García, R. Cea-Olivares, J. Organomet. Chem. 693 (2008) 3166.
[168] J.E. Drake, R.J. Drake, L.N. Khasrou, R. Ratnani, Inorg. Chem. 35 (1996) 2831.
[169] D. Dakternieks, R. Di Giacomo, R.W. Gable, B.F. Hoskins, J. Am. Chem. Soc. 110 (1988) 6541.
[170] A.K. Singh, V. Srivastava, J.K. Basumatary, T.P. Singh, A.K. Saxena, Phosphorus Sulfur Silicon Relat. Elem. 89 (1994) 31.
[171] J.E. Drake, M.L.Y. Wong, J. Organomet. Chem. 377 (1989) 43.
[172] A.K. Singh, J.K. Basumatary, T.P. Singh, B. Padmanabhan, J. Organomet. Chem. 424 (1992) 33.
[173] V. Srivastava, J.K. Basumatary, A.K. Singh, T.P. Singh, A.K. Saxena, Phosphorus Sulfur Silicon Relat. Elem. 85 (1993) 175.
[174] M. Wieber, S. Lang, N. Graf, Phosphorus Sulfur Silicon Relat. Elem. 85 (1993) 31.